Understanding Scale-down of Oxygen Dependent Biocatalysis

Dias Gomes, Mafalda

Publication date:
2018

Document Version
Publisher's PDF, also known as Version of record

Understanding Scale-down of Oxygen Dependent Biocatalysis

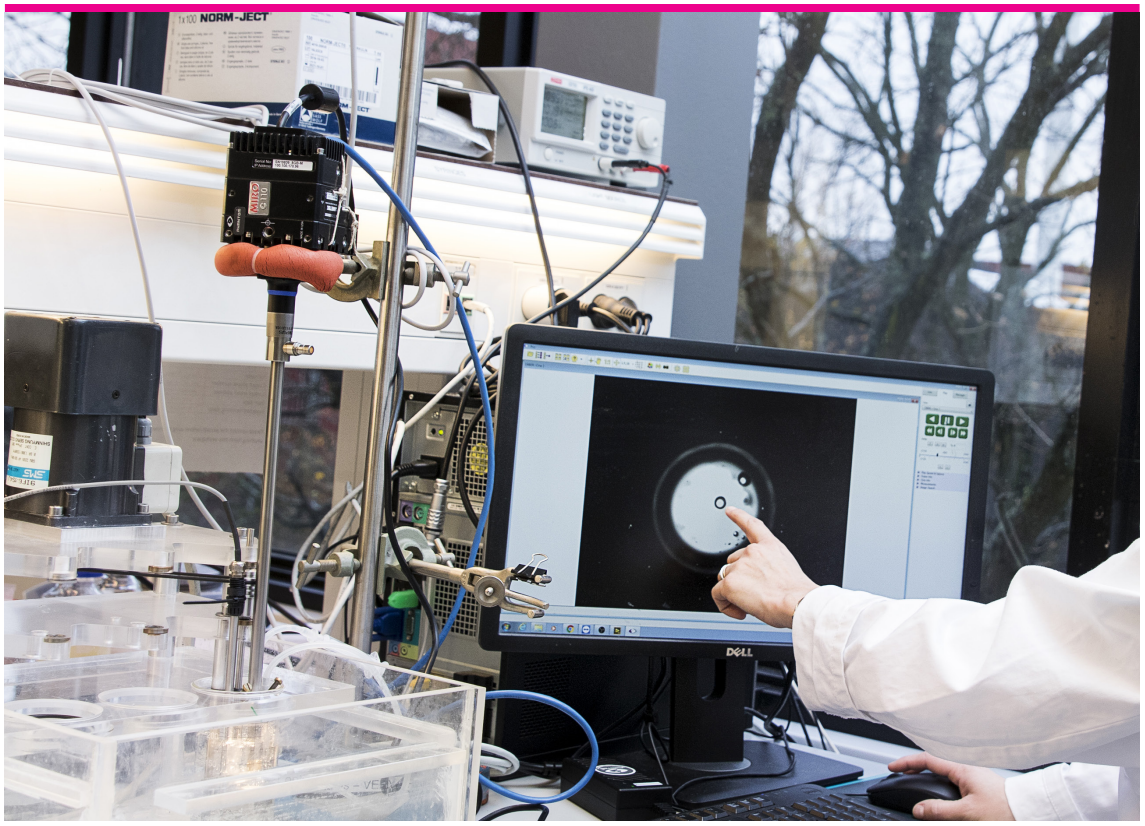

Mafalda Dias Gomes

PhD Thesis

October 2018

DTU Chemical Engineering
Department of Chemical and Biochemical Engineering

Understanding Scale-down of Oxygen Dependent Biocatalysis

Mafalda Dias Gomes

PhD Thesis
October 2018

DTU Chemical Engineering
Department of Chemical and Biochemical Engineering

Address: Process and Systems Engineering Center (PROSYS)

Department of Chemical and Biochemical Engineering

Technical University of Denmark

Building 229

Dk-2800 Kgs. Lyngby

Denmark

Phone: +45 4525 2800

Web: www.kt.dtu.dk/forskning/prosys

Print: STEP

DTU Chemical Engineering
Department of Chemical and Biochemical Engineering

Abstract

Biocatalysis has been raising great interest in industrial chemical synthesis, particularly in the development of new biocatalytic routes for oxidation reactions. Oxidation reactions are widely used in the chemical industry, however, traditional chemocatalytic processes are poorly selective, carried out under harsh reaction conditions and generate significant quantities of waste. In contrast, enzymes used to catalyse oxidation reactions offer exquisite selectivity and the ability to work under mild reaction conditions, which contributes to the development of sustainable industrial processes. Besides these great benefits, biocatalysis offers the possibility to modify and tune the biocatalyst, adapting it towards the process needs. Through protein engineering, modifications can be made to an enzyme, which influence its performance. Protein engineering methods offer an extra degree of freedom to the process design task, enabling orders of magnitude improvements compared to process engineering methods. However, process limitations have to be identified at an early stage of process development to define targets for protein engineering research.

Most oxidative enzymes require molecular oxygen as an oxidant, which is conventionally supplied to the reaction by aeration in a stirred tank reactor. Although oxygen is an environmentally friendly oxidant which is inexpensive and abundant, its supply to a reaction is usually the primary constraint that prevents the implementation of biocatalytic oxidations in industry. Moreover, it also makes these reactions difficult to study at the laboratory scale. This can be due to either poor biocatalyst stability in the presence of gas-liquid interfaces or to reaction rates being limited by either oxygen transfer into the liquid medium or biocatalyst kinetics. In this context, this thesis proposes a scale-down approach to investigate the main limitations of biocatalytic oxidation reactions, at an early stage of process development. This approach aims to acquire fundamental understanding of the biocatalyst kinetics and stability, under relevant process conditions dictated by industrial targets.

In the first part of the work, a systematic methodology based on reaction trajectory analyses was applied, in order to identify the major limitations of an oxidase-catalysed reaction. Glucose oxidase was used as a model enzyme and the major process limitations identified were related to oxygen

transfer rate and enzyme kinetics. The maximum biocatalyst load in order to avoid oxygen transfer limitations was found for the reactor setup used. Furthermore, the kinetic parameters for GOx were determined using a tube-in-tube reactor and the K_{MO} (0.843 mM) was found to be higher than the solubility of oxygen in aqueous solutions (0.265 mM). This result indicates that the enzyme efficiency is compromised when the reaction is carried out under typical operational conditions (aeration at atmospheric pressure).

In the second part of the work, the stability of NAD(P)H oxidases towards gas-liquid interfaces was investigated. For the first time, an *in situ* experimental method that quantifies the gas-liquid interfacial area inside an aerated stirred tank reactor was developed. This method enabled the investigation of kinetic stability of enzymes in the presence of gas-liquid interfaces, similar to large-scale bioreactors. It was found that the half-life of NAD(P)H oxidases decreased with an increase in gas-liquid interfacial area. Results demonstrated that mechanical stirring and the presence of gas-liquid interfacial area each have an individual effect on enzyme deactivation. Therefore, the effect of mechanical stirring was studied in the absence of gas-liquid interface and the deactivation rate of NAD(P)H oxidase increased with an increase in power input per volume of the reactor. It is proposed that the deactivation is caused by molecular collisions in the reactor and that their frequency increases with higher stirring power input. The stability of these enzymes was also studied in the absence of stirring and in the presence of gas-liquid interfaces, in a laboratory scale bubble column. It was shown that these oxidases deactivated faster with the increase of interfacial area and that the presence of oxygen in the gas feed enhanced the deactivation rate. With these findings, a conceptual stability map identifying the causes for enzyme deactivation as a function of mechanical stirring and gas supply was elaborated.

Finally, a scale-down approach to investigate and understand biocatalytic oxidations was developed. This approach is based on an industrially driven philosophy and on the results for kinetics and stability of oxygen dependent biocatalysts obtained here. It suggests scale-down experiments depending on the limitation that is being investigated: kinetics or stability. The outcome of this approach contributes to the establishment of practicable solutions to improve biocatalytic oxidation processes and ultimately, to accelerate their implementation in industry.

Dansk Resumé

Biokatalyse har de seneste år vakt stor interesse inden for industriel kemisk syntese, nærmere bestemt som et grønt alternativ til traditionelle redoxreaktioner. Traditionelle Oxidative redoxreaktioner benyttes i stor stil i den kemiske industri, dog er disse oftest forbundet med høj reagens promiskuitet, lav stereoselektivitet og lavt udbytte hvis ikke krasbørstige procesvilkår benyttes. Erstattes den traditionelle kemiske katalysator i stedet for med enzymer, kan ikke kun langt mildere procesvilkår benyttes, men også en langt højere substrat og produktselektivitet opnås. Udover at dette faktum potentielt set gør skiftet til enzymer økonomisk rentabelt, biddrager det også til højne bæredygtigheden i den kemiske industri. Foruden disse i forvejen store fordele ved biokatalyse, er det muligt at foretage ændringer i enzymets peptidstruktur og aminosyresekvens, og dermed skræddersy katalysatormaterialet, så det passer perfekt til den ønskede proces. Dermed tilføres en ekstra frihedsgrad til proces design dilemmaet, der kan have langt større effekt på udbyttet end selve procesteknologien. Dette ændre dog ikke på at det er yderst vigtigt at kortlægge begrænsninger fastsat af den baglæggende teknologi, inden ændringer i enzymet udføres.

De fleste oxidase enzymer benytter, navnet tro, oxygen eller ilt som elektronaccepter. Ilten tilføres oftest til reaktionen via beluftning og omrøring i en konventionel omrørt tank reaktor. Selvom oxygen er en miljøvenlig, let tilgængelig og billig elektronaccepter ender det oftest med at være den reaktant som forhindre anvendelsen af oxidativ biokatalyse i industrien såvel som præcise studier i laboratoriet. Dette skyldes enten selve enzymkinetikken, gas/væske masseoverførelsesproblemer, eller at enzymet henfalder i kontaktfladen mellem gas og væske. I denne sammenhæng foreslås der i denne afhandling en fremgangsmåde til at nedskalere og undersøge begrænsende faktorer af biokatalytiske oxidationsreaktioner på et tidligt stadium af procesudvikling. Denne tilgang har til formål at opnå grundlæggende forståelse for enzymkinetikken og stabiliteten under relevante procesbetingelser dikteret af industrielle mål.

I den første del af arbejdet blev en systematisk metode baseret på reaktionsforløb analyser anvendt for at identificere de væsentligste begrænsninger af en oxidase-katalyseret reaktion. Glukose oxidase (GOx) blev anvendt som et modelenzym, og masseoverførelse samt enzymkinetik blev

identificeret som de vigtigste procesbegrænsninger. Den maksimale enzymkoncentration for at undgå iltoverførselsbegrænsninger blev bestemt for den anvendte reaktoropsætning (130 mg L^{-1}, kLa = 120 h^{-1}). Endvidere blev de kinetiske parametre for GOx bestemt under anvendelse af en tube-in-tube reaktor, og KMO (0.843 mM) viste sig at være højere end opløseligheden af oxygen i luft i vandige opløsninger (0.265 mM). Dette resultat indikerer, at enzymeffektiviteten er kompromitteret, når reaktionen udføres under typiske driftsbetingelser (beluftning ved atmosfærisk tryk).

I anden del af arbejdet blev stabiliteten af NAD(P)H oxidase over for gas-væske-kontaktflader undersøgt. For første gang blev en in situ eksperimentel metode, der kvantificerer gas-væske-kontaktfladeområdet inde i en beluftet omrørt tankreaktor udviklet. Denne metode muliggjorde undersøgelsen af kinetisk stabilitet af enzymer ved tilstedeværelsen af samme gas-væske-kontaktflader som i store bioreaktorer. Det blev konstateret, at halveringstiden for NAD(P)H-oxidaser faldt med en stigning i gas-væske-kontaktfladen. Resultater viste, at mekanisk omrøring og tilstedeværelsen af en gas-væske-kontaktflade hver har en individuel virkning på enzyminaktivering. Effekten af mekanisk omrøring blev derfor undersøgt i fravær af gas-væske-grænseflade, og henfaldshastigheden for NAD(P)H oxidase steg med en stigning i effekt pr. Volumen af reaktoren. Det foreslås, at inaktiveringen skyldes molekylære kollisioner i reaktoren, og at deres frekvens stiger med øget omrøringshastighed. Stabiliteten af disse enzymer blev også studeret i fravær af omrøring og ved tilstedeværelse af gas-væske-kontaktflader i en laboratorieskala boblekolonne. Det blev påvist, at disse oxidaser henfalder hurtigere med forøgelsen af kontaktfladeområdet, og at tilstedeværelsen af ilt i gasforsyningen forøger inaktiveringshastigheden. På baggrund af disse fund blev der udarbejdet en fremgangsmåde til identifikation af årsagerne til enzyminaktivering som en funktion af mekanisk omrøring og gasforsyning.

Til sidst blev der udviklet en nedskaleringstilgang til undersøgelse og forståelse af biokatalytiske oxidationer. Denne tilgang er baseret på en industrielt tilgang og på resultaterne for kinetik og stabilitet af iltafhængige enzymer beskrevet i denne afhandling. Det foreslås at nedskalingsforsøg tilrettelægges afhængigt af den begrænsning, der undersøges: kinetik eller stabilitet. Resultatet af denne tilgang bidrager til etablering af praktiske løsninger til forbedring af biokatalytiske oxidationsprocesser og i sidste ende at fremskynde deres brug i industrien.

Preface

This thesis has been written to fulfil the requirements for a PhD degree in Chemical Engineering. The work here presented was developed over the period of September 2015 to October 2018 and was supervised by Professor John M. Woodley. The research was mostly conducted at the Process and Systems Engineering Centre (PROSYS) within the Department of Chemical and Biochemical Engineering at the Technical University of Denmark (DTU). The work presented in Chapter 5 was carried out during an external stay at the Department of Chemical and Biomolecular Engineering at Georgia Institute of Technology (GaTech) in Atlanta, Georgia, USA under the guidance of Professor Andreas Bommarius and Dr Bettina Riebel Bommarius.

The work was partly funded by the Technical University of Denmark and by the European Union (EU) project ROBOX (grant agreement n° 635734) under EU's Horizon 2020 Programme Research and Innovation actions H2020-LEIT BIO-2014-1. The EU project enabled several positive collaborations within the project partners, that supplied the enzymes required for this research.

Kgs. Lyngby, October 2018

Mafalda Dias Gomes

Acknowledgements

I would like to express my sincere gratitude to my supervisor John for the constant support, scientific vision and mentorship during my PhD project. Thank you for challenging me to do this PhD and for always believing in me. I have truly enjoyed our discussions, your thought-provoking questions and your immense knowledge on the field of biocatalysis. Your guidance not only helped me to develop and grow as a researcher but also as a person.

Thank you to my friend Murray for being a great lab mate and travel partner and for all the support in overcoming the numerous obstacles that I have faced through this project. Thank you for your friendship. I am also grateful for my co-supervisor Mathias, for the guidance on the laboratory work and for always being available to discuss my work.

I am grateful to former and present colleagues at PROSYS for creating an enjoyable work environment. In particular, I would like to thank my colleagues and friends Catarina, Christian, Sebastian and Rowan for reading parts of my thesis and contributing with valuable comments and also Asbjørn, Leander, Morten, Ricardo, Rolf and Teresa for the great companionship and all the fun we had in the last three years. A special thanks to Tannaz for being a wonderful office mate, for the motivation and good company.

I would like to acknowledge Andy and Bettina for welcoming me at Georgia Tech, sharing great ideas and contributing to fruitful scientific discussions. I am also grateful to my lab mates at Georgia Tech for making me feel welcome during my external stay.

A big thank you to my family and friends in Portugal, especially to my mother and sister, for the unconditional support through this journey, even though not fully understanding what I was doing.

Finally, I would like to dedicate this thesis to my husband Rafael and thank him for his extraordinary patience and encouragement throughout this project, especially during the writing process. Thank you for always being by my side. "*Tudo é possível a quem crê*".

Contents

Nomenclature

Roman Letters

A	Gas-liquid interfacial area (m^2)
a	Specific gas-liquid interfacial area (m^{-1})
Bo	Bond number
$C_{½}$	Half-concentration
d_b	Gas bubble diameter (mm)
d_{32}	Sauter mean diameter (mm)
d_0	Nozzle diameter (mm)
d_e	Equivalent diameter of a bubble (mm)
D	Impeller diameter (m)
g	Gravitational acceleration (m s^{-2})
H	Henry´s constant (atm L mol^{-1})
k_{cat}	Enzymatic reaction constant (µmol min^{-1} mg^{-1})
k_d	Deactivation rate constant (h^{-1})
k_la	Volumetric mass transfer coefficient
K_{iu}	Uncompetitive inhibition constant
K_u	Unfolding equilibrium constant
K_M	Michaelis constant
K_{ic}	Competitive inhibition constant
L	Bubble column height (cm)
M	Morton number
m_B	Mass of biocatalyst
m_P	Mass of product
m_S	Mass of substrate
N_p	Impeller power number
N	Impeller rotational speed
N_i	Number of bubbles in a bin
p_{O_2}	Partial pressure of oxygen (atm)
P_A	Area probability density function
P_N	Number probability density function
P_V	Volume probability density function
P/V	Power input per reactor volume (W L^{-1})
Q	Gas flow rate (m^3 s^{-1})

Q_q	Theoretical transition flow rate (m s^{-1})
R	Reynolds number
t	Time
T_m	Melting temperature of a protein (°C)
T_{50}	Temperature of half inactivation (°C)
U	Rising velocity of a bubble (m s^{-1})
v_{max}	Maximum volumetric enzymatic reaction rate (µmol L^{-1} min^{-1})
V	Volume (m^3)
$[E]$	Concentration of enzyme (mg_{CFE} L^{-1})
$[S]$	Concentration of substrate (mmol L^{-1})
$[O_2]$	Concentration of oxygen in solution (mmol L^{-1})
$[O_2]^*$	Saturation concentration of oxygen (mmol L^{-1})

Greek Letters

ρ_g	Gas density (kg m^{-3})
ρ_l	Liquid density (kg m^{-3})
$\bar{\rho}$	Average density of the medium (kg m^{-3})
μ	Viscosity (Pa s)
σ	Surface tension (kg m^{-1} s^{-1})
θ	Residence time of a bubble in the bubble column (s)
$\tau_{½}$	Half-life of an enzyme (h)
ε	Gas hold-up
$\triangle G_u$	Gibbs free energy of protein unfolding (J mol^{-1})

Abbreviations

AOX	Alcohol oxidase
AAP	Aminoantipyrine
ADH	Alcohol dehydrogenase
Cat	Catalase
CFE	Cell free extract
DCHBS	Sodium 3,5-dicloro-hydroxybenzenesulfonate
DNA	Deoxyribonucleic acid
DTT	Dithiothreitol
EC	Enzyme commission
FAD	Flavin adenine dinucleotide
GOx	Glucose oxidase
HRP	Horseradish peroxidase
NAD(P)H	Nicotinamide adenine dinucleotide (phosphate)
NOX	NAD(P)H oxidase
OTR	Oxygen transfer rate
TiTR	Tube-in-tube reactor
TTN	Total turnover number
UV-Vis	Ultraviolet-visible light

Chapter 1.

General Introduction

1.1 Background

Biocatalysis

The field of biocatalysis involves the use of enzymes or non-growing microbial organisms to catalyse chemical reactions. Here, we define biocatalysis as the application of enzymes as catalysts to convert a reactant, termed substrate, into a product of commercial interest. Enzymes are renewable catalysts (produced by fermentation), which can operate under mild conditions and offer excellent regio and stereoselectivity (Pollard and Woodley, 2007). These properties are highly attractive for industrial chemical processing, which traditionally relies on the use of metal catalysts. For instance, the exquisite selectivity of enzymes enable the elimination of costly protection and de-protection steps in a chemical synthesis (Truppo, 2017; J.M. Woodley, 2017) and, the fact that enzymatic reactions are often carried out in aqueous media, under mild temperatures and pH, reduces chemical waste and contributes to the development of sustainable processes (Sheldon and Woodley, 2018).

The extraordinary advantage of biocatalysis when compared to chemo-catalysis is the opportunity to use a tunable catalyst. It is indeed possible to manipulate enzymes through protein engineering (Chen and Arnold, 1993; Davids et al., 2013; Hammer et al., 2017). Nowadays, the catalytic properties of an enzyme can be altered towards the synthesis of industrially interesting molecules (Arnold, 2018; Bornscheuer et al., 2012). Enzymes are proteins found in nature and are capable of catalysing chemical reactions that are usually carried out at low concentrations and rates. However, the natural environment of an enzyme is very different from the operational conditions of a bioreactor and, in order to use them as biocatalysts, high catalytic activity, stability and tolerance to large substrate and product concentrations are necessary. With the development of recombinant DNA

technology, it is possible to change the amino acid structure of an enzyme, by modifying its amino acid sequence (Lalonde, 2016; Strohmeier et al., 2011). These alterations allow the improvement of enzyme activity, stability and selectivity and therefore, create biocatalysts capable of meeting industrial process requirements. Another protein engineering approach to tune enzyme characteristics is directed evolution (Arnold et al., 2001; Cahn et al., 2017; Hammer et al., 2017). This method uses natural selection to evolve proteins with desired properties. It does not require knowledge of the crystal structure of a protein, which can be beneficial to accelerate the development of robust enzymes (Turner, 2009). However, it requires high-throughput computational methods for screening and selection from the large number of different mutations generated (Porter et al., 2016). Overall, with the established techniques of protein engineering, there is a possibility to change an enzyme and adapt it to a desired process rather than adapt the process to an enzyme. This additional degree of freedom that biocatalysis offers allows orders of magnitude improvements that could never be achieved using only process engineering methods. However, in order to develop an industrial biocatalytic process faster and more effectively, there is a need to integrate these two fields of research. Protein engineering needs targets based on process requirements (Woodley, 2017). Therefore, process engineers can identify the limitations of a reaction system and thus give directions for protein engineering research.

Enzymes as Industrial Biocatalysts

Enzymes are classified according to the type of reaction catalysed. There are 6 classes of enzymes established by the *Enzyme Commission* (EC), which are presented in Table 1.1. There are multiple subclasses, defined based on the chemical groups involved in the reaction. To date, enzymes have been predominantly applied in the pharmaceutical industry (Choi et al., 2015; Woodley, 2008; Woodley, 2017). Examples of highly relevant products include the synthesis of sitagliptin and atorvastatin (Ma et al., 2010; Savile et al., 2010). The former is the active ingredient in Januvia®, an antidiabetic drug commercialized by Merck, and is catalysed by a transaminase. The latter, is the active ingredient of Lipitor®, used to lower the cholesterol (commercialized by Pfizer), which is catalysed in two steps using a combination of three enzymes: ketoreductase, glucose dehydrogenase and halohydrin dehalogenase. Generally, for the synthesis of pharmaceuticals, the purity of a product is one of the most significant parameters for the purposes of high quality standards required in this industrial sector. Therefore, the selectivity of enzymes is one of the most appealing features of biocatalysis for the production of pharmaceutical ingredients.

Table 1.1. Enzymes classification and nomenclature (EC = Enzyme Commission).

EC Class	Reaction catalysed	Subclasses examples
EC 1 Oxidoreductases	Redox reactions	Dehydrogenases, oxidases
EC 2 Transferases	Group transfer from one substance to another	Transaminases
EC 3 Hydrolases	Formation of two products from one substrate by hydrolysis	Lipases, dehalogenases
EC 4 Lyases	Group removal from substrates	Aldolases, decarboxylases
EC 5 Isomerases	Geometric or structural changes within one molecule	Isomerases, mutases
EC 6 Ligases	Join together two molecules coupled with breakdown of ATP	Synthetase

Nevertheless, the environmental benefits of using enzymes as biocatalysts are also of great importance. Indeed, biocatalysis fulfils the demands for safer and cleaner industrial processes due to the renewable features of enzymes. However, its application will have a higher impact on the development of sustainable processes if applied more broadly to commodity and fine chemicals where production volumes are much higher. Today, there are still few enzymatic industrial processes for lower priced, high volume chemicals. This trend results from a lower economic margin for the process development (Price et al., 2016). In this industrial sector, the economic metrics are of major importance to implement a successful and profitable process (Tufvesson et al., 2011). The process has to be highly efficient and the biocatalyst very robust, which makes its design and development more complex and challenging, in contrast with the pharmaceutical sector. In general, as the market price of a product decreases, its production process has to be more efficient. Therefore, process engineering methodologies become essential to extend the application of biocatalysis to every sector of the Chemical Industry.

Oxidising Enzymes as Biocatalysts

Enzymes have gained a considerable interest in the Chemical Industry for the development of oxidative biocatalysis (Dong et al., 2018; Hollmann et al., 2011; Martínez et al., 2017; Turner, 2011; Wang et al., 2017; Xu, 2005). The major attraction of these enzymes is that the oxidant is usually molecular oxygen, which is mild compared to metal catalysts usually used in conventional chemical processes. Additionally, redox biocatalytic reactions are controlled and readily achieved because of the superb selectivity of enzymes and the high redox potential of biological oxidizing agents (favours reaction thermodynamics towards product formation) (Burton, 2003). Oxidising enzymes are part of a major class of enzymes denominated oxidoreductases and are divided into subclasses according to the nature of the electron acceptor and the reaction products, as illustrated in Figure 1.1.

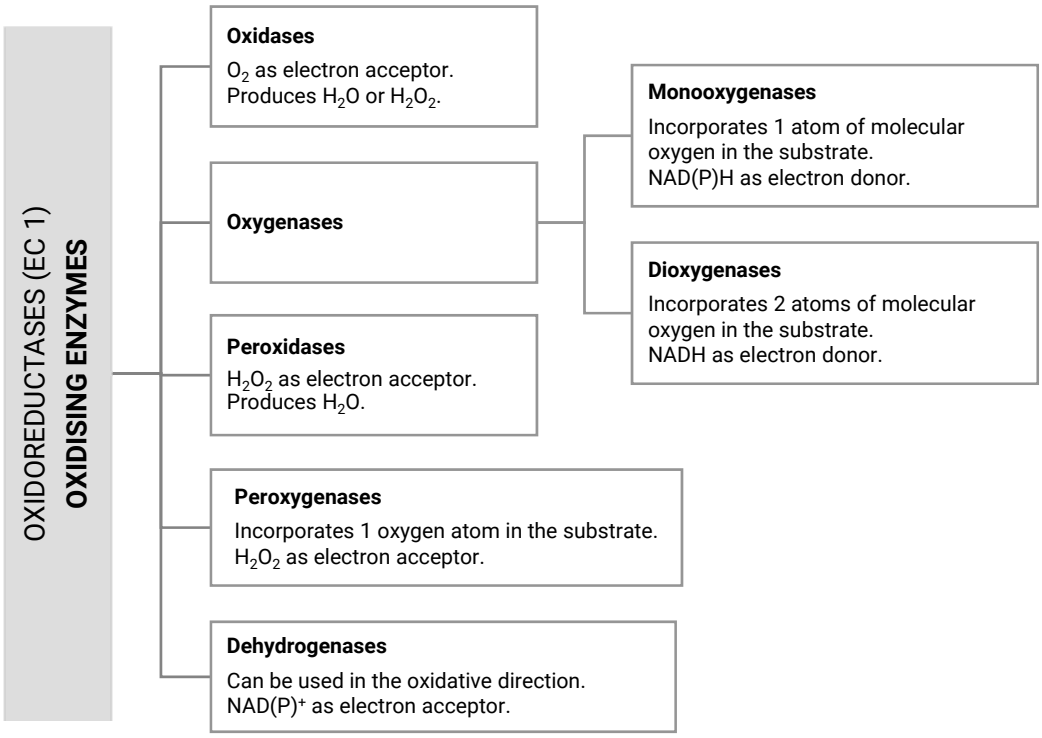

Figure 1.1. Classification of industrially relevant oxidising enzymes based on the *Enzyme Commission* (EC) nomenclature.

Oxidative enzymes can have roles in the primary or secondary metabolism of living organisms and there is often a need for cofactors to facilitate electron transfer. The cofactor requirement of these enzymes can impose constrains on the development of an industrial process since they are required in stoichiometric amounts and can be considerably expensive (Dumeignil et al., 2018). Therefore, *in situ* cofactor regeneration systems are necessary to develop economically feasible processes (Truppo, 2012) and to favour the reaction equilibrium towards product formation (Abu and Woodley, 2015; Ferrandi et al., 2014).

Oxidases and oxygenases are oxygen dependent enzymes. Dehydrogenases become oxygen dependent when coupled with NAD(P)H oxidase for cofactor regeneration. Therefore, when performing reactions using these enzymes, molecular oxygen is required. Conventionally, oxygen is continuously supplied by aerating a stirred tank reactor, which generates gas-liquid interfaces. The principles behind oxygen transfer to aqueous solutions are explained in the following section.

The enzymes studied in this thesis are oxidases: glucose oxidase (GOx EC 1.1.3.4) and NAD(P)H oxidase (NOX EC 1.6.3.2). The first enzyme was used as a model system to investigate and identify process limitations in a reaction catalysed by an oxidase. The second enzyme, which is applied for cofactor regeneration, usually coupled with alcohol dehydrogenases to oxidise alcohols to ketones or aldehydes, was used to investigate enzyme stability at gas-liquid interfaces. GOx is described in detail in Chapter 2 and NOX in Chapter 3, 4 and 5.

Oxygen Transfer

Oxygen is usually transferred from the air into the aqueous medium, where enzymatic oxidation reactions take place. The rate at which oxygen is required depends on the biocatalyst activity (enzyme kinetics) and on the stoichiometry of the biooxidation reaction. Providing sufficient oxygen is indeed a complex task in reaction engineering because of the low solubility of oxygen in aqueous solutions. At 25 °C the concentration of oxygen in water saturated with air at atmospheric pressure is 0.265 mM, a value that decreases with temperature increase and with the presence of other solutes (Onken and Liefke, 1989).

The transfer of oxygen from a gas bubble to a liquid solution is described by the Two-Film Theory (Whitman, 1923), where the diffusion of oxygen determines the transport phenomena. It assumes an equilibrium between the two films at the gas-liquid interface and a stagnant layer on both sides (Figure 1.2). The oxygen diffusion through the gas film is fast whereas the diffusion through the liquid film drives the oxygen transfer. The driving force for mass transfer, which is the difference between the oxygen concentration in the bulk and the concentration at the gas-liquid interface (oxygen saturation concentration, $[O_2]^*$), is low due to the poor solubility of oxygen in aqueous media. The equilibrium concentrations of each side of the gas-liquid interface can be related by Henry's law, defined in equation (1.1), where H is the Henry's constant and $[O_2]$ the oxygen concentration in equilibrium with a gas phase, with partial pressure p_{O_2}.

$$p_{O_2} = H[O_2] \tag{1.1}$$

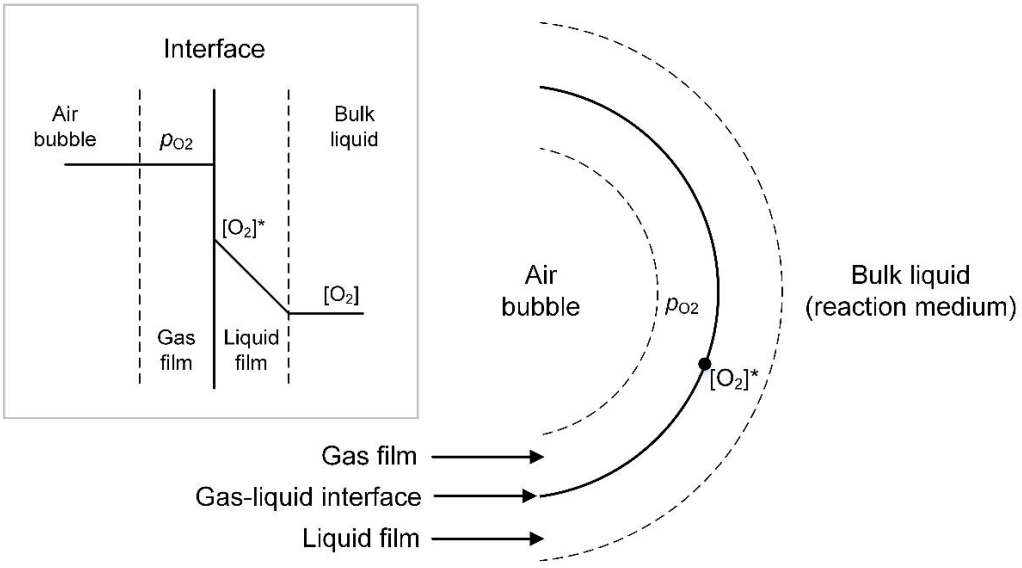

Figure 1.2. Oxygen transfer from the gas to the liquid phase. p_{O2} is the partial pressure of oxygen and $[O_2]^*$ its saturation concentration. Concentration profiles of oxygen in the gas and liquid films, based on the Two-Film Theory (top left corner).

Overall, the oxygen transfer rate (OTR) is dependent on the mass transfer coefficient through the liquid film (k_l), the driving force for the transfer (ΔC) and the gas-liquid interfacial area per unit volume available (a) (equation (1.2)).

$$\mathrm{OTR} = k_l a([O_2]^* - [O_2]) \tag{1.2}$$

Conventionally, aerated stirred tanks have been the most common type of reactors to run aerobic processes because of their extreme flexibility. In order to achieve high dispersion of air in the media, turbulent flow is required and the interfacial area of the bubbles is hard to determine. Therefore, k_l and a have been lumped together as one constant termed *volumetric mass transfer coefficient* (k_la). The k_la is dependent on fluid dynamics and rheology and is empirically correlated with the power per unit volume to the reactor, the superficial gas velocity and the viscosity of the medium (Garcia-Ochoa and Gomez, 2009; Van't Riet, 1979). It is very dependent on the reactor scale and geometry and is used to quantitatively describe the oxygen transfer rate (Gabelle et al., 2011). Indeed, it may not be intuitive but k_la increases with scale and consequently, the oxygen transfer rate increases as well. This is due to a larger contribution of the gas phase through the superficial gas velocity. The superficial gas velocity (m s^{-1}) is the velocity of gas rising through the reactor, assuming a single gas plug flow rising through the tank and is calculated from the gas flow rate divided by the cross sectional area of the tank. As the volume increases, for the same vvm of gas (volume of gas per volume of liquid per minute), the superficial gas velocity tends to increase, which contributes to higher k_la compared to laboratory scales. Additionally, in large reactors, the inlet gas pressure increases with the increase of liquid height, resulting in higher solubility of oxygen. Therefore, the increase in driving force also contributes to higher oxygen transfer as the reactor scale increases (Stocks, 2013).

The oxygen requirements to develop an industrial biooxidation process can limit reaction rates (Nordblad et al., 2018; Nordkvist et al., 2007; Pedersen et al., 2015) and biocatalyst stability (Bhagia et al., 2018; Bommarius and Karau, 2005). Therefore, in order to develop biooxidations in the direction of industrial feasibility, these two possible constraints have to be identified at an early stage of process development. Furthermore, the reasons for such limitations must be understood to accelerate process design and development. We believe that this understanding provides a direction to a more focused research on the enzymes and can give targets to protein engineers when process optimization strategies are not enough to the development of such reactions.

In fact, there are a few ways to overcome process limitations related to oxygen supply by, for example, using bubble-free methods to avoid enzyme inactivation (Van Hecke et al., 2009) or using oxygen enriched air to increase oxygen transfer rates (Lara et al., 2011). However, to the extent of our knowledge, very few studies focus on understanding this problem. In this thesis, we have tried to understand the effect of oxygen supply in biocatalytic oxidations and we have proposed a unique

approach to study these reactions in the laboratory scale, never forgetting the industrial application. The scale-down approach developed in this thesis is based on a scale-down philosophy established for fermentation processes. Therefore, the scale-up and scale-down of bioprocesses are introduced in the following section.

Scale-Up and Scale-down of Bioprocesses

Scale-up can be defined as the activity of moving a reaction form the laboratory to the industrial scale with the purpose of establishing a commercial process. This task is very challenging because the conditions and solutions found in the laboratory may not be transferable to large scale bioreactors. The scale-up of bioprocesses has been widely covered in literature with respect to fermentation processes (Charles, 1985; Garcia-Ochoa and Gomez, 2009; Hardy et al., 2017; Hewitt and Nienow, 2007; Neubauer and Junne, 2010) however, there is no clear consensus on a satisfactory approach for all types of processes. Actually, in industry, scale-up is mainly performed based on empirical knowledge from highly experienced professionals (Stocks, 2013) and has been based on the classic trial-and-error approach. For instance, the most common example of a scale-up methodology is to keep certain factors the same while increasing scale, such as power input per volume, mixing time and geometric similarity (Paul et al., 2004). However, while some factors are maintained, others can change drastically, which can result in serious economic repercussions (Noorman, 2016). Therefore, in order to understand the behaviour of a process at an early stage of its design task, scale-down approaches have been developed, for fermentation processes (Delvigne and Noorman, 2017; Nienow et al., 2013). Such studies consider two main aspects: the basic fluid dynamics, which relates to e.g. mechanical stirring and the fluid viscosity; and the characteristics of the microorganism that e.g. determines the oxygen demand for aerobic processes (Nienow et al., 2011). Currently, four milestones on the scale-down process have been recognized (Noorman, 2011):

1. Description of the large scale process analysing the operational conditions and rate limiting steps;
2. Mimic the large scale environment in the laboratory to keep the process under the same rate limitations and operational conditions;
3. The laboratory research is performed at medium or high- throughput rate with low risk and cost;
4. Improvements obtained at small scale are transferred and implemented in large scale, with a reduced risk of failure.

This four steps approach, guided by an industrial perspective, creates a broader understanding of the process prior to scale-up.

The industrial targets and consequently the operational conditions of a fermentation process are very different from biocatalytic processes, especially concerning productivities (2 g L^{-1} h^{-1} and 20 g L^{-1} h^{-1}, respectively). As a result, the challenges to be faced during scale-up will be different. Nevertheless, the scale-down philosophy developed for fermentations can be applied for enzymatic reactions.

1.2 Scope

The scope of this thesis is to propose a scale-down approach for the development of biocatalytic oxidation processes. Even though this approach is driven by industrial requirements, its main objective is to acquire fundamental understanding of the biocatalyst kinetics and stability and to incorporate the knowledge gained into the process design task. The experimental work presented here, is focused on investigating the influence of molecular oxygen on these two aspects. Furthermore, the kinetic stability of oxidases in the presence of gas-liquid interfaces is explored in detail and the rationale for enzyme deactivation in such environments is suggested. Finally, these findings are integrated with the principles of process engineering towards the implementation of biocatalytic oxidations in industry.

In this thesis, the biocatalyst is assumed to be always in the format of cell free extract. Other biocatalyst formats such as whole-cells and immobilized enzymes are not discussed here. Fermentation processes are also not part of the scope of this thesis and are here referred to simply as the process to produce enzymes used as biocatalysts for organic synthesis.

1.3 Thesis Outline

This thesis is structured in 9 chapters and its contents are summarised below:

Chapter 1 gives a general introduction to biocatalysis and its benefits in comparison with chemical catalysis for organic synthesis. Oxidative biocatalysis is introduced together with the associated process limitations. Furthermore, scale-up and scale-down of bioprocesses are presented.

Chapter 2 consists on applying a reaction trajectory methodology to determine the limitations of a biocatalytic oxidation reaction catalysed by an oxidase. Kinetic limitations are highlighted and the experiments were performed using glucose oxidase as a model system.

Chapter 3 presents a method to study the kinetic stability of oxygen dependent enzymes towards gas-liquid interfaces, in a stirred tank reactor. The method developed was applied to investigate the effect of gas-liquid interfaces on the kinetic stability of NAD(P)H oxidase.

Chapter 4 investigates the effects of mechanical stirring on the kinetic stability of NAD(P)H oxidases and attempts to correlate kinetic and thermodynamic stability of the different NAD(P)H oxidases studied.

Chapter 5 studies the effect of gas-liquid interfaces and the presence of oxygen on the kinetic stability of NAD(P)H oxidases in a bubble column.

Chapter 6 discusses the different causes of enzyme deactivation in the presence of gas-liquid interfaces and mechanical stirring.

Chapter 7 proposes a scale-down approach for the development of industrial biocatalytic oxidation processes.

Chapter 8 concludes the thesis and **Chapter 9** gives future research perspectives.

Chapter 2.

Kinetic Mapping Experiments

This chapter forms the basis of a recently published paper: *Nordblad, M Dias Gomes, M Meissner, MP Ramesh, H and Woodley, JM (2018) Scoping Biocatalyst Performance using Reaction Trajectory Analysis, Org. Process Res. Dev. 22 (9), 1101 DOI: 10.1021/acs.oprd.8b00119.*

2.1. Summary

In this chapter, a systematic experimental methodology to assess the performance of oxidase-catalysed reactions is presented and tested. Glucose oxidase (GOx) was used as a model system and the main process limitations found are related to the reaction rate. More specifically, the limitations are associated with enzyme kinetics and oxygen transfer into solution. Therefore, an experimental map for operating conditions was developed for GOx and subsequently, a conceptual regime map to illustrate kinetic limitations was designed for oxygen dependent biocatalysis.

2.2. Introduction and Motivation

Biocatalysis is increasingly becoming a feasible alternative to traditional chemical synthesis since enzymes applied as biocatalysts show excellent regio and stereoselectivity under mild reaction conditions, which meets the growing demands for cleaner and safer industrial processes (Sheldon and Woodley, 2018; Woodley, 2008; Woodley et al., 2013). Recently, the availability of enzymes capable of catalysing industrially relevant reactions has increased (Demming et al., 2018; Gkotsi et al., 2018) and there is a considerable interest in using oxidases (Liu et al., 2018; Martínez et al., 2017). Oxidases are attractive to industry because they can selectively oxidise a broad range of substrates, in contrast to conventional organic process chemistry, which requires the use of protection and de-protection steps to guide the addition of oxygen (Hollmann et al., 2011; Pickl et al., 2015).

Secondly, oxidases use molecular oxygen as the electron acceptor which is usually reduced to hydrogen peroxide (Figure 2.1), and these two molecules are among the most environmental friendly oxidants in comparison with other oxidising agents, such as permanganate and peroxyacids (Vennestrøm et al., 2010).

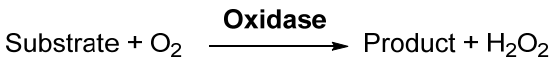

Figure 2.1. General oxidation reaction catalysed by an oxidase enzyme.

Alcohol oxidases (AOX) are a particular type of oxidase that catalyse the oxidation of alcohols into their corresponding aldehydes or ketones and require flavin-based cofactors (Goswami et al., 2013). The flavin adenine dinucleotide (FAD) is associated with the redox centre of the enzyme and is involved in transferring the hydride ion, which originates from the alcohol substrate, to molecular oxygen, leading to the formation of hydrogen peroxide (H_2O_2) (Chaiyen et al., 2012; Mattevi, 2006). Flavoenzymes are very attractive for industrial application since they can catalyse reactions without the need for external cofactors. In order to avoid enzyme deactivation, H_2O_2 is usually scavenged by the addition of catalase that converts it into water and oxygen (Figure 2.2).

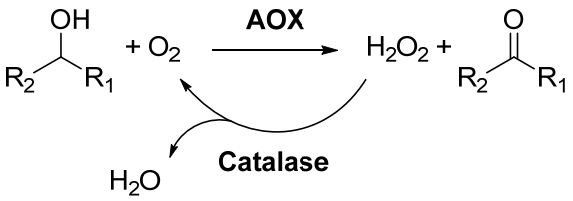

Figure 2.2. Oxidation of an alcohol to a ketone or aldehyde catalysed by an alcohol oxidase (AOX) coupled with a catalase to degrade the hydrogen peroxide into water and oxygen.

However, despite the attractive properties of oxidases, the implementation of biocatalytic oxidation reactions at an industrial scale has some challenges, mostly related to the requirement for molecular oxygen. First, this gas is poorly soluble in water (0.265 mM, using air at atmospheric pressure and 25 °C) and the kinetics of an oxidase can be limited by the oxygen concentration in solution (Nordkvist et al., 2007; Pedersen et al., 2015). Additionally, the reactions may be limited by the oxygen transfer rate from the gas to the liquid phase, when high productivities are required (Hoschek et al., 2017) and finally, the stability of the enzymes can be compromised in the presence of gas-liquid interface (Bhagia et al., 2018; Bommarius and Karau, 2005; Van Hecke et al., 2009).

Methodology based on Reaction Trajectory Analysis

With the purpose of moving oxidative biocatalysis towards industrial application, there is a need to address the specific limitations related to oxygen-dependent enzymes at an early stage of process development. In order to accelerate this process and to identify the major limitations of a

biocatalyst, a methodology based on time-course reactions was developed by Nordblad *et al.* (2018). This methodology can be applied to any biocatalytic reaction and, with simple and systematic experiments, the bottleneck of an enzymatic reaction can be identified.

In brief, the methodology consists of three sequential experiments where the biocatalyst load and substrate concentration are varied and the interpretation and understanding of the results is based on a graphical analysis of the reaction trajectories. As illustrated in Figure 2.3, the experiments follow the substrate conversion over time and, specifically for enzymatic oxidation reactions, are carried out in three sequential steps:

1. In the first experiment, time-course data is collected at relevant operational conditions, such as temperature, pH, stirring speed, aeration rate and substrate and biocatalyst concentrations. These conditions are defined based on a preliminary characterisation of the enzyme, for example data about enzyme activity, pH, temperature and oxygen demand. The substrate and biocatalyst concentrations should be defined in order to run the experiment during a reasonable period of time. Therefore, a complete conversion curve (up to 100 % conversion) can be obtained. This experiment, termed *benchmark experiment*, establishes the reaction behaviour. In other words, it defines if the reaction rate varies with time (higher-order kinetics) or not (zero-order kinetics).

2. In the second experiment, all conditions are maintained except the biocatalyst load. By varying the biocatalyst concentration the main limitation of the system can be identified: mass transfer (oxygen transfer rate), biocatalyst kinetics or stability. If the latter two limitations are found, we move to the third experiment. Otherwise, if mass transfer is identified, step one should be repeated under non mass transfer limitations because they conceal the biocatalyst performance. Mass transfer limitations are noncatalytic related, so the initial reaction conditions should be modified to eliminate them. This objective can be achieved by reducing the biocatalyst load or changing operational conditions related to the laboratory equipment (e.g.: agitation, aeration rate and gas phase composition).

3. For the last experiment, the substrate concentration is varied and the other conditions used in the second experiment are kept constant. The results obtained will indicate the underlying mechanism of the main limitation identified (biocatalyst kinetics or stability). In Figure 2.3, the possible parameters causing process limitations are listed and the graphical analysis illustrates how to identify them.

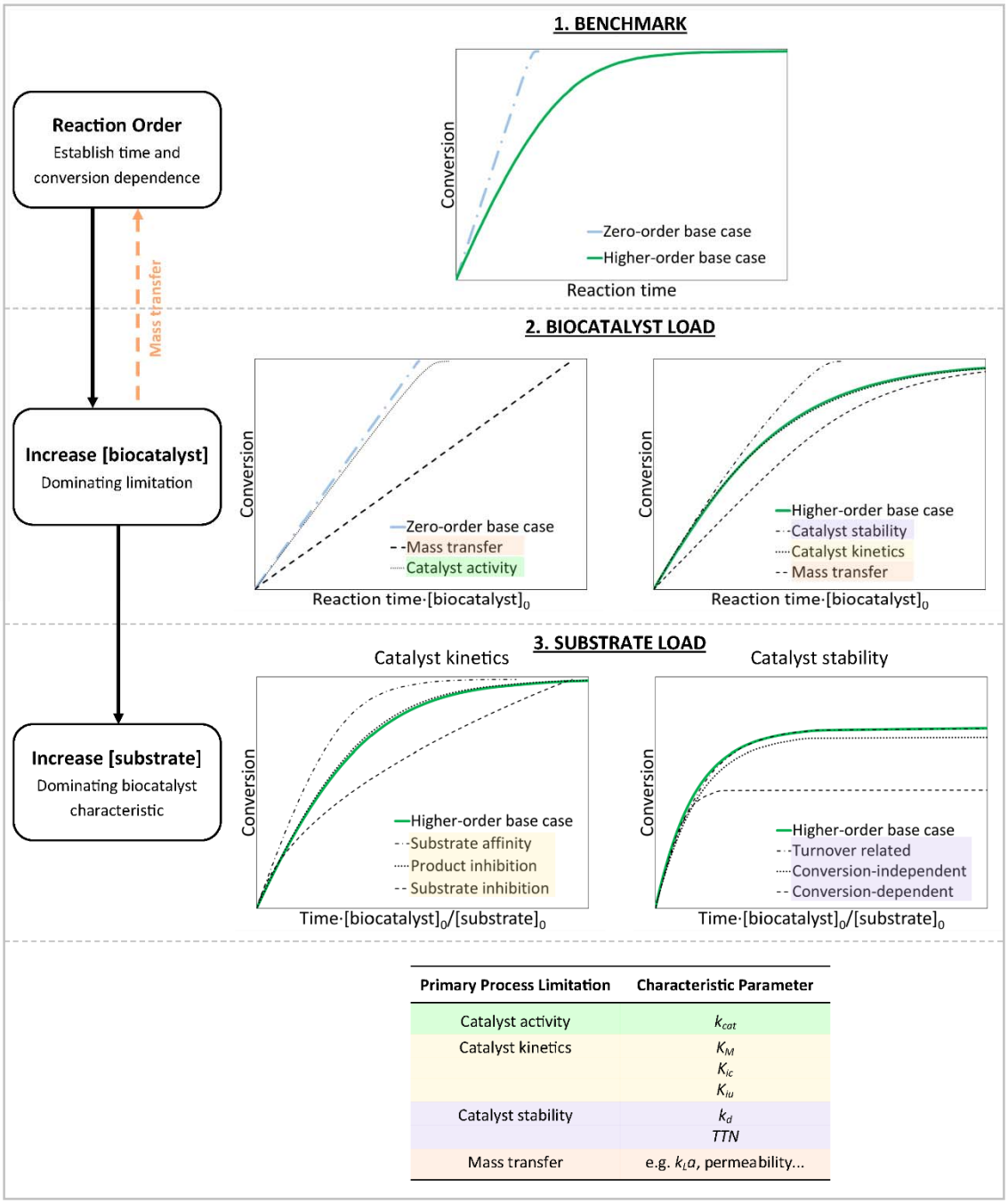

Primary Process Limitation	Characteristic Parameter
Catalyst activity	k_{cat}
Catalyst kinetics	K_M K_{ic} K_{iu}
Catalyst stability	k_d *TTN*
Mass transfer	e.g. k_La, permeability...

Figure 2.3. Illustration of the methodology to establish process and catalyst limitations. 1. Benchmark experiment to determine reaction order under given conditions; 2. Biocatalyst load experiment to determine process limitations; 3. Substrate load experiment to determine catalyst limitations. Trajectories show an increase in the varied parameter. Catalyst activity limited: k_{cat} - turnover frequency; Kinetically limited: K_M – Michaelis constant, K_{ic} - competitive inhibition constant, K_{iu} - uncompetitive inhibition constant; Enzyme stability limited: k_d - first-order rate constant for inactivation, TTN - total turnover number; Mass transfer limited: k_La - overall volumetric mass transfer coefficient. This figure is from Nordblad et al. (2018).

Glucose Oxidase as a Model System

Glucose Oxidase (GOx E.C. 1.1.3.4) catalyses the oxidation of glucose to glucono-lactone, which (at neutral pH) spontaneously forms gluconic acid and the byproduct hydrogen peroxide (Figure 2.4). Oxygen is required to perform the reaction and half the stoichiometric requirement is supplied in the form of molecular oxygen by bubbling air into the bioreactor, with the residual being supplied by decomposing hydrogen peroxide using added catalase. This enzyme is mostly used in the food industry as an additive with preservative purposes, or for glucose sensors and assays (Dubey et al., 2017; Wong et al., 2008).

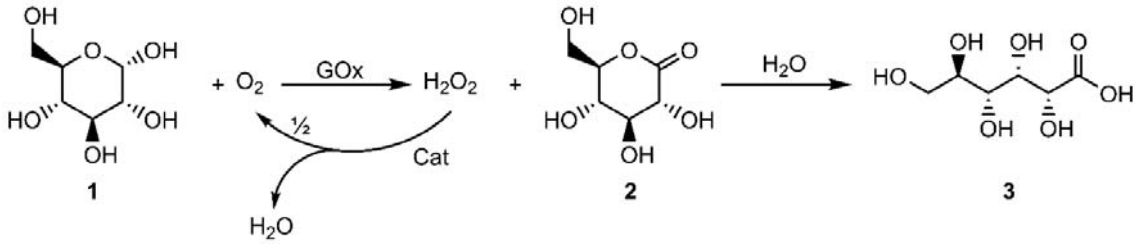

Figure 2.4. Oxidation of glucose (1) to glucono-lactone (2), which instantly hydrolyses to gluconic acid (3), and includes the generation of hydrogen peroxide. The reaction is catalyzed by glucose oxidase (GOx) and the hydrogen peroxide is decomposed to water and oxygen by catalase (Cat).

GOx, as other oxidases, has been shown to follow a ping pong bi bi (substituted) enzyme kinetic mechanism (Gibson et al., 1964). Glucose, the primary substrate to be oxidised, reacts with the oxidised form of the enzyme and then the oxidised substrate, glucono-lactone, is released. Afterwards, the reduced form of the enzyme reacts with oxygen to produce hydrogen peroxide and regenerate the oxidised form of the enzyme. Therefore, the enzyme mechanism can be divided into two parts (1) reductive half-reaction, where the enzyme is reduced by the main substrate and (2) oxidative half-reaction, the part of the redox catalytic cycle where the enzyme is reoxidised. More specifically, in the case of a flavoenzyme oxidase, this step relates to the reoxidation of the reduced flavin by oxygen (Gadda, 2012; Leskovac et al., 2005; Romero et al., 2018).

The enzymatic rate expression for the ping pong bi bi mechanism can be simplified in equation (2.1) (Cornish-Bowden, 2014; Ringborg and Woodley, 2016).

$$\frac{r}{[E]} = \frac{k_{cat}[S][O_2]}{[S][O_2] + K_{MO}[S] + K_{MS}[O_2]} \tag{2.1}$$

The k_{cat} is the maximum specific activity of the enzyme, the K_{MO} and K_{MS} are the Michaelis constants (binding constants) for oxygen and glucose and$[E]$, $[S]$ and $[O_2]$ are the concentrations of enzyme, glucose and oxygen, respectively.

Although GOx is not a particularly interesting biocatalyst from a synthetic chemistry perspective, it is still a very robust oxidase, which makes it useful as a model system to study the process

engineering challenges related to oxygen dependent enzymes. Therefore, the present work used GOx as a model system to identify the major limitations of an oxidation reaction catalysed by an oxidase and implemented the methodology mentioned above to find them. Furthermore, the kinetic parameters of the enzyme were determined using a flow reactor that can be pressurized and therefore test oxygen concentrations in aqueous solution higher than at atmospheric pressure (Ringborg et al., 2017).

2.3. Materials and Methods

Reagents

Glucose oxidase (GOx) from *Aspergillus niger*, was supplied by DuPont Industrial Biosciences (Wageningen, The Netherlands) as a freeze-dried powder with a total protein content of 51.25% (determined by BCA method) and activity of 16.2 U/mg of lyophilized powder (1 Unit (U) decomposes 1 µmol of glucose per minute at pH 7.5, 25 °C, 100 mM glucose). Catalase with ≥3000 U/mg of activity was acquired from Sigma-Aldrich (St. Louis, MO, USA) (1 Unit (U) decomposes 1 µmol of H2O2 per min at pH 7.0, 25 °C, 10 mM H_2O_2). Analytical grade D-glucose and sodium D-gluconate were obtained from Thermo Fisher Scientific (Waltham, MA, USA); potassium dihydrogen phosphate and dipotassium hydrogen phosphate were acquired from VWR (Radnor, PA, USA) and sodium hydroxide from Sigma-Aldrich (St. Louis, MO, USA).

Procedure for Enzyme Kinetics Determination

Spectrophotometric Assay

The quantification of glucose oxidase activity was measured by following a secondary reaction with hydrogen peroxide (H_2O_2). Horseradish peroxidase (HRP) catalyses the reaction between 4-aminoantipyrine (AAP), sodium 3,5-dichloro-2-hydroxybenzenesulfonate (DCHBS) and H_2O_2, which forms a pink product. The formation of this product was measured by an increase in absorbance at 515 nm in a spectrophotometer. The apparent kinetic parameters were estimated using Michaelis Menten kinetics.

Automated Tube-in-tube Reactor (TiTR)

These experiments were performed in a tubular flow reactor developed by Ringborg et al. (2017) where the initial rates were found for different glucose concentrations and different oxygen concentrations. The TiTR was pressurized up to 2 bar to achieve oxygen concentrations above atmospheric pressure. Gluconic acid was measured by UV-Vis detection, as carried out in HPLC. The kinetic parameters were found by fitting all the data points in a kinetic equation that describes reaction with two substrates (equation (2.1)).

Experimental Setup and Procedure for Reaction Trajectory Experiments

Batch reactions were carried out in a stirred tank reactor (MiniBio with my-Control from Applikon Biotechnology (Delft, The Netherlands)). The reactor contained a metal sparger, two Rushton turbines, as well as temperature and pH control. Stirring (500 rpm) and aeration rate (1 volume of air per volume of liquid per minute (vvm)) were kept constant. Experiments were performed under the following conditions: operating temperature of 25 °C, 200 mM phosphate buffer at pH 7.5, working volume of 150 mL, and catalase concentration of 5 mg/L (15 860 U/L) to ensure total H_2O_2 conversion. Glucose concentrations were varied from 10, 20, and 200 mM, and GOx concentrations of 10, 20, 50, and 100 mg/L (mg of lyophilized powder with an activity of 18 U mg^{-1} of powder). Reactions were carried out until complete oxidation of glucose was achieved, followed by measuring dissolved oxygen in the liquid phase using a Fiber-Optic Oxygen Sensor Probe from PyroScience (GmbH, Aachen, Germany). Samples of 1 mL were taken at regular intervals (which varied between experiments to fit with the added catalytic activity) and were analysed by HPLC.

Glucose and gluconic acid in the samples were analysed by HPLC using the same procedure described by Toftgaard Pedersen et al. (2017).

2.4. Results and Discussion

In order to run time-course experiments to determine the major limitations of an alcohol oxidase reaction system, relevant operational conditions such as substrate and enzyme concentration must be identified. Therefore, a simple and traditional spectrophotometric assay was performed to determine apparent Michaelis-Menten kinetic parameters of GOx. It should be noted that the kinetic parameters determined are apparent since GOx is an oxidase and oxygen (cosubstrate) was tested at a fixed concentration (0.265 mM). By definition, apparent kinetic parameters are the observed kinetic constants in conditions where the enzyme is not fully saturated with a substrate (Cornish-Bowden, 1979). In this particular case, the substrate is oxygen.

The apparent K_{MS} was found to be 7.2 mM and the apparent k_{cat} was 17.9 U mg^{-1} (Figure 2.5 (right)). Results showed no evidence of substrate inhibition. To verify if there were no other limitations running the assay, GOx concentration was varied at a fixed glucose concentration (100 mM). It was observed as a linear increase of the initial rates with the increase of enzyme concentration (Figure 2.5 (left)), which demonstrated that the v_{max} was only dependent on the enzyme concentration under these conditions. It is important to note that the highest enzyme concentration tested was 0.04 mg mL^{-1} so the HRP reaction was not the rate limiting step. In summary, these experiments gave an indication about reaction rates and the substrate concentration required to carry out a reaction which rate is only dependent on the biocatalyst concentration (zero-order kinetics).

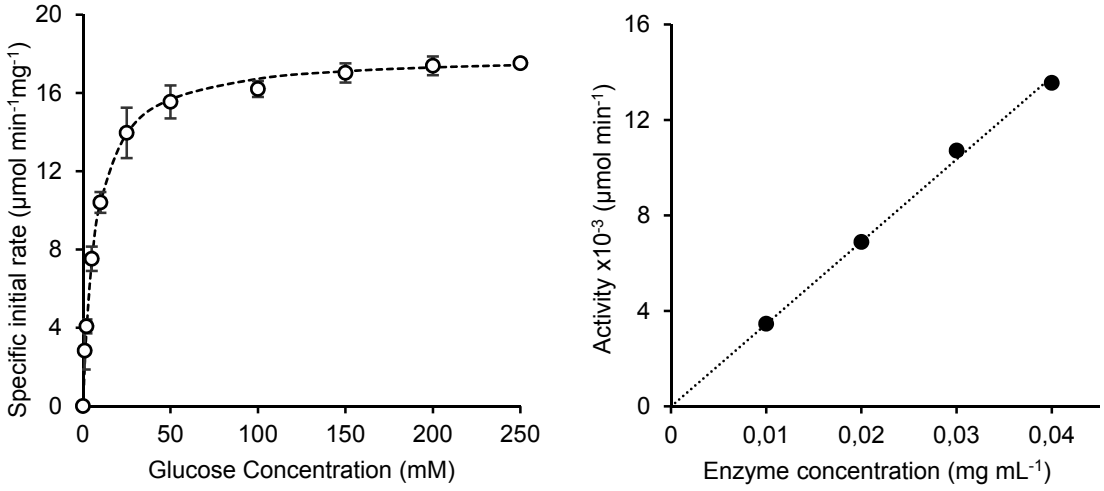

Figure 2.5. (Left) GOx activity as a function of substrate concentration, using the spectrophotometric assay. Michaelis-Menten kinetics is represented by the dotted line. The assay was run at 25 ° C, 1 mL cuvettes, phosphate buffer, pH 7.5 and GOx concentration of 0.02 mg mL^{-1} for 2 min. Experiments performed in triplicate. (Right) Initial rates as a function of GOx concentration using 100 mM of glucose. Experiments were carried out in triplicate.

After identifying the GOx kinetics, the starting operational conditions for a batch reaction of the glucose oxidation using GOx were selected. The substrate concentration was above the determined K_{MS} (10 mM) and the enzyme concentration (10 mg L^{-1}) was chosen so a reasonable reaction time (5 h) was achieved.

The methodology to identify the bottlenecks of the oxidation reaction was used (Nordblad et al., 2018) and an initial reaction trajectory experiment was performed. Results indicated a higher-order kinetics behaviour since the reaction rate changes over time (base case, Figure 2.6). In order to distinguish which type of phenomena is slowing down the reaction, a second experiment with double the biocatalyst load and the same glucose concentration was carried out. Results showed no sign of enzyme inactivation and revealed that the reaction was limited by the kinetics of the enzyme (Figure 2.7). To identify the dominating kinetic limitation under these conditions, the glucose load was increased to 20 mM. The analysis revealed that the reaction was limited by substrate affinity (K_M limitation, Figure 2.8). It turns out that the reaction was carried out at a substrate concentration beneath the Michaelis–Menten constant for glucose, showing a conversion/time-dependent reaction. These results also indicate that the kinetic parameters found were indeed apparent and that the oxygen concentration may have an effect on the enzyme kinetics and consequently on the reaction rate.

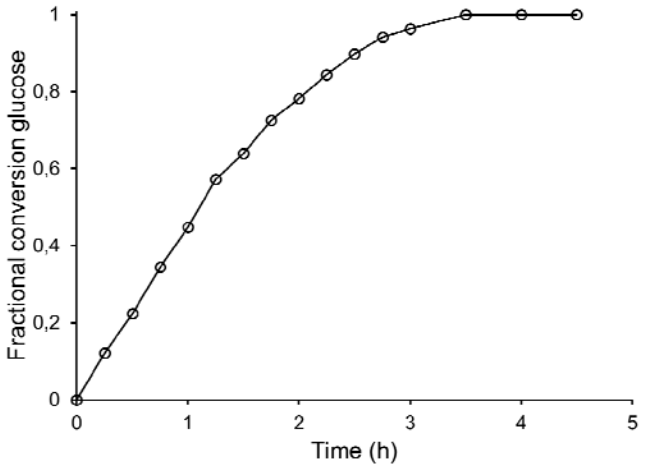

Figure 2.6. Biooxidation of 10 mM of glucose to gluconic acid at 25 °C and pH 7.5 in an aerated stirred tank reactor (500 rpm and 1 vvm of air) with 10 mg L^{-1} of GOx.

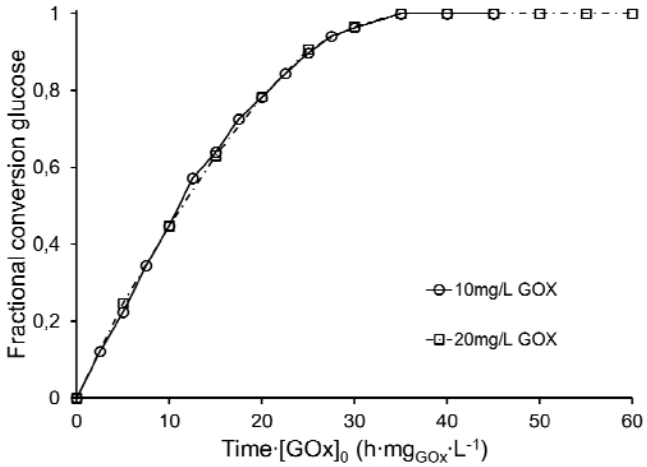

Figure 2.7. Effect of biocatalyst load on the biooxidation of 10 mM of glucose for different GOx concentrations.

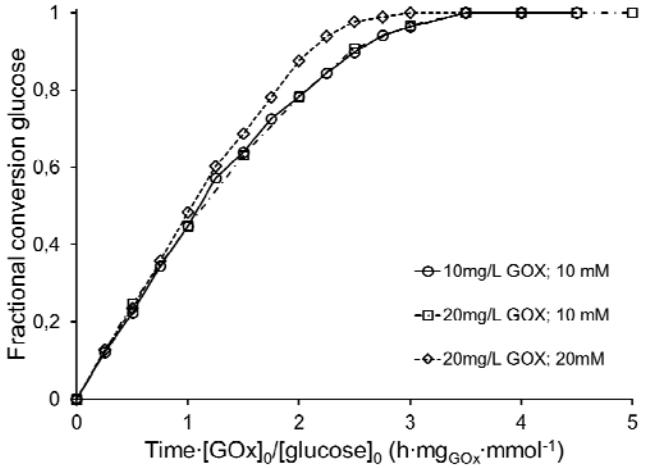

Figure 2.8. Effect of increased substrate load on the biooxidation of glucose.

In order to eliminate kinetic limitations related to substrate affinity (K_{MS}), an experiment with higher glucose concentration (200 mM) was conducted. These results exhibited zero-order reaction behaviour (Figure 2.9) showing a constant rate over the course of the reaction. Following the methodology, the biocatalyst load was increased and an improvement in reaction rate was observed (Figure 2.10). However, the rate enhancement going from 50 to 100 mg L^{-1} of biocatalyst was not proportional, thus indicating mass transfer limitations under these conditions. For this specific reaction, the mass transfer limitation is related to the oxygen supply into the reactor. Under these aeration and agitation rate conditions, it is not possible to increase the oxygen transfer rate from the gas to the liquid phase further. Therefore, to achieve substantially higher reaction rates, it would be necessary to increase the scale (since gas–liquid mass transfer typically improves with scale) (Stocks, 2013), an improvement in the aeration/agitation system, or an increase in the (partial) pressure of oxygen used for aeration, which would increase the driving force for oxygen mass transfer (Garcia-Ochoa and Gomez, 2009). The path taken to investigate the limitations of the GOx reaction system is illustrated in Figure 2.11. The experimental map summarizes the impact of glucose and enzyme concentration on the identified limitations.

To sum up, three major conclusions can be drawn from the applied methodology results: (1) the enzyme kinetics is dependent on enzyme concentration and on oxygen concentration. This is because kinetic limitations were observed when running the reaction with a glucose concentration higher than the apparent K_{MS} (7.2 mM), (2) when the glucose concentration was increased, the reaction rate was limited by the oxygen transfer rate (OTR), which indicated that the OTR has to be improved in order to achieve higher productivities, (3) more experiments should be carried out to investigate the influence of oxygen on the enzyme kinetics, which could give a better understanding of this oxidase and its reaction system.

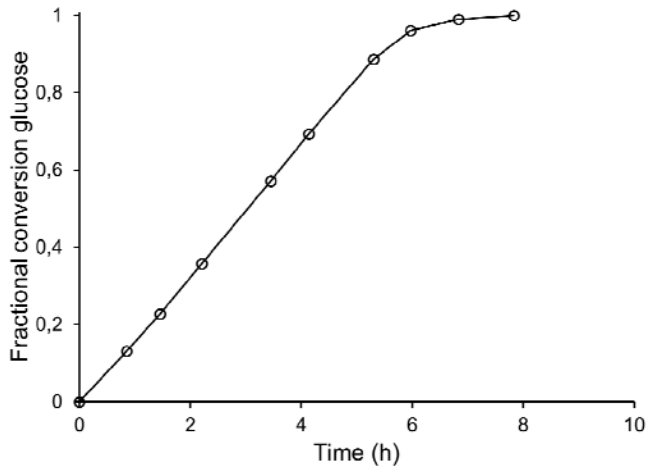

Figure 2.9. Biooxidation of 200 mM of glucose to gluconic acid at 25 °C and pH 7.5 in an aerated stirred tank reactor (500 rpm and 1 vvm of air) with 50 mg L^{-1} of GOx.

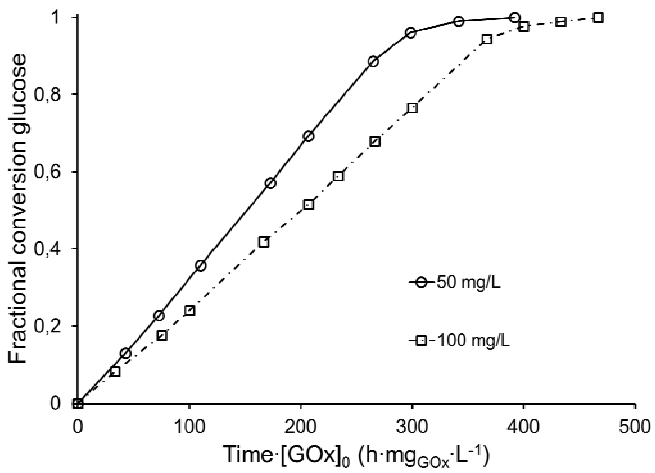

Figure 2.10. Effect of biocatalyst load on 200mM of glucose conversion for two GOx concentrations.

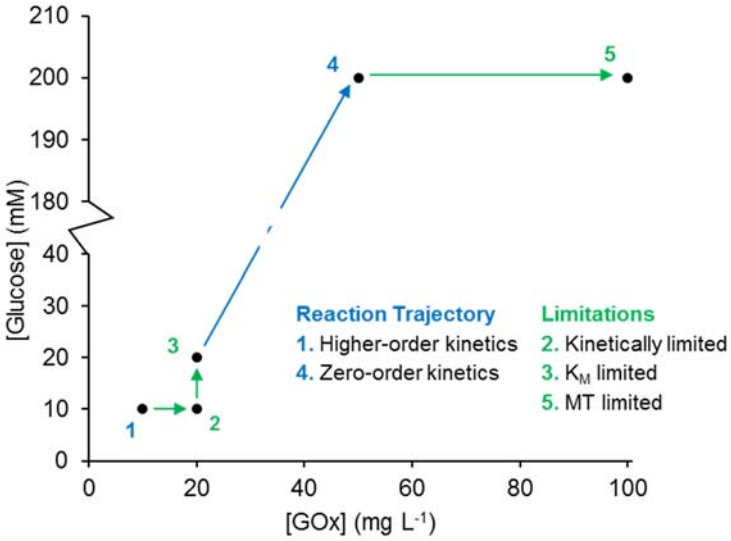

Figure 2.11. Experimental map of GOx illustrating the limitations of the reaction system. MT = mass transfer, which is related to oxygen transfer.

Consequently, a recently developed apparatus by Ringborg et al. (2017) was used to determine real enzyme kinetics parameters. This reactor can be pressurized, which allowed the study of the effect of different oxygen concentrations, greater than the atmospheric pressure, on the initial reaction rates (Figure 2.12). The results obtained in the TiTR are summarized in Table 2.1 together with the results obtained by the spectrophotometric assay. With the calculated parameters from the TiTR data, the K_{MS} apparent was estimated and compared with the value obtained in the spectrophotometer assay. The results are very similar, confirming the veracity of the data collected in the TiTR.

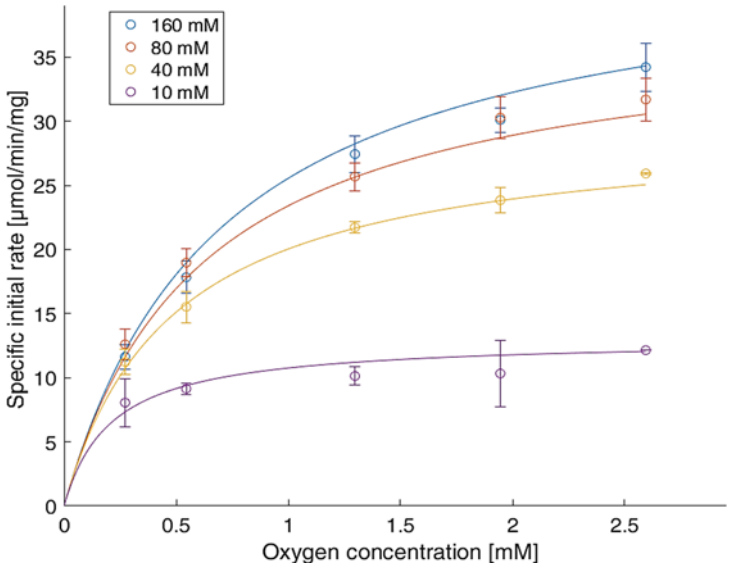

Figure 2.12. Enzyme activity as a function of oxygen concentration for GOx, obtained in the Tube-in-Tube reactor (25 °C and up to 2 bar). The reaction was performed in triplicate for all concentrations. Error bars reflect standard deviation.

Table 2.1. Kinetic parameters of GOx. Spec. assay = spectrophotometric assay and TiTR = tube-in-tube reactor.

	k_{cat} (µmol min^{-1} mg^{-1})	$K_{MS\ apparent}$ (mM)	K_{MS} (mM)	K_{MO} (mM)
Spec. Assay	17.9 [*1]	7.21	-	-
TiTR	51.90±4.72	7.13 [*2]	29.80 ± 6.38	0.843 ± 0.165

*1 These are apparent k_{cat} values estimated based on lower concentration of oxygen (0.27 mM).
*2 These values were estimated based on the K_{MS} obtained in the TiTR by the following equation: $K_{MS\ apparent} = K_{MS} / (1 + (K_{MO}/p_{O2}))$. Parameters estimated in the TiTR were fitted using equation (2.1)

For instance, looking into Figure 2.12, it can be seen that the enzyme activity is strongly dependent on the oxygen concentration. The reaction rate is faster with an increase of oxygen concentration in the aqueous phase. According to the K_{MO} found in the TiTR, the enzyme kinetics are oxygen limited when the reaction is carried out using air at atmospheric pressure as the K_{MO} is higher than the solubility of oxygen in water (1 atmosphere and 25 °C, 0.265 mM). Therefore, the kinetic constants estimated using the spectrophotometric assay results are limited by the oxygen concentration under atmospheric conditions.

Essentially, the results showed that the observed kinetic parameters of GOx are strongly dependent on oxygen concentration. Indeed, when GOx is used in an aerated reactor at atmospheric pressure, the enzyme efficiency is limited. In order for this enzyme to work at a higher efficiency, reactions must be carried out at concentrations above the K_{MO} and K_{MS} so the reaction rate is only dependent on the enzyme concentration (i.e. zero-order kinetics). Therefore, collecting full enzyme kinetic data for oxygen-dependent enzymes is essential to evaluate the biocatalyst efficiency. Overall, true kinetic parameters are key inputs for process development, particularly when using oxidases as the main limitation may be related to oxygen. Based on the

outcome of the methodology experiments and on the kinetic parameters of GOx, a regime map indicating the limitations zones was obtained. This reaction system is limited by oxygen transfer for GOx concentrations above 130 mg L^{-1}, approximately, as showed in Figure 2.13 . This limitation is strongly related with the scale at which the experiments were performed therefore, as mentioned before, it can be overcome by scaling up the system. Furthermore, the system can be kinetically limited if the glucose concentration is below the K_{MS} (30 mM). In that case, the reaction will be slower, resulting on a lower slope for the oxygen consumption rate.

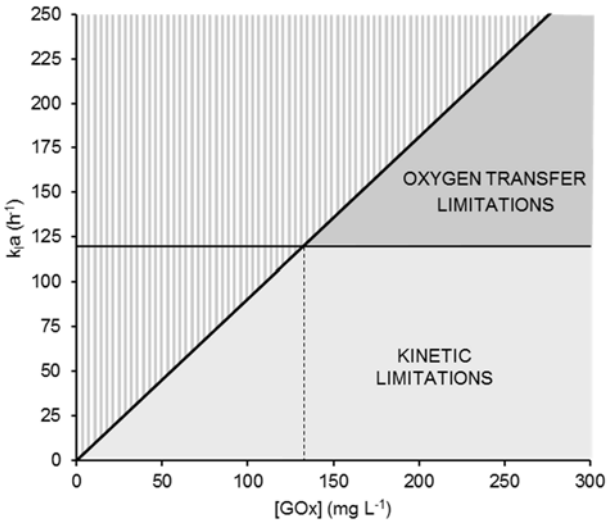

Figure 2.13. Regime map illustrating the process limitations of GOx-catalysed oxidation. The oxygen consumption rate was determined from the reaction rate and its stoichiometry. The k_La for the laboratory reactor was estimated based on the maximum reaction rate obtained, when the rate did not increase with the increase of GOx concentration (120 h^{-1}).

2.5. Conclusions

The methodology developed by Nordblad et al. (2018) to determine the performance of a biocatalyst was successfully tested using glucose oxidase as a model system. The study demonstrates that with the proposed methodical strategy and graphical analysis of the results, it is possible to identify the main process limitations. This methodology therefore allows users to design a regime map of the major limitations of the system, as a function of substrate concentration and biocatalyst load. It should be emphasized that the starting conditions are not important to a successful outcome of the methodology, what matters is the systematic experimental approach. The results from GOx experiments showed that the main process limitations were related to the enzyme kinetics and to the oxygen transfer rate. Based on this analysis and on the experimental map obtained for GOx, a conceptual regime map of process limitations for oxygen dependent biocatalysts is proposed (Figure 2.14). To obtain quantitative boundaries for kinetic limitations, the real kinetic parameters must be determined. Regarding oxygen transfer limitations, these are defined by the equipment and scale at which the experiments are carried out. In the end, the product value determines the process operational conditions. The biocatalyst load is defined based on its process cost margin and productivity, the required oxygen transfer rate on the productivity and finally, the substrate concentration is naturally based on the product concentration demand.

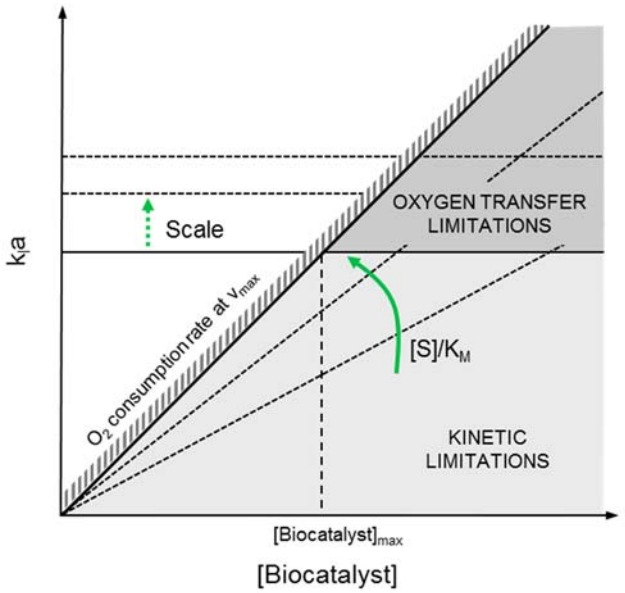

Figure 2.14. Conceptual regime map for oxygen dependent biocatalysts. [S] corresponds to the concertation of both oxygen and main substrate, as well as the K_M. Above the oxygen consumption rate at v_{max} is not possible to operate.

Chapter 3.

Stability Mapping Experiments

This chapter is intended for later publication. The image analysis methods presented here were developed in collaboration with Rayisa Moiseyenko, Andreas Baum and Thomas Jørgensen from the Department of Applied Mathematics and Computer Science, Technical University of Denmark.

3.1. Abstract

The enzymatic oxidation of alcohols for the production of their corresponding carbonyl compounds is of great interest in the synthesis of fine chemicals. Alcohol dehydrogenases are frequently used to catalyse such reactions due to their high catalytic specificities and selectivities. However, dehydrogenases are cofactor dependent oxidoreductases, meaning they require stoichiometric amounts of $NAD(P)^+$ as an electron acceptor, which is expensive and chemically unstable. Thus, strategies for efficient cofactor regeneration are essential for large scale application of these enzymes. An effective means of regenerating $NAD(P)^+$ is through the use of NAD(P)H oxidases that require molecular oxygen as a co-substrate. In large scale biocatalytic processes, agitation and aeration are necessary for sufficient oxygen transfer into the liquid phase, both of which have been shown to significantly increase the rate of enzyme deactivation. As such, the aim of this study was to identify the existence of a correlation between enzyme stability and gas-liquid interfacial area inside a bioreactor. This was done by measuring the kinetic stability of NAD(P)H oxidase after incubation at various power inputs per volume and gas phase compositions in an aerated stirred tank reactor. It was found that enzyme deactivation was proportional to the increase of interfacial area up to a certain limit, where the power input per volume appeared to have a higher impact. Furthermore, the presence of oxygen increased the NAD(P)H oxidase deactivation rate at low interfacial areas. Finally, a correlation between the enzyme half-life and specific interfacial area (a) was obtained and the areas achieved were found in the range of those in large scale bioreactors. Therefore, we conclude that the method developed in this contribution

can be used to help predict the behaviour of biocatalysts stability under industrial relevant conditions concerning gas-liquid interfacial areas.

3.2. Introduction and Motivation

Oxidoreductases (EC 1) are enzymes that catalyse oxidation and reduction reactions. As biocatalysts, these enzymes have attracted significant interest for industrial application in the synthesis of chemicals not only for pharmaceuticals but also for the production of lower value chemicals (Dong et al., 2018; Martínez et al., 2017; J.M. Woodley, 2017). Since these enzymes are cofactor-dependent and cofactors have a high cost and are required in stoichiometric amounts, there is a need to regenerate them. Therefore, cofactor regeneration systems are essential to lower the cost of such reactions and drive them to completion by shifting the equilibrium towards the product of interest (Truppo, 2012).

Alcohol dehydrogenases (ADHs) are oxidoreductases enzymes (EC 1.1.1.1) that can catalyse the oxidation of alcohols to ketones (or aldehydes), which are important building blocks for the production of many important chemicals (Liu et al., 2018). The NAD(P)$^+$ cofactor is necessary as an electron acceptor (Figure 3.1). As mentioned before, a cofactor regeneration system is required for practical application of these enzymes and there are several regeneration strategies that can be used (Brummund et al., 2015; Ferrandi et al., 2014; Hummel and Gröger, 2014). One of particular interest is the use of NAD(P)H oxidases (NOXs) (Kroutil et al., 2004; Rehn et al., 2016). NOXs have the great benefit of using molecular oxygen as an electron acceptor, which is inexpensive and abundant. Additionally, it favours the oxidative direction of the ADH reaction since the cofactor system is thermodynamically favourable due to the presence of molecular oxygen (Figure 3.1).

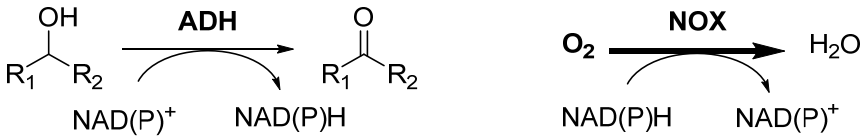

Figure 3.1. Oxidation of primary or secondary alcohols to ketones or aldehydes catalysed by an ADH. NOX system for nicotinamide cofactor regeneration.

When NOX is used for cofactor regeneration in industrially relevant ADH catalysed oxidations, oxygen needs to be supplied at high rates to achieve the target productivities (Sheldon and Woodley, 2018; Tufvesson et al., 2011; J.M. Woodley, 2017). For example, for a medium value product, a productivity of 10 g L^{-1} h^{-1} is required thus, to produce a molecule with a molecular weight of 100 g mol^{-1}, an oxygen transfer rate of 100 mmol L^{-1} h^{-1} is necessary (for a stoichiometry of 1 mol of oxygen per mol of product). However, the presence of a head space in a reaction vessel is not enough to achieve such rate. As a result, aeration and stirring are essential to achieve high oxygen

transfer rates (Law et al., 2006). Generally, oxygen is supplied by sparging air bubbles into the liquid and stirring is used to break the bubbles, increase dispersion and consequently create high gas-liquid interfacial area. In this environment, the biocatalyst is inevitably exposed to a gas-liquid interface. Some enzymes are known to deactivate in the presence of such interfaces (Bhagia et al., 2018; Bommarius and Karau, 2005; Mohanty et al., 2001; Perriman et al., 2007; Van Hecke et al., 2011). However, the correlation between protein stability and gas-liquid interfacial area is not well understood. It should be noted that a protein in solution exposed to gas bubbles in a turbulent flow inside a bioreactor is very different from a quiescent liquid enzyme solution exposed to a gas-surface. Therefore, to study the deactivation of an enzyme in a tube with an open lid is not sufficient to understand the effect of real process conditions on the biocatalyst. Thus, enzymes have to be exposed to conditions in the laboratory similar to the ones at industrial scale.

The method developed here uses an endoscopic probe connected to a high speed camera to measure the size of bubbles inside the reactor. This technique has been applied before to study the influence of different process conditions, such as agitation speed and gas flow rate, on bubble size distributions. (Junker et al., 2007; Raimundo et al., 2016). In the present work, we go a step further and an image processing algorithm was used for quantifying the interfacial area at different oxygen supply conditions, which was subsequently correlated with the deactivation of the biocatalyst. NOX was selected for investigation not only because of its industrial relevance but specifically because it is an oxidase. This is particularly interesting since oxygen is required for the reaction to take place but at the same time it can have a negative effect on the enzyme stability. The aim of this contribution is to better understand the correlation of enzyme stability and gas-liquid interfacial area, under industrial process conditions. So the present work investigates the deactivation of a water-forming NOX from *Streptococus mutans* (Petschacher et al., 2014) under different power inputs per volume (P/V). Additionally, air and nitrogen were sparged to study the influence of the presence of oxygen in the deactivation of the enzyme.

3.3. Experimental Section

Materials

A water forming NAD(P)H oxidase (NOX) from *Streptococcus mutans* (Petschacher et al., 2014) was kindly supplied by InnoSyn (Geleen, The Netherlands) as a cell free extract (CFE) formulation. Potassium dihydrogen phosphate and dipotassium hydrogen phosphate, purchased from VWR (Radnor, PA, USA), were used to prepare potassium phosphate buffer. NADPH tetrasodium salt (β-nicotinamide-adenine dinucleotide phosphate, reduced) was acquired from VWR (Radnor, PA, USA). NOX activity was in average 850 U/mL_{CFE}. One unit corresponds to 1 µmol of NADPH consumed per minute.

Bioreactor and Optical Method Setup

NOX was incubated in a stirred tank reactor, with a total volume of 250 mL, designed and built in-house. The bioreactor contained two Rushton turbines, two baffles and a metal sparger. The optical probe for visualising bubbles inside the reactor (Figure 3.2) consisted of a high speed camera, an endoscope and a light source.

The camera was a monochrome Phantom Miro C110 (Vision Research, Wayne, NJ, USA) that could capture videos of 800 fps (frames per second) at a resolution of 1289 x 1024 pixels. It was connected to a computer through an Ethernet cable to collect and store the video data. It was attached to the endoscope by a C-mount lens adaptor. The endoscope was a 10 mm high definition (HD) laparoscope from Olympus (Tokyo, Japan). It was positioned on the side of the first impeller so the bubbles were dragged horizontally in that region, avoiding attachment to the probe and blocking the optics. In order to illuminate the bioreactor and create a contrast between the gas bubbles and the liquid, a back lighting source (LED matrix from Cree, Durham, NC, USA) was installed inside the vessel. The LED was placed in a custom made stainless steel housing. It could supply 24 Watts and 2200 lumens and was connected to an external power supply that enabled control of the light intensity under different incubation conditions.

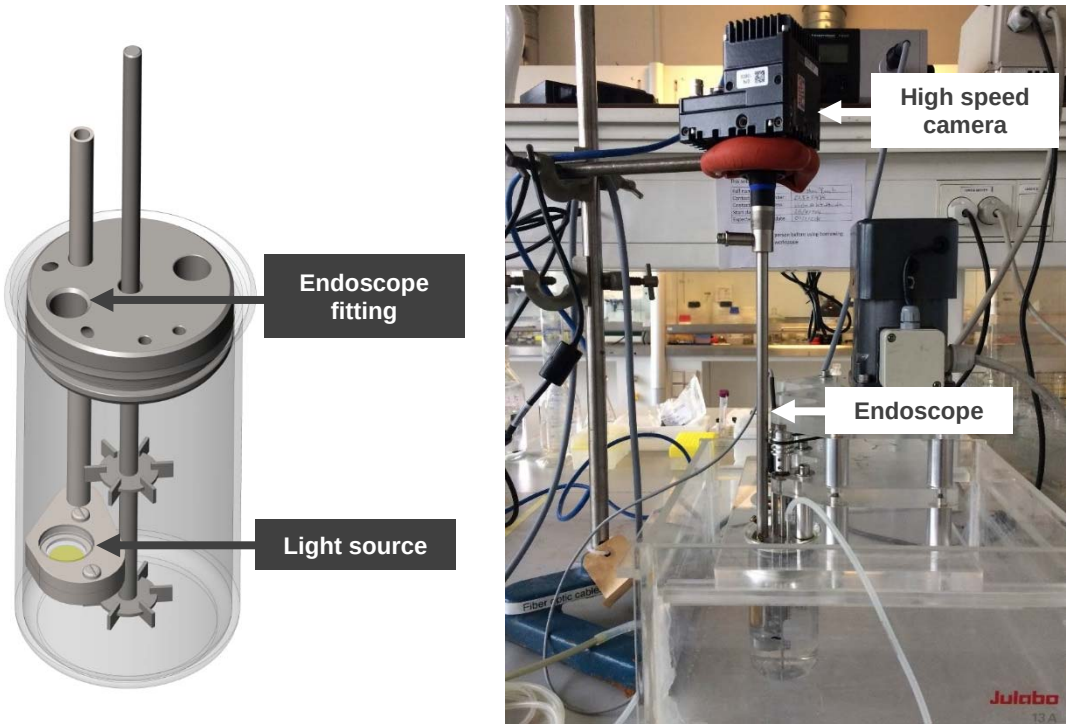

Figure 3.2. Setup of the bioreactor with an optical probe incorporated. (Left) Scheme of the reactor showing the two Rushton turbines and the light source. (Right) Picture of the complete setup highlighting the high speed camera and the endoscope.

Procedure

In order to study the effect of agitation and aeration in the stability of NOX, the power input to the reactor and the composition of the gas phase were varied. Experiments were carried out at power inputs per volume of 0.5, 1, 1.5, 2, 3, 4 and 5 W L^{-1} and with a constant aeration rate of 1 vvm, using both air (21 % oxygen) and nitrogen. The impeller stirring speed was estimated based on defined power inputs per volume, using equation (3.1). All experiments were carried out on aqueous solutions and so the density and viscosity of water at 25 °C were assumed for the calculations.

For all conditions tested, the enzyme was incubated in the reactor, with a working volume of 150 mL, at a concentration of 1 g_{CFE} L^{-1} in 50 mM phosphate buffer at pH 7.5. Incubations were performed at 25 °C and for 6 hours. A control experiment was performed under the same conditions but in a static solution (without stirring and aeration).

The NOX solution was sampled at regular periods of time and stored on ice to stop further enzyme inactivation. Subsequently, the enzyme solution was assayed for residual activity, relative to a sample with no inactivation (time zero), by following the NADPH consumption at 340 nm in a spectrophotometer. Activity was measured at 25 °C using 1 mL cuvettes, 50 mM KPi pH 7.5, 0.20 mM NADPH and 0.05 g_{CFE} L^{-1}. At the same time the protein solution was sampled to measure its activity, a video sample was taken from the reactor in order to measure the area of the corresponding gas-liquid interface. The videos captured a minimum of 800 fps and were stored for data analysis. Then, these were analysed using image analysis algorithms to detect the bubbles' diameter and further generate a bubble size distribution for each reactor condition. The image analysis technique applied in this work is described in the next section. The gas hold-up was determined experimentally by the difference between the liquid level in the reactor with and without aeration and stirring. Measurements were carried out in triplicate. The data flow diagram in Figure 3.3 illustrates the data collection and analysis procedure.

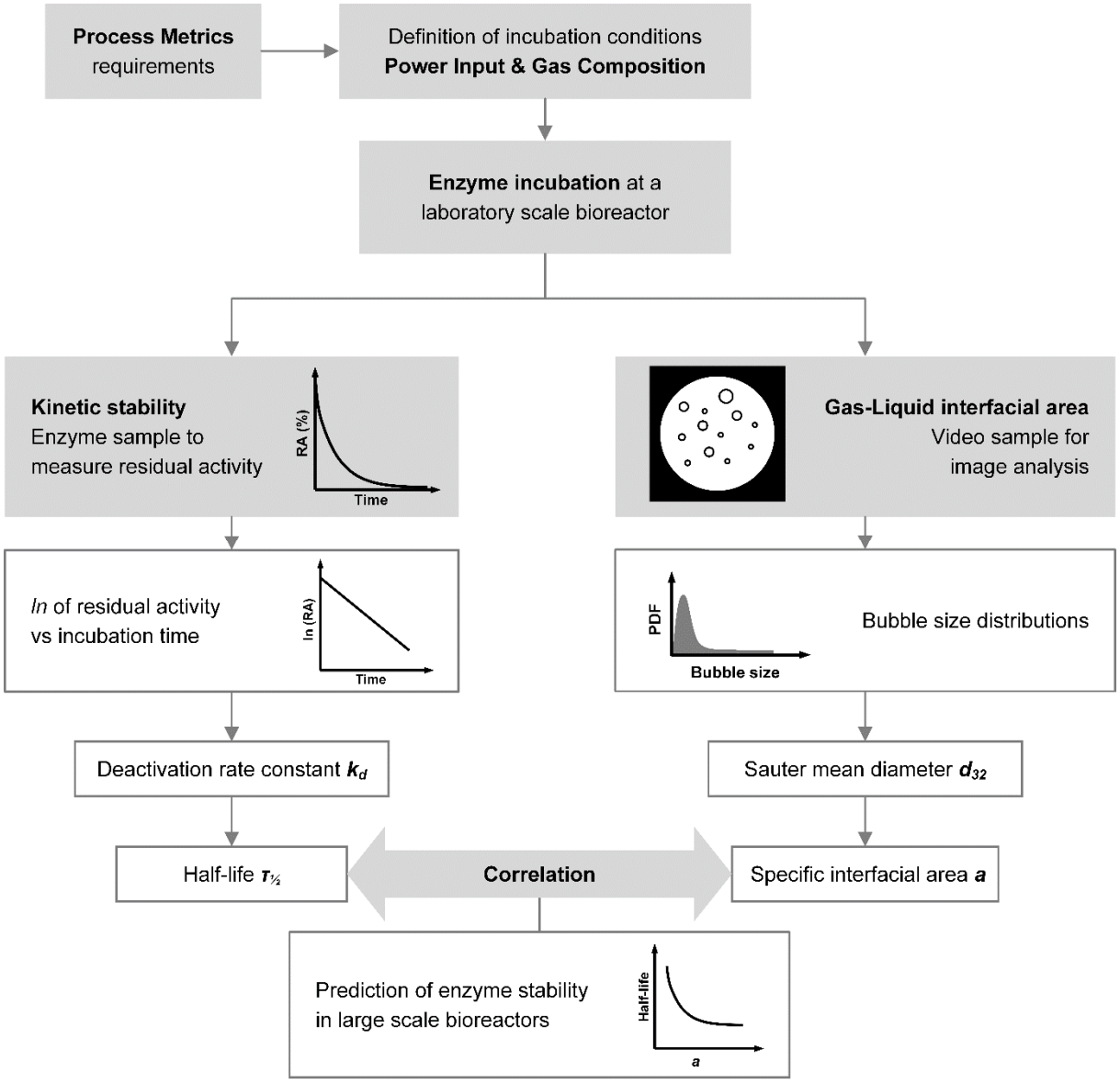

Figure 3.3 Data flow diagram of the methodology developed to determine enzyme stability at specific gas liquid interfacial areas achieved in large scale reactors.

3.4. Image Analysis for Bubble Size Determination

Image processing algorithms were implemented in order to estimate the number of bubbles visible in each video frame. The criterion chosen for counting a bubble is to observe a sufficiently large arc of an ellipse present in the image. From experimentation, we found that requiring 120 degrees of arc in general identified the objects we anticipated as representing bubbles. Successively, the primary axis of the associate elliptic fit was used to estimate the size of a bubble. The essential part of the processing was based on an elliptical arc detector published by Pătrăucean et al. (2012). The size of the image region being input to the image algorithm and the image resolution (scale) automatically determines the image processing parameters according to the so-called Helmholtz

principle (Lowe, 1985). This principle states that an observed geometric structure is perceptually meaningful only if its number of occurrences is very small in a random situation in order to reduce the number of false positive detections.

The elliptic arc detector operates on spatial gradients occurring in the grey scale images. The scale at which the image is represented becomes important because it influences the characteristic of the gradients. Downscaling the image is therefore needed to allow the algorithm to detect the structures of interest (Grompone von Gioi et al., 2012). In our case, the presence of small bubbles (relative to the scale) actually made it necessary to upscale the image (we applied a nearest neighbour filter). The amount of upscaling/downscaling is determined simply from experimentation. In some cases, it can be necessary to apply the elliptic arc detector at a couple of scales if the size of the bubbles vary a lot.

A second problem arises due to an area composed of circular arc segments due to inhomogeneous illumination (darker background in Figure 3.4 (a)). It was of major interest to use as large a detection area as possible to gain optimal detectability of the method and to remove obstructive image features, which would lead to false positive detections. To do so, the constant video background was removed by subtraction of the average video frame (Figure 3.4 (b)). Nevertheless, the algorithm would occasionally detect a double border of the bubbles leading to double detection/counting. This issue was solved by checking whether a detected ellipse contains another ellipse in its interior. In such cases the smaller one was neglected (Figure 3.4 (b)). A minimum of 800 frames was used for the analysis of each video.

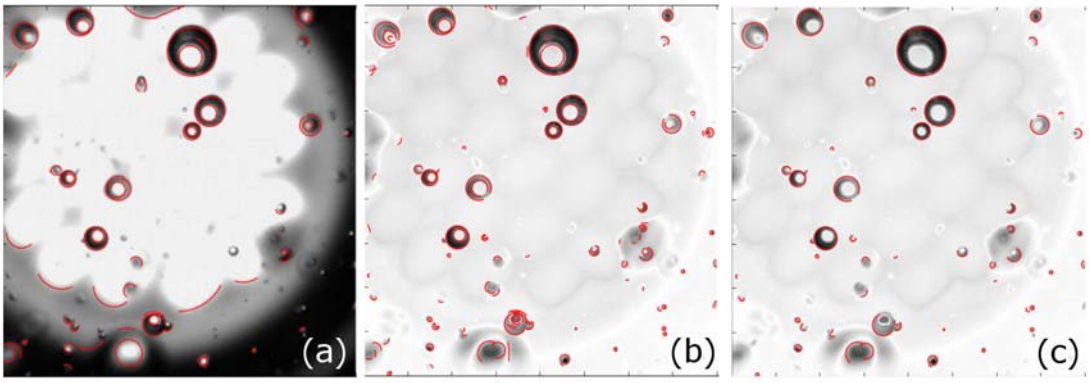

Figure 3.4. A typical frame from the setup under varying stages in the image processing with the red lines indicating detected objects characterized by having an elliptic shape. (a) is the original image, (b) is the image after upscaling to detect small bubbles, and background removal, (c) shows the result of eliminating double detection.

The selected scaling factor and contrast settings were chosen by applying scaling factors from 0.1 to 1, with a step of 0.1 and a contrast factor from 1 to 8, with a stepsize of 1 and manually deciding which parameters gave the best performance from a given number of image frames.

The algorithm was validated using video samples of 1 mm glass beads. This calibration method allowed the conversion of image pixels to physical size and the mode of the number, area and volume distributions was found to be approximately 41 pixels. As a result, it was assumed 41 pixels represent a 1 mm object. Details of the calibration are presented in the Supporting Information in the end of the chapter.

3.5. Results and Discussion

Effect of Aeration and Mixing on NOX Kinetic Stability

First, by comparing the NOX incubation in quiescent solution with the different mixing conditions, it is clearly observed that aeration and stirring have a negative effect on enzyme stability (Figure 3.5 (left)). Secondly, results showed that the residual activity of NOX decreases faster with an increasing power input. Furthermore, to investigate if the presence of oxygen had an influence in the NOX deactivation, the feed gas composition was varied between air (21 % of oxygen) and nitrogen. It was found that NOX was more stable when nitrogen was sparged to the reactor. Nevertheless, to better compare the results among the power inputs and feed gases tested, the deactivation rate constant and enzyme half-life were calculated for all cases. As can be seen in Figure 3.5 (right), it was observed that the deactivation kinetics were close to first-order. Accordingly, first-order deactivation kinetics were assumed and the deactivation rate constant (k_d) was estimated from the slope of the natural logarithm of the residual activity over time (Sadana, 1988). The figures for all investigated conditions are presented in Table 3.1.

When air was supplied, the results from Table 3.1 revealed that the half-life of NOX decreases with the increase of power input. With respect to nitrogen, the same behaviour was observed for the lowest power inputs tested, although, from 2 to 4 WL^{-1}, it appears that the half-life slightly increases. Nevertheless, the values obtained are within experimental variability, so a clear conclusion cannot be drawn for higher mixing conditions when nitrogen was supplied. It can also be seen that NOX is generally more stable with nitrogen, as mentioned before. However, the difference of the enzyme stability between the two gases tends to decrease with an increase in power input. These results indicate that there are several phenomena affecting protein deactivation and that the presence of oxygen is not the only cause. As the power input increases, the gas-liquid interfacial area increases as well and the enzyme is more exposed to the interface, which enhances its inactivation. In order to further understand the reasons of NOX deactivation, the interfacial area in the reactor was measured and correlated with the enzyme half-life.

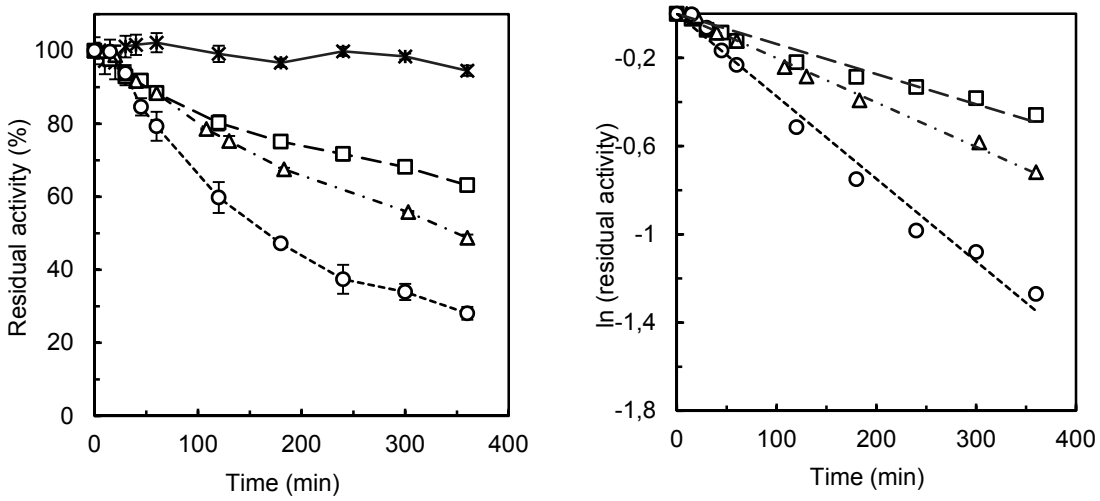

Figure 3.5. (Left) Residual activity of NOX at different P/V conditions: (×) Quiescent solution, (□) 0.5 WL^{-1}, (△) 1 WL^{-1}, (○) 2 WL^{-1}. Activity was measured in triplicate. Error bars reflect standard deviation and may not be visible since it was always below ± 5 %. (Right) First-order kinetic deactivation curve from the data presented in the left graph.

Table 3.1. Deactivation rate constants (k_d) and half-life of NOX at different power inputs per volume sparging air (21 % oxygen) and nitrogen. The relative errors of the deactivation constants for power inputs up to 2 WL^{-1} were below ± 3 % and for power inputs higher than 3 WL^{-1} were below ±8 %.

Power input (WL^{-1})	**Air**		**Nitrogen**	
	k_d (min^{-1})	*Half-life (min)*	k_d (min^{-1})	*Half-life (min)*
0.5	-1.4×10^{-3}	507	-7.8×10^{-4}	711
1	-2.0×10^{-3}	345	-1.6×10^{-3}	430
1.5	-4.0×10^{-3}	176	-	-
2	-3.7×10^{-3}	185	-3.2×10^{-3}	219
3	-	-	-3.0×10^{-3}	233
4	-	-	-2.6×10^{-3}	265
5	-5.8×10^{-3}	121	-	-

Determination of the Gas-Liquid Interfacial Area in the Bioreactor Setup

When air is sparged to a stirred tank reactor, small gas bubbles are created and the biocatalyst is inevitably exposed to gas-liquid interfaces. Preliminary tests were carried out to decide whether the aeration or the stirring had a major effect on changing the interfacial area in the setup. It was found that the stirring speed had a higher impact on changes in gas-liquid interfacial area and these could be detected by the optical probe (Figure 3.6). Therefore, in the experiments performed, different interfacial area conditions were obtained by changing the stirring speed of the impeller. The stirring speed is reported in terms of power input to the reactor (P/V) to compare the results closely with those applied at industrial scale. Thus, the energy inputs used in the experiments were

selected based on the values used in industrial reactors. However, higher power inputs were also tested to better understand the effect of high interfacial areas on protein stability.

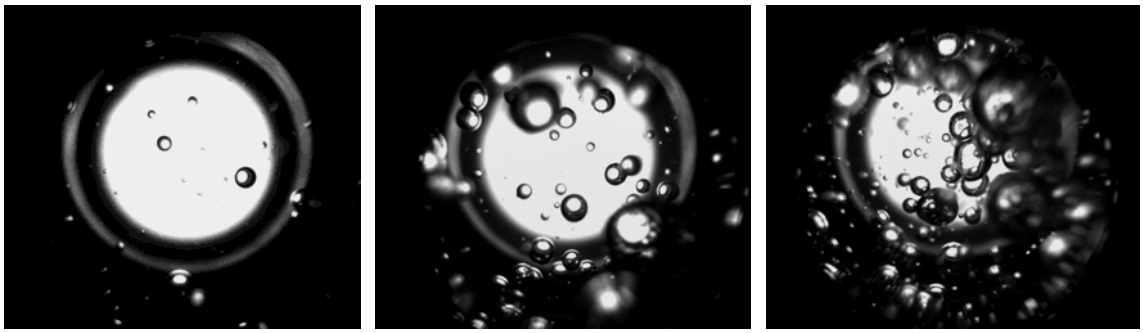

Figure 3.6. Regime of the bubbles inside the reactor at an aeration rate of 1 vvm and different power inputs. (left) 1 WL^{-1}; (centre) 2 WL^{-1} and (right) 5 WL^{-1}.

From the video samples, bubble size distributions for all power inputs tested were obtained using the image analysis technique (Figure 3.7). The video processing algorithm gives vectors that contain the diameter and frequency of the detected bubbles. Then, the number, area and volume distributions are calculated for all conditions tested. Although air and nitrogen were used, no difference was found in the bubble size between these two gases, as it was expected. Furthermore, this analysis was performed assuming spherical bubbles. This assumption was verified within the mixing conditions tested by the videos collected, as observed in Figure 3.4 and Figure 3.6. Thus, the distributions obtained showed the same shape as the ones observed at the same reactor position in the work developed by Laakkonen et al. (2005), which reports bubble size distributions in different zones of an aerated stirred reactor.

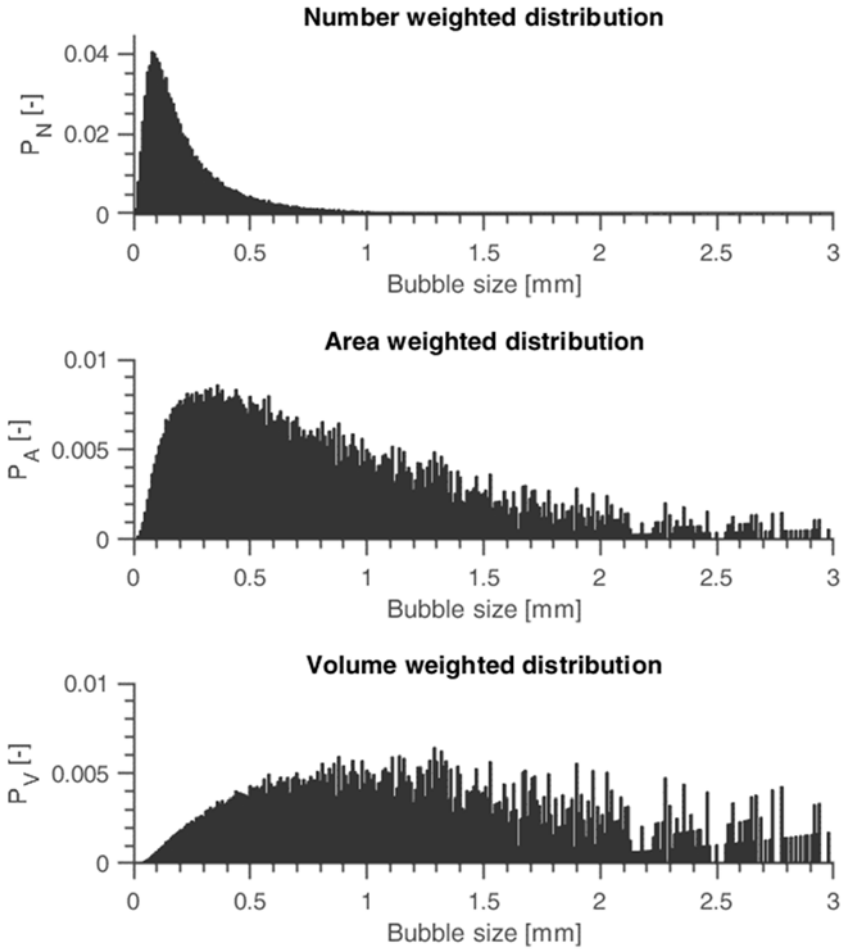

Figure 3.7. Bubbles' size distributions at a power input of 2 WL^{-1} and a gas flow rate of 1 vvm. The distributions were calculated based on number, area and volume probability density functions of the bubbles' diameter (P_N, P_A, and P_V). Distributions were discretized in 60 bins.

With the purpose of estimating the gas-liquid interfacial area for all mixing conditions, the area and volume distributions are extremely important. The distributions take into consideration the large bubbles in the reactor, which contribute more to the interfacial area. It can be seen from the number distribution that small bubbles dominate the reactor. Whereas looking into the area and volume distributions, the mode is increasing. Therefore, the Sauter mean diameter (d_{32}) was used to calculate an average size of the bubbles since it is based on the mean diameter of area and volume distributions. The results obtained are presented in Figure 3.8 and show that the d_{32} does not change significantly with the increase of power input per volume. However, more bubbles are detected in the reactor at higher power inputs, as observed in Figure 3.6. This can be explained by the increase of gas holdup with the increase of power input per volume to the reactor. With higher stirring rates the bubbles were kept longer inside the liquid, increasing the interfacial area available. Therefore, the gas-liquid interfacial area was higher for larger power inputs because the mixing increased the residence time of the bubbles in the reactor, which was measured by the gas holdup. In Figure 3.8, the effect of the power input per volume on these two variables is shown. It should be noticed that the gas hold up and the bubbles' size are dependent on the reactor scale

and geometry therefore, these two variables may behave differently in large scale bioreactors (Bach et al., 2017).

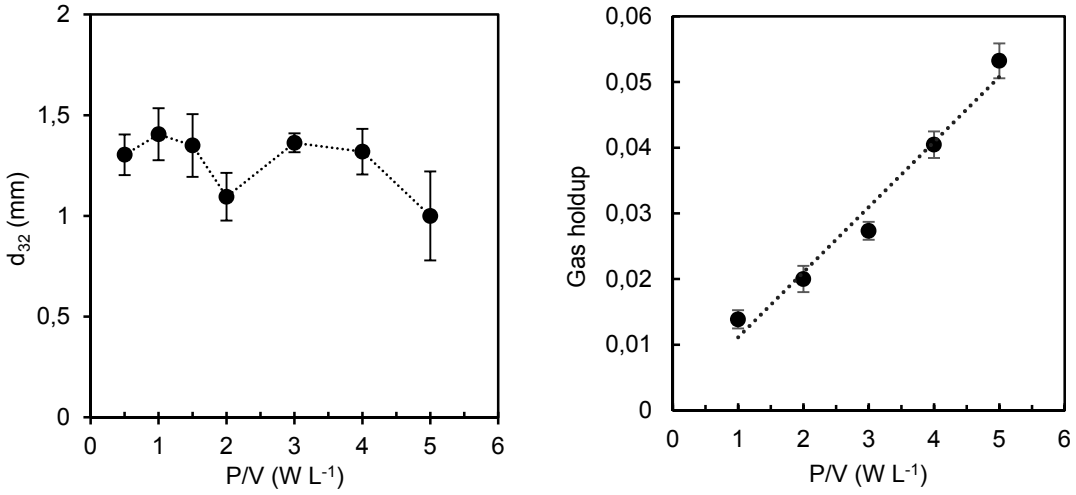

Figure 3.8. Sauter mean diameter, d_{32}, (Left) and gas holdup (Right) at a gas flow rate of 1 vvm for different power inputs per volume (P/V) in a 150 mL reactor. Error bars represent standard deviations of 5 video samples for the d_{32} and 3 measurements for the gas hold up. The line in the gas holdup measurements represents a linear regression with a R^2 of 97 % (gas holdup = 0.0103·P/V).

Finally, the interfacial area was calculated using the Sauter mean diameter (d_{32}) and the gas holdup. This was expressed in terms of specific interfacial area, which is the ratio of the gas-liquid interfacial area and the reactor volume. In Figure 3.9, a correlation was established and it was found that the specific interfacial area (a) increased with the increase of power input. Indeed, these two parameters cannot be separated when the bioreactor is aerated.

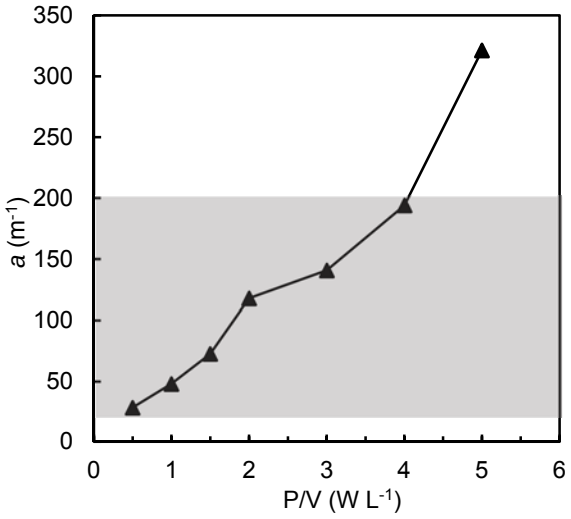

Figure 3.9. Correlation of specific interfacial area (a) and power input per volume to the reactor (P/V). The shaded area represents the range on specific interfacial areas obtained in large scale bioreactors.

Furthermore, comparing the results with mechanical agitated contactors, it was found that the specific interfacial areas achieved in this study were within the range of the ones observed in large scale reactors (20 -200 m^{-1}, from Paul et al. (2004)). This result is very promising since it demonstrates that specific interfacial areas of an industrial aerated stirred reactor can be mimicked at a small-scale. The method developed here allows enzyme incubation much closer to industrially relevant conditions, using smaller enzyme amounts compared to larger scale reactors (e.g. pilot plant scale). Therefore, this gives the possibility of studying protein stability in the presence of gas-liquid interfaces in a turbulent flow regime prior to process scale- up. Based on these findings, we propose a scale-down approach that is illustrated on Figure 3.10.

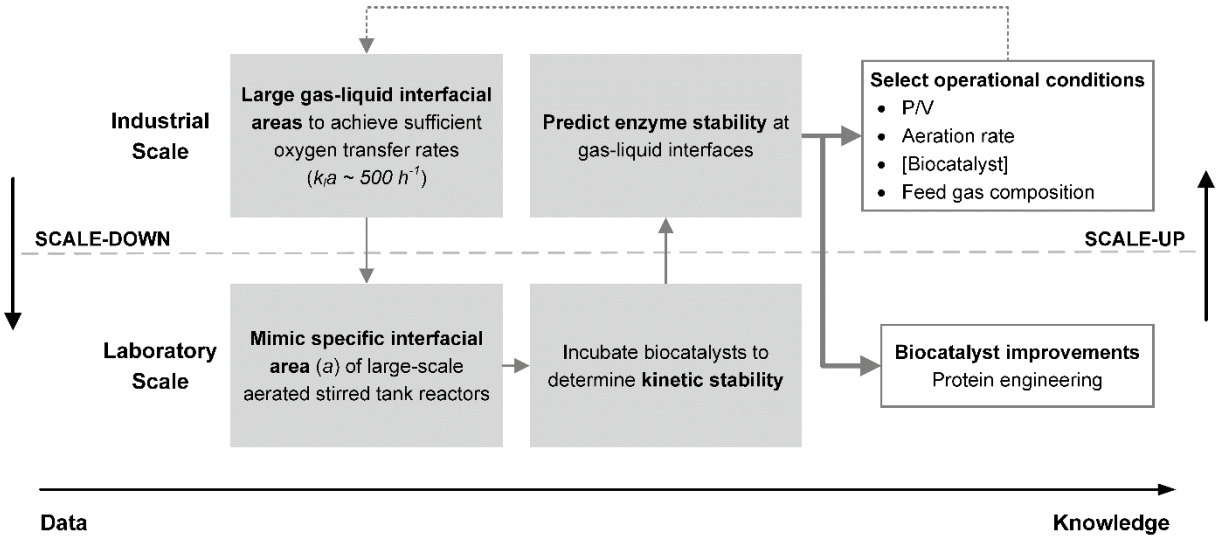

Figure 3.10. Scale-down approach to determine enzyme stability at gas-liquid interfacial areas similar to large scale bioreactors.

Correlation of NOX Stability with Gas-Liquid Interfacial Area

With the purpose of understanding the deactivation of NOX at gas-liquid interfaces, a correlation between the enzyme half-life and the specific interfacial area is presented in Figure 3.11. As expected, results showed that the NOX half-life decreased with the increase of interfacial area. The same behaviour is observed in the presence of both air and nitrogen. Additionally, two distinct regions can be seen in the plot: a regime for above or below a = 75 m^{-1}.

In the regime of low interfacial areas (< 75 m^{-1}), sparging air decreases the enzyme half-life in comparison with supplying nitrogen. This result indicates that the oxygen present in the feed gas may be causing overoxidation of certain amino acid residues in the protein. On the other hand, for higher gas-liquid interfacial areas, the difference in the NOX half-life between the two gases decreases. This observation points to the belief that the presence of oxygen is not the major reason for NOX deactivation but rather the presence of the gas-liquid interface per se.

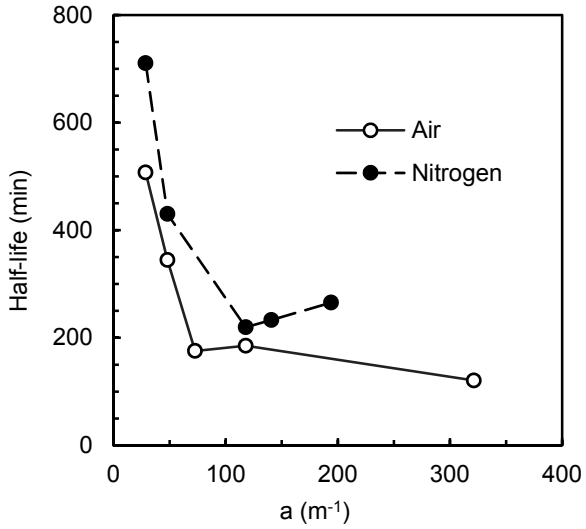

Figure 3.11. Half-life of NOX as function of different specific interfacial area conditions at a gas flow rate of 1 vvm.

Looking more closely into the correlation, for a > 75 m^{-1}, the stability of NOX reaches a plateau, even though the interfacial area is increasing. There is a point at which it appears that the mixing is having more influence in the deactivation comparing with the interfacial area. Indeed, the interfacial area is changed by increasing the stirring speed and in these results the two factors cannot be separated. Thus, in order to further investigate the effect of agitation, an experiment without aeration was run in the same setup at power inputs of 0.5, 1 and 2 WL^{-1} (experimental section described in Chapter 5).

Table 3.2. NOX half-life for a non-aerated and aerated system at 1 vvm. The relative errors of the deactivation constants were below ± 3 %.

Power input (WL^{-1})	**Half-life (min)**		
	No Aeration	**Nitrogen**	**Air**
0.5	760	711	507
1	431	430	345
2	235	219	185

Results presented in Table 3.2 showed that for the lower power input the presence of air reduced the half-life of NOX, which supports the idea that oxygen has an effect on NOX stability. However, for 1 and 2 WL^{-1}, the presence of a gas phase did not change NOX stability significantly. This behavior shows that the presence of gas is not the dominant cause of protein inactivation when the system is being agitated. Therefore, the deactivation of NOX was caused by three distinct parameters: stirring, presence of a gas-liquid interface and the presence of oxygen. In order to understand in which extent each of these parameters are deactivating the enzyme, they need to

be investigated separately. Thus, experiments were performed isolating stirring from aeration and the results are presented in Chapter 5 and 6. Nevertheless, the method developed here allows the study of the influence of these parameters together on the biocatalyst stability, which is extremely relevant to evaluate the deactivation of enzymes under real process conditions.

3.6. Conclusions

In conclusion, we have developed and applied an experimental laboratory method that studies the kinetic stability of enzymes towards gas-liquid interfaces and that mimics specific gas-liquid interfacial areas of industrial bioreactors. The distinct aspect of this method is that it uses an image processing algorithm for *in situ* quantification of the gas-liquid interfacial area in an aerated stirred tank reactor. Therefore, it allows understanding of the kinetic stability of a biocatalyst at an early stage of process development, under industrially relevant operational conditions. The method was tested by investigating the kinetic stability of NAD(P)H oxidase at gas-liquid interfaces and it was found that the deactivation rate of this enzyme increased with an increase in gas-liquid interfacial area. It was also observed that for large gas-liquid interfacial areas, the power input per volume was the dominating cause of deactivation. The phenomena of enzyme deactivation at gas-liquid interfaces is still not fully understood thus, it is necessary to isolate the possible operational conditions that cause protein deactivation (Chapters 4 and 5). Finally, a correlation between NOX half-life and specific gas-liquid interfacial area was successfully obtained under the experimental conditions. This correlation demonstrates that the approach developed here can be applied further to predict kinetic stability of enzymes in the presence of industrially relevant gas-liquid interfacial areas. Furthermore, the knowledge gained can be used to guide protein engineers to improve the biocatalyst.

3.7. Acknowledgements

The research for this work has received funding from the European Union (EU) project ROBOX (grant agreement n° 635734) under EU's Horizon 2020 Programme Research and Innovation actions H2020-LEIT BIO-2014-1. Any statements herein reflect only the author's views. The European Union is not liable for any use that may be made of the information contained herein. The authors acknowledge PhD Christian Bach for his assistance in the development of the optical method and the Matlab code for the bubble size distributions analysis.

3.8. Theory

This section describes principles regarding agitation in an aerated stirred tank reactor, mass transfer of oxygen from the feed gas to the liquid medium and estimation of the gas-liquid interfacial area. Furthermore, probability density functions based on number, area and volume for calculating bubble size distributions are also defined.

Mixing

Mixing is essential in biooxidation processes due to its influence in controlling oxygen transfer rates from the gas to the liquid phase, where the reaction takes place. Stirring is directly related to the gas-liquid interfacial area available in the vessel since it controls the breakup of the bubbles and their residence time in the system. The choice of the impeller is also of great importance in the reactor design because it defines the flow pattern inside the tank. High gas-liquid interfacial areas (small bubble diameters) are required to increase the mass transfer coefficient ($k_l a$). Therefore, a high-shear impeller such as a Rushton turbine was selected. Furthermore, baffles (metal plates positioned on the sides of the vessel) were also used to increase the axial velocity component, which promotes fluid circulation (Paul et al., 2004).

Agitation is usually measured in terms of the power consumption per unit volume of reaction medium and for industrial bioreactors the average ranges from 1 to 2 W/L (ca. 100 m^3 vessels) (Paul et al., 2004; Stocks, 2013). To determine the power input per volume (P/V), the power input (P) to the system can be calculated from equation (3.1).

$$P = N_p \cdot \bar{\rho} \cdot N^3 \cdot D^5 \tag{3.1}$$

P is function of the impeller power number (N_p), average density of the medium ($\bar{\rho}$), impeller rotational speed (N) and impeller diameter (D). N_p depends on the impeller type and its Reynolds number (equation (3.2)). For the Rushton turbine used, the impeller number was assumed 5 from the graphic presented by Paul et al. (2004) (D = 0.025 m and Re > 10^3).

$$Re = \frac{\bar{\rho} \cdot N \cdot D^2}{\mu} \tag{3.2}$$

Gas-Liquid Interfacial Area

According to the two-film theory, the transport of oxygen from gas to liquid phase is dependent on the diffusion coefficient through the liquid film, the concentration gradient of oxygen and the interfacial area available (Whitman, 1962). This theory assumes that the gradient of the gas side is insignificant. The oxygen transfer to the liquid can be described by equation (3.3), where the mass

transfer coefficient (k_l) and the specific surface area (a) are treated as one overall volumetric mass transfer coefficient known as the k_la.

$$OTR = k_l a \cdot ([O_2]^* - [O_2]) \tag{3.3}$$

In order to obtain high oxygen transfer rates, a high k_la is necessary, which is dependent on the available transfer area per volume of liquid. In other words, a large gas-liquid interfacial area increases the k_la. The present work aims to estimate this interfacial area and, for that, the following definition was used.

$$a = \frac{A}{V_l} = \frac{6 \cdot \varepsilon}{(1-\varepsilon) \cdot d_{32}} \tag{3.4}$$

The specific interfacial area (a) is the ratio of the total interfacial area in a gas liquid dispersion (A) and the liquid volume (V_l). It is dependent on the gas hold-up (ε) and on the average bubble diameter that is commonly expressed by the Sauter mean diameter (d_{32}) (Bach et al., 2017; Garcia-Ochoa and Gomez, 2004). The gas hold-up is the ratio of the volume of gas and the total volume of the gas-liquid dispersion. The Sauter mean diameter is the mean diameter based on the average of gas-liquid surface and is presented in equation (3.5). This can be estimated based on bubble size distributions in the reactor.

$$d_{32} = \frac{\sum N_i d_{B,i}^3}{\sum N_i d_{B,i}^2} \tag{3.5}$$

The gas hold-up and the average bubble size diameter were experimentally determined in this contribution.

Bubble Size Distributions

In order to estimate the Sauter mean diameter, size histograms of the bubbles, detected by the video analysis, were calculated. The observed diameters of the gas bubbles were divided into a series of intervals with the same size termed bins (i). The probability density function for the bubbles diameter based on the number of detected bubbles is given by equation (3.6),

$$P_N\left(\bar{d}_{B_j}\right) = \frac{N_i}{\sum_i N_i} \tag{3.6}$$

The $\bar{d}_{B_j}$ is the average size of a bubble and N is the number of bubbles in a bin. By definition, the sum of all probabilities must be equal to one (equation (3.7)).

$$\sum_i P_N(\bar{d}_j) = 1 \tag{3.7}$$

As it is intended to estimate the gas-liquid surface area, it is important to evaluate the impact of the area and volume distributions on the bubbles' diameter estimation. The probability density functions based on the surface area and volume of the bubbles are given by equations (3.8) and (3.9).

$$P_A\left(\bar{d}_{B_j}\right) = \frac{N_i \cdot \bar{d}_{B_j}{}^2}{\sum(N_i \cdot \bar{d}_{B_j}{}^2)} \tag{3.8}$$

$$P_V\left(\bar{d}_{B_j}\right) = \frac{N_i \cdot \bar{d}_{B_j}{}^3}{\sum(N_i \cdot \bar{d}_{B_j}{}^3)} \tag{3.9}$$

3.9. Supplementary Information

Optical Method Calibration

In order to convert the image pixels to a physical size, a calibration using glass beads with a defined diameter in a controlled environment was used (Junker et al., 2007). The glass beads had a diameter of 1 mm and were purchased from VWR (Radnor,PA,USA). These beads were placed in a 250 mL bioreactor with a working volume of 150 mL of water. A power input per volume of 2 W L^{-1} was applied and the size distributions obtained are presented in Figure 3.12. Several gas bubbles were entrapped in the liquid due to the agitation and consequently they were detected in the calibration.

The gas bubbles entrapped in the reactor dominate the number size distribution. However, when the area and volume distributions are calculated, it is clear that the peak around 40 pixels corresponds to the glass beads. The mode of the peaks represent the average size of the detected beads. This was found to be 40.7, 41.3 and 42.0 for the number, area and volume distributions, respectively. Therefore, an average of 41 pixels was assumed correspond to 1 mm and this was used throughout the analysis of all collected video data presented in this chapter.

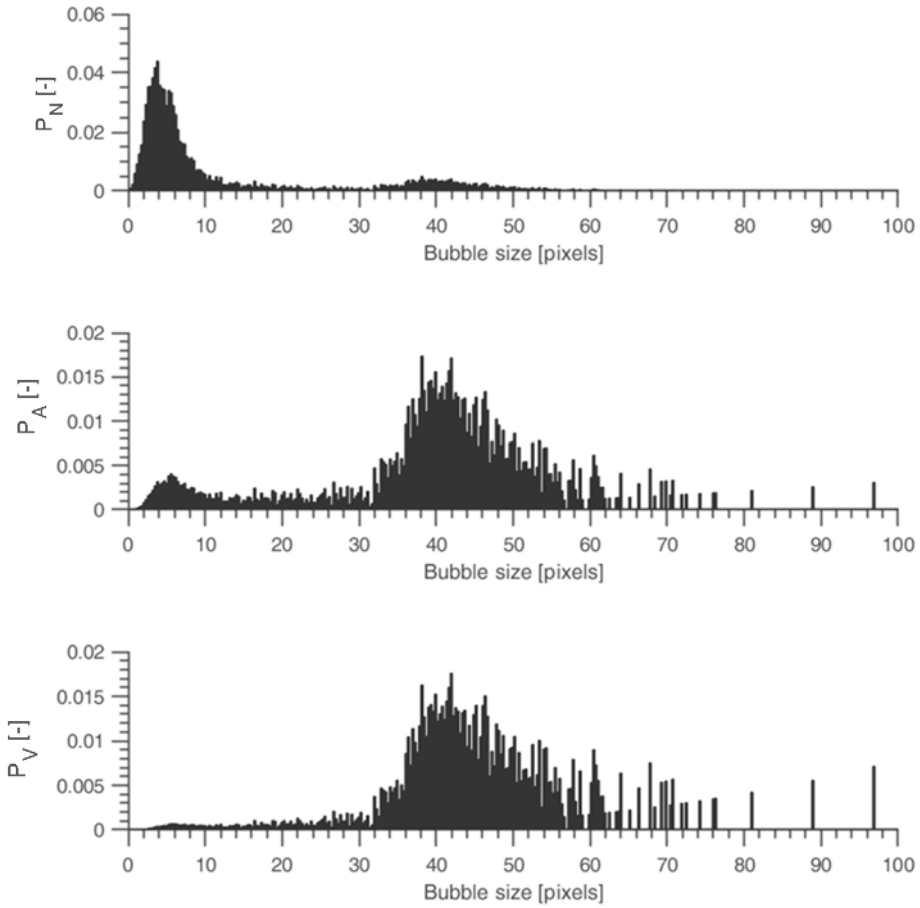

Figure 3.12. Probability density function of number, area and volume distributions (P_N, P_A, and P_V, respectively) of 1 mm glass beads in a stirred tank reactor with a working volume of 150 mL.

Chapter 4.

Effect of Mechanical Stirring on the Kinetic Stability of NAD(P)H Oxidases

This chapter is intended for later publication together with Dr. Sebastian Bartsch and Dr. Andreas Vogel from c-LEcta GmbH, Leipzig, Germany.

4.1. Abstract

NAD(P)H oxidases are industrially relevant enzymes since they can be used for the regeneration of the nicotinamide cofactors required by alcohol dehydrogenases in the oxidative direction. NAD(P)H oxidases are oxygen dependent enzymes therefore, reactor aeration and stirring are necessary to achieve target industrial productivities. Understanding NAD(P)H oxidases stability under relevant process conditions is of great interest for its application at industrial scale. Most of the stability studies in the field concern thermodynamic stability measurements, which do not indicate the "*lifetime*" of a biocatalyst under relevant operational conditions. Therefore, in the present work, the effect of the stirring power input on the kinetic stability of NAD(P)H oxidases was investigated. It was found that NAD(P)H oxidases deactivate faster with the increase of power input and we propose that protein-protein collisions are the cause for the observed biocatalyst deactivation. Furthermore, the residual activity of different NAD(P)H oxidase variants at a power input of 1 WL^{-1} was measured and compared with their independently measured thermostability. No clear correlation between thermodynamic and kinetic stability was found. Lastly, the effect of the cell lysis method on the kinetic stability of the enzymes was analysed. Lysis using detergent resulted in less stable enzymes, which showed that the enzyme formulation has a great impact on the biocatalyst stability.

4.2. Introduction and Motivation

In order to apply an enzyme as a biocatalyst to produce an industrial relevant chemical, stirring is required to obtain homogeneity in large scale reactors (Xue and Woodley, 2012). Furthermore, if the enzyme is an oxidase, which requires molecular oxygen as a cosubstrate, mixing is essential to break the air bubbles in the liquid medium to promote oxygen transfer into solution (Goswami et al., 2013; Martínez et al., 2017). However, these conditions can harm the enzyme and promote its deactivation (Colombié et al., 2001a). In the development of biocatalysis towards lower value chemicals, the biocatalyst stability becomes a bottleneck because the biocatalyst cost contribution margin is lower than that for pharmaceutical compounds (Lima-Ramos et al., 2014; Woodley, 2013). Understanding the causes for enzyme deactivation under process conditions is thus essential to improve the stability of biocatalysts in the right direction.

When a reactor is mechanically stirred using an impeller, shear forces exist related to the flow velocities in the liquid. In the 1970s, these forces were suggested as the cause for protein deactivation, as firstly showed by Charm & Wong (1970) and further supported by Tirrell & Middleman (1975). However, Thomas et al. (1979) have demonstrated that alcohol dehydrogenase is much less sensitive to shear than other enzymes reported in earlier studies. Likewise, Thomas & Dunnill (1979) showed that sheared solutions of catalase and urease had no significant losses in activity. In addition, the authors claimed that shear forces alone are not as effective in causing protein deactivation as it was believed. One of the explanations for this is that a protein molecule is much smaller than the Kolmogorov length scale of turbulence and the eddies are unlikely to cause shear damage to an enzyme in solution (Ghadge et al., 2005; Kolmogorov, 1991). There have been many publications concerning the effect of shear on enzymes' stability, and these were comprehensively reviewed by Thomas & Geer (2011). From all the debate and experimental work performed, it was concluded that shear alone is rarely or never the cause for protein deactivation.

Although shear forces have been demonstrated not to degrade enzymes, protein deactivation has been observed upon mechanical agitation (Chapter 3). In fact, it has been previously shown that stirring deactivates enzymes and reasons other than shear have been proposed as the explanation. Colombié et al. (2000, 2001a and 2001b) suggested that lysozyme deactivation was caused by collisions between native and inactive protein. Previously, Caussette et al. (1997) showed the existence of a self-catalytic enzyme inactivation enhanced by stirring due to a high rate of protein-protein molecule collisions. Therefore, with the purpose to investigating the effect of mechanical agitation on the stability of oxidase enzymes, incubation experiments in a bioreactor of different NAD(P)H oxidases (NOXs) were performed in quiescent solution and at different impeller power inputs per volume. In order to characterise the results, the kinetic stability of the enzymes was studied and correlated with the energy input for stirring to the reactor.

Enzyme stability can have different meanings depending on how it is measured. A step further to better understand the stability of a biocatalyst is to relate thermodynamic and kinetic stability (John M. Woodley, 2017). Commonly, enzyme stability is referred to as the tendency of a protein to reversibly unfold, which is a measure of thermodynamic stability. This is usually represented by the melting temperature of the protein (T_m) or the free energy of unfolding (ΔG_u) (Bommarius and Broering, 2005). On the other hand, kinetic stability is a measure of the time scale that a protein remains active before it is irreversible denatured. This is generally measured by the enzyme half-life of denaturation (Sanchez-Ruiz, 2010). Although this parameter is extremely useful because it indicates the "lifetime" of a biocatalyst, there are fewer reported studies on proteins' kinetic stability. In addition, unfolding and deactivation are somehow associated, but how kinetic and thermodynamic stability are related is not fully understood. Although protein unfolding leads to a loss in enzymatic activity, both phenomena are different processes that are quantified in different ways (Polizzi et al., 2007). A summary of the various enzyme stability measurements are presented in Table 4.1.

In the present contribution, we determined the deactivation rate constants and half-lives of three NOXs at different power inputs and we correlated it with the enzymes' melting temperature in order to find a relationship between kinetic and thermodynamic stability. The NOXs selected have been thermodynamically stabilized via protein engineering to improve their melting temperature. In brief, the work developed here had two distinct goals: to investigate the effect of power input on the deactivation of NOX and to correlate its kinetic and thermodynamic stability. Furthermore, the effect of the cell lysis method on NOX kinetic stability was also investigated.

Table 4.1. Summary of enzyme stability measurements. Adapted from Polizzi et al. (2007).

Type of stability	Measurements and Units	Definition
Thermodynamic	**Melting temperature** T_m (deg.)	Temperature of which half of the enzyme is in the unfolded state.
	Free energy of unfolding ΔG_u (energy mol^{-1})	Change in Gibbs free energy from the folded to the unfolded state.
	Unfolding equilibrium constant K_u ($conc._u$ $conc._f{}^{-1}$)	Concentration ratio of unfolded and folded protein.
	Half-concentration $C_{½}$ (conc.)	Concentration of denaturant required to unfold half of the protein.
Kinetic	**Deactivation rate constant** k_d (time $^{-1}$)	Overall rate constant for going form native to deactivated protein.
	Half-life $\tau_{½}$ (time)	Time required by an enzyme to reach 50 % of its residual activity.
	Temperature of half-inactivation T_{50} (deg.)	Incubation temperature to reduce by half the residual activity during a defined period of time.
	Total turnover number *TTN* ($mol_{product}$ mol_{enzyme}^{-1})	Moles of product produced over the biocatalyst lifetime.

4.3. Experimental Section

Materials

Six different water-forming NAD(P)H oxidases (NOXs) were kindly supplied by c-LEcta (Leipzig, Germany) in the format of a lyophilised cell free extract powder. These enzymes differed by the number of mutations added to the wild type, in order to improve its thermosability, and on the cell lysis method employed (Table 4.3). The source organism of the enzymes is unknown. All the chemicals used were purchased from VWR (Radnor, PA, USA). Potassium dihydrogen phosphate and dipotassium hydrogen phosphate were used to prepare potassium phosphate buffer. NADPH tetrasodium salt (□-nicotinamide-adenine dinucleotide phosphate, reduced) was used as the substrate for the enzyme activity assays.

Table 4.3. Overview of the NOXs used in the experiments. Activities reported are per mg of lyophilised powder. One unit corresponds to the consumption of 1 μmol min^{-1} of NADPH.

Enzyme ID	Enzyme	Activity (U/mg)	T_m (°C)	Sequence information	Cell lysis method
NOXwt-D	NOX-31	1.9	41	wt plus smNOX mutations *	Detergent
NOX1-D	NOX-29	0.93	47	1st generation stabilized, plus smNOX mutations	Detergent
NOX2-D	NOX-30	1.4	51	2nd generation stabilized, plus smNOX mutations	Detergent
NOXwt-ND	NOX-31	3.4	41	wt plus smNOX mutations	Homogenization
NOX1-ND	NOX-29	2.1	47	1st generation stabilized, plus smNOX mutations	Homogenization
NOX2-ND	NOX-30	1.7	51	2nd generation stabilized, plus smNOX mutations	Homogenization

*Mutations applied in *Streptococus mutans* NOX reported by Petschacher et al. (2014).

Bioreactor Setup

The NOXs were incubated in a stirred tank reactor with a total volume of 250 mL designed and built in-house, similar to the one described in Chapter 4. The bioreactor contained two Rushton turbines, two baffles and a metal sampling port. The stirring speed was controlled by an external motor. Since the effect of stirring power input per volume was investigated, the head space was completely eliminated to avoid introducing air into the liquid from the vortex created around the impeller (Figure 4.12). To account for the sampling volume, the reactor was run flooded.

For these experiments, a light source and a borescope were used inside the reactor in order to maintain hydrodynamics and 'material' surface area the same as in the experiments carried out in Chapter 3. This decision was taken so the results with and without aeration could be compared.

Figure 4.12. Scheme of the reactor setup without head space. The reactor lid was adapted to slide inside the reactor for a working volume of 150 mL

Procedure

To study the effect of mechanical stirring on the stability of a given NOX, the stirring power input per volume was varied. Experiments were carried out at power inputs of 0.5, 1, 2, 3, 4 and 5 WL^{-1}. For each experiment, the reactor was filled with 160 mL enzyme solution with a concentration of 0.16 g_{CFE} L^{-1} in 50 mM KPi buffer at pH 7. The enzyme was incubated at 21 °C for a period of 6 hours. Control experiments were carried out in quiescent solution to account for time deactivation dependence. A summary of all experiments is presented in Table 4.3.

Samples were collected at regular periods of time and stored on ice to stop further enzyme inactivation. A disposable syringe attached to the sample port was used to take samples and was very carefully handled so no air bubbles were introduced in the system. Then, the enzyme solution was assayed for residual activity, relative to a sample with no inactivation (time zero), by following the NADPH consumption at 340 nm in a spectrophotometer. Activity was measured at 25 °C using 1 mL cuvettes, 50 mM KPi pH 7 and 0.20 mM NADPH.

Table 4.4. Experiments map. The tick marks are the experiments performed and discussed in the following section.

	Power input (WL^{-1})						
Enzyme ID	Quiescent	0.5	1	2	3	4	5
NOXwt-D	✓	✓	✓	✓	✓	✓	✓
NOX1-D	✓	-	✓	✓	-	-	-
NOX2-D	✓	-	✓	✓	-	-	-
NOXwt-ND	-	-	✓	-	-	-	-
NOX1-ND	-	-	✓	-	-	-	-
NOX2-ND	-	-	✓	-	-	-	-

4.4. Results and Discussion

Effect of Mechanical Stirring on NOXs Deactivation

The first part of the work was focused on understanding the effect of stirring in the deactivation of NOX, in the absence of gas-liquid interface. In order to do so, NOXwt-D was incubated with stirring at different power inputs per volume and its residual activity was measured over time. As expected, results showed that with an increase in power input the kinetic stability of the enzyme decreased (Figure 4.13A). Moreover, two other NOXs, NOX1-D and NOX2-D, were incubated at 1 and 2 WL^{-1} and the same behaviour as NOXwt-D was observed (Figure 4.13 B and C). In fact, these results are in line with the observations presented in the previous chapter.

In order to estimate the deactivation of NOXs in solution, a control experiment was performed in quiescent conditions (without any stirring). By doing so, it was possible to measure the time effect on the enzyme deactivation when dissolved in an aqueous solution. Furthermore, for a quantitative comparison between all NOXs tested, the deactivation rate constant (k_d) and the enzyme half-life were calculated. It was found that deactivation kinetics were close to first-order by following the residual activities over time. Therefore, a first-order deactivation kinetics was assumed to all cases. Results are presented in Table 4.5.

A

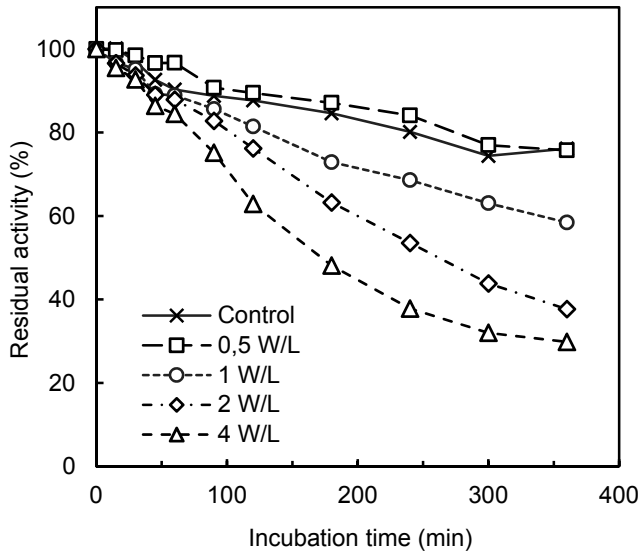

B

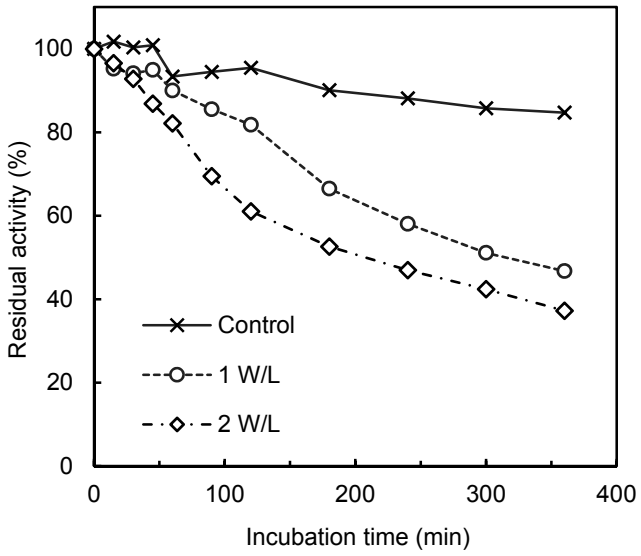

C

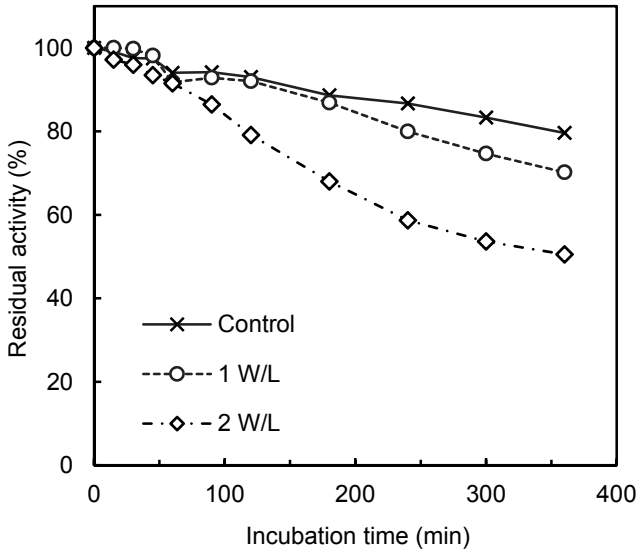

Figure 4.13. Residual activity of NOXwt-D (A), NOX1-D (B) and NOX2-D (C) at different stirring conditions. Incubation experiments were carried out in 50 mM of KPi buffer pH 7 with an enzyme concentration of 0.16 g_{CFE}/L. Activities were measured in triplicate and the standard deviation was always below ± 3 %.

In this chapter, the experiments were performed in a highly controlled environment, where no gas-liquid interface was present. Nevertheless, it was observed that enzymes deactivate in the presence of mechanical stirring. As discussed in the introduction, the size of the eddies in the Kolmogorov length scale of turbulence is too large in comparison with the size of a small protein like NOX (~50 Da), meaning that shear forces cannot be responsible for inducing protein deactivation. Thus, we believe that is the frequency of collisions which is causing the loss of enzyme stability. As the power input per volume (P/V) increases, the probability of a protein molecule to collide with another and with the reactor walls is higher. The probability of collisions

increases with the P/V because the enzymes contact more often with the impeller. Therefore, enzyme-enzyme collisions are more frequent. It is suspected that the enzyme inactivation is related to active-inactive protein interactions because of the observed formation of precipitates, possibly aggregates of inactive protein. This phenomena was first seen with lysozyme and it was described by Caussette *et al.* (1997). Nevertheless, to the best of our knowledge, it is the first time that this phenomena is observed with an oxidase. Indeed, deactivated proteins expose their hydrophobic residues so the interaction between active protein and aggregates increases the contact between native protein and hydrophobic surfaces, which also induces enzyme deactivation (Wu et al., 1993).

Furthermore, with an increase of power input per volume, faster deactivation rates were observed. As can be seen in Figure 4.14, the deactivation rate constant of NOXwt-D increases in proportion to the power input per volume (P/V). Moreover, the relationship between these two variables was also previously observed for lysozyme (Colombié et al., 2000). Therefore, these results support the proposed collision theory since at higher P/V the probability of an enzyme collision is higher.

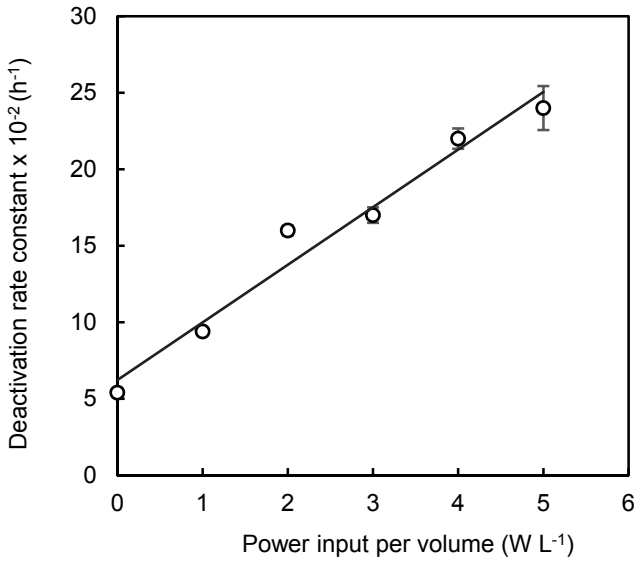

Figure 4.14. Dependence of the NOXwt-D deactivation constant (k_d) on the power input per volume (P/V) to the reactor. The enzyme was incubated in 50 mM KPi buffer pH 7 with a concentration of 0.16 g_{CFE}/L. The line represents a linear regression with a R^2 = 97 % (k_d = 3.8·P/V + 6.2). The relative error of the deactivation rate constant was below ±6 %.

Table 4.5. Deactivation rate constants (k_d) and half-life of NOXs at various power inputs. The relative error of the deactivation rate constant was below ±6 % for all stirring conditions.

	NOXwt-D		**NOX1-D**		**NOX2-D**	
Power input (W L^{-1})	k_d (h^{-1})	*Half-life* (*h*)	k_d (h^{-1})	*Half-life* (*h*)	k_d (h^{-1})	*Half-life* (*h*)
Control	0.054	12	0.030	23	0.038	18
1	0.094	7.3	0.13	5.4	0.05	12
2	0.16	4.3	0.18	3.8	0.12	5.8
3	0.17	4.2	-	-	-	-
4	0.22	3.1	-	-	-	-
5	0.24	2.9	-	-	-	-

Effect of Protein Engineering on the Kinetic Stability of NOX

In the second part of this study, a comparison between the different NOXs was made. NOX1 and NOX2 have been genetically modified and their melting temperatures were improved (Table 4.3). As a result, the NOX thermodynamic stability was increased by protein engineering. However, at a power input per volume of 1 WL^{-1}, the kinetic stability measurements from the incubation experiments showed that NOX1 deactivated faster than NOXwt. Figure 4.15 showed that the kinetic stability at 1 WL^{-1} of the first generation mutant of NOXwt (NOX1) was not improved. On the other hand, the kinetic stability of NOX2 was better. These results indicate that improving enzyme thermostability may not directly result on an improved kinetic stability, towards mechanical stirring.

In order to understand if the same trend as at 1 WL^{-1} was observed under other mixing conditions, experiments performed in quiescent medium (control) and at 2 WL^{-1} were compared. Figure 4.16 illustrates the half-life for the three NOXs at different power inputs. Regarding the control conditions, it was observed that NOX1 kinetic stability was better than NOX2. However, when the solution was stirred, the NOX2 appears to be more stable. Moreover, as the power input increases, the difference between the half-life of the wild type and the mutants is very little. In conclusion, a correlation between the NOX melting temperature and half-life was not observed and the impact of increased thermostability on kinetic stability is not straightforward.

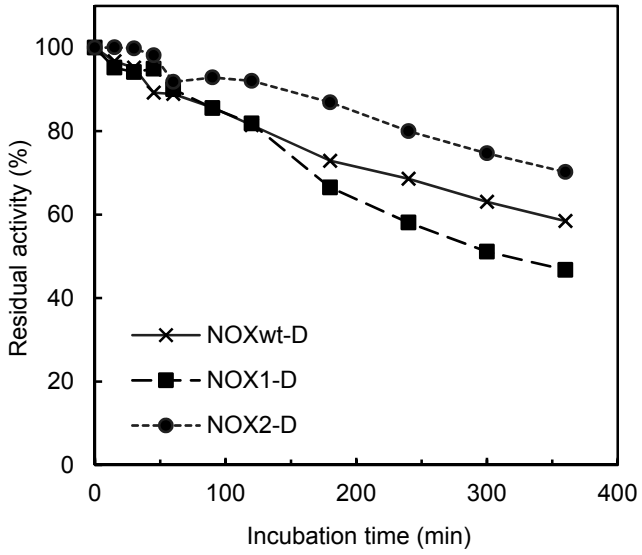

Figure 4.15. Residual activity of different NOXs at a power input of 1 WL^{-1}. Incubation experiments were performed in 50 mM of KPi buffer pH 7 with an enzyme concentration of 0.16 g_{CFE}/L. Activities were measured in triplicate and the standard deviation was always below ± 3 %.

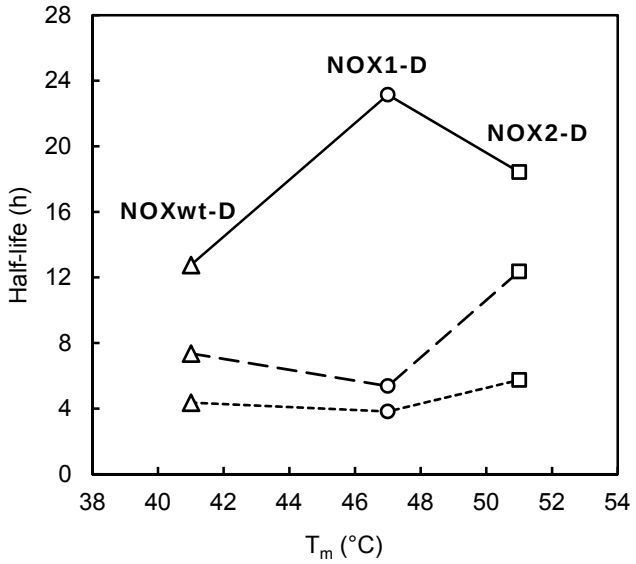

Figure 4.16. Correlation between kinetic stability and thermostability of NOXs at different stirring conditions. (△) NOXwt-D, (□) NOX1-D and (○) NOX2-D. T_m is the melting temperature of the enzymes. (Full line) control, (Large dashed line) 1 WL^{-1} and (Small dashed line) 2 WL^{-1}.The relative error of the half-life was below ± 6 % for all conditions.

Effect of Cell Lysis Methods on the Stability of NOX

Lastly, the reactor was aerated in order to investigate if the presence of gas-liquid interface increased the deactivation rate of NOX. However, as the aeration started, the foam formation could not be controlled. As a result, the experiments were impossible to carry out due to a significant loss of enzyme solution volume. Nevertheless, to run a reaction catalysed by NOX, molecular oxygen must be supplied and aeration is the most common method. Next, we realised that the cell lysis method used detergent. Since detergent is surface active it can generate a lot of foam. So, after discussing with the enzyme supplier, the cells were disrupted by homogenization, without the use of any detergent. Afterwards, the new NOX were tested again at different stirring conditions, without aeration, for a comparison between the two cell lysis methods (Figure 4.17). The half-life was re-calculated and is presented in Table 4.6.

The enzyme formulation prepared using homogenization appears to be more stable at a power input of 1 WL^{-1} for NOXwt and NOX1. NOX2 does not follow the same trend as NOXwt and NOX1 since the observed half-life of NOX2-D is higher than NOX2-ND. On the other hand, the activity of all NOXs increased when detergent was not used (Table 4.3). From these results, the NOXwt without the use of detergent appears to be the most kinetically stable enzyme, at a power input of 1 WL^{-1}, even though it is not the enzyme with the highest thermostability. Thus, it is important to measure the enzyme kinetic stability to better understand enzyme behaviour under industrial relevant operational conditions. Moreover, these results showed that great care should be taken concerning the enzyme formulation. The process to produce the biocatalyst that will be used to develop an enzymatic reaction has a strong influence on the biocatalyst activity and stability. Therefore, a systematic integration of protein engineering strategies with process engineering must be developed for a faster development of new biocatalytic processes.

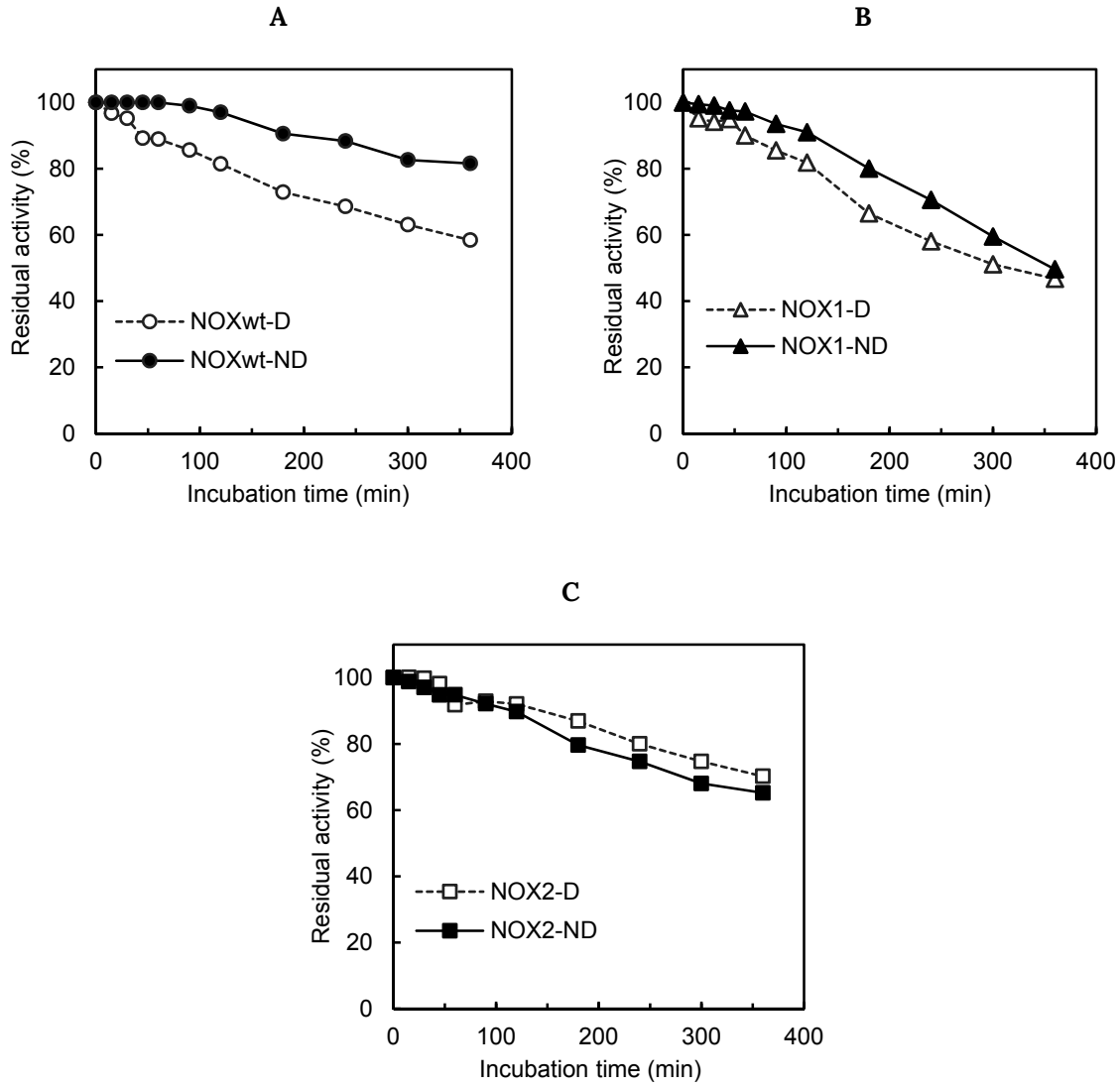

Figure 4.17. Comparison of the residual activity of two different formulations of NOXwt (A), NOX1 (B) and NOX2 (C) at a power input of 1 WL^{-1}. NOX-D were enzyme formulations prepared using detergent for the cells lysis and NOX-ND were formulations prepared without detergent. Activities were measured in triplicate and the standard deviation was always below ± 3 %.

Table 4.6.Half-life of NOXs formulations prepared using two different cell lysis methods at a power input of 1 WL^{-1}. The relative errors of the half-life are below ± 5 %.

	Detergent *Half-life (h)*	**No Detergent** *Half-life (h)*
NOXwt	7.3	21
NOX1	5.4	7.1
NOX2	12	10

4.5. Conclusions

The present work has revealed that NAD(P)H oxidases deactivate when mechanically stirred without the presence of gas-liquid interfaces. To the extent of our knowledge, the results here presented showed for the first time a proportional increase of NOX deactivation rate with the increase of stirring power input per volume. We believe that the enzyme deactivation is associated with collisions between native and inactive protein resulting from the mechanical stirring, because with the increase on power input, the frequency of collisions between protein molecules inside the reactor is higher. Furthermore, the comparison of three NOXs variants thermodynamic and kinetic stability showed no correlation between the enzymes' half-life and melting temperature. Lastly, it was found that the enzyme formulation affects the NOX activity and stability. These findings demonstrate the relevance of kinetic stability measurements under conditions in which the enzymes are exposed when used as biocatalysts in industrial processes. Besides, until the correlation between thermodynamic and kinetic stability is not fully understood, experiments to measure both are required. In conclusion, in order to use an enzyme as a biocatalyst, its kinetic stability should be investigated under similar conditions to industrial processes.

4.6. Acknowledgements

The research for this work has received funding from the European Union (EU) project ROBOX (grant agreement n° 635734) under EU's Horizon 2020 Programme Research and Innovation actions H2020-LEIT BIO-2014-1. Any statements herein reflect only the author's views. The European Union is not liable for any use that may be made of the information contained herein. The authors acknowledge Søren Madsen, from the Workshop in the Department of Chemical and Biochemical Engineering at DTU, for the technical drawings and for building the reactor setup. Thomas G. Andersen is acknowledged for his contribution to the experimental part of the work.

Chapter 5.

Effect of Gas-Liquid Interfaces on the Kinetic Stability of NAD(P)H Oxidases

This chapter is intended for later publication. The work presented here was developed in collaboration with Professor Andreas Bommarius and Dr Bettina Riebel Bommarius as part of my external stay at Georgia Institute of Technology in Atlanta, Georgia, USA.

5.1. Abstract

One of the major drawbacks for many biocatalysts is their poor stability under industrial process conditions. A particularly interesting example is the supply of oxygen to biooxidation reactions, catalysed by oxidases, oxygenases or alcohol dehydrogenases coupled with NAD(P)H oxidases, which require molecular oxygen as an oxidant or electron acceptor. Commonly, oxygen is supplied to the bioreactor by air sparging. In order to ensure sufficient oxygen transfer from the gas to the liquid phase, stirring is essential to disperse the gas bubbles and create high gas-liquid interfacial area. Studies indicate that the presence of gas-liquid interfaces induce enzyme deactivation by protein unfolding which then readily aggregate and can precipitate (Bommarius and Karau, 2005; Caussette et al., 1999). This contribution has examined the effect of gas-liquid interfaces on the kinetic stability of two NAD(P)H oxidases (NOX) (EC1.6.3.2). A bubble column apparatus was successfully developed to define and quantify the gas-liquid interfacial area. The results showed, for both NOXs tested, that enzyme deactivation increases with the increase of gas-liquid interfacial area. Both air and nitrogen induce protein deactivation but air enhances the rate of stability lost. Furthermore, from the comparison between the two NOXs and the literature, the extent of protein deactivation was found to be enzyme dependent.

5.2. Introduction and Motivation

The integration of biocatalysis into the production of pharmaceuticals and fine chemicals continues to make progress. An enzyme's ability to operate under mild conditions is of great importance but it is their excellent selectivity that draws attention for wider applications in chemical synthesis (Pollard and Woodley, 2007; Woodley et al., 2013). Additionally, biocatalysis offers economic and environmental advantages over chemical routes, contributing to the development of more sustainable industrial processes (Sheldon and Woodley, 2018; J.M. Woodley, 2017). However, despite the many benefits of biocatalysts, their stability under relevant process conditions is still a drawback to the increased usage of enzymatic catalysis (Bommarius, 2015).

Oxidoreductases are a class of enzymes that is becoming increasingly relevant, as it was mentioned in Chapter 4 (Dong et al., 2018). These can perform oxidation reactions to produce molecules with industrial interest, that are difficult to obtain in a single step using non-biocatalytic processes (Birmingham and Turner, 2018; Grogan, 2018; Turner, 2012). In particular, oxidation of alcohols to ketones or aldehydes, essential to produce building blocks for many valuable chemicals, can be catalysed using Alcohol Oxidases (AOXs) and Alcohol Dehydrogenases (ADHs). ADHs have been most commonly used since there are more discovered enzymes with activity and selectivity towards molecules of interest (Brummund et al., 2015; Liu et al., 2018). However, these enzymes require $NAD(P)^+$ as an electron acceptor, which is an expensive cofactor and needs to be recycled to achieve an economically feasible process (Rehn et al., 2016). Therefore, NAD(P)H oxidases (NOXs) can be used for this purpose. For both of these systems, using AOX or ADH/NOX, molecular oxygen is needed as an oxidant in stoichiometric amounts. This particularity is highly attractive for industrial manufacturing processes, as it avoids the use of harmful metal oxidants. However, it comes with some limitations, especially regarding the biocatalyst stability under the target process conditions.

Usually, oxygen is supplied to a stirred bioreactor by sparging air into the liquid media. Stirring is essential to break the gas into small bubbles, increase their residence time in the reactor and then ensure sufficient oxygen transfer from the gas to the liquid phase. To achieve industrially relevant productivities (Tufvesson et al., 2011; J.M. Woodley, 2017), fast oxygen transfer from the gas to the liquid phase is needed. Therefore, to obtain a high mass transfer coefficient (k_la) a large gas-liquid interfacial area is desired. However, it has been shown that the presence of gas-liquid interfaces can deactivate certain biocatalysts. For instance, Donaldson et al. (1980) observed that acid phosphatase deactivates in the presence of air-liquid interfaces and that the rate of deactivation is dependent on air-liquid contact time in a laminar flow reactor. Later, it was found that lysozyme deactivates when in contact with air-liquid interfaces and also in the presence of nitrogen (Caussette et al., 1999; Colombié et al., 2001a). Around the same time, Patil et al. (2000) and Mohanty et al.(2001) have also shown that lipases deactivate in the presence of surface aeration. Likewise,

Bommarius & Karau (2005) found that formate dehydrogenase deactivates towards gas-liquid interfaces (using both air and oxygen). Further, Findrik et al. (2014) revealed that the increase of aeration in a stirred tank reactor decreased the stability of D-amino acid oxidases. Finally, recent work developed in shake flasks demonstrates that cellulases deactivate at the air-liquid interface too (Bhagia et al., 2018). However, Toftgaard Pedersen et al. (2015) showed that galactose oxidase did not lose activity when exposed to air aeration. As it can be seen, there is no clear trend to define if a protein is stable or not towards gas-liquid interfaces.

Since sparging air into a stirred tank reactor is still the most efficient and economical way of supplying oxygen to biooxidations, the presence of gas-liquid interfaces are unavoidable. As mentioned before, the stability of the biocatalyst is crucial for successful application of biocatalytic oxidations in industry. Therefore, the reasons for protein inactivation in the presence of such interfaces must be better understood. This is especially relevant for oxidases, since oxygen is a cosubstrate in the reaction. Furthermore, methods that allow the study of the deactivation of these proteins in the presence of gas-liquid interfaces should be further developed.

In order to explore the effect of gas-liquid interfacial area on the stability of oxygen dependent enzymes, a bubble column was built based on previously published work by Bommarius & Karau (2005) where, inter alia, the deactivation of formate dehydrogenase (FDH) at gas-liquid interfaces was studied. The bubble column design was reproduced and used specifically for NOXs. The present work investigates the stability of two water-forming NOXs from *Lactobacillus sanfranciscensis* (Lountos et al., 2006) and from *Lactobacillus plantarum* (NoxV) (Park et al., 2011) towards gas-liquid interfaces and aims to correlate the extent of protein deactivation with the availability of the interfacial area. Aqueous solutions of both enzymes were bubbled with air (21% oxygen) through a bubble column. As the presence of oxygen is known to over-oxidise some amino acid residues in oxidases (Slavica et al., 2005), the stability of these enzymes was also tested in the presence of nitrogen gas (no oxygen available). Control experiments in quiescent solutions were also carried out to account for time dependent protein deactivation. Furthermore, the causes of enzyme deactivation in the presence of a gas-liquid interfacial were addressed and discussed.

5.3. Theory

Quantification of gas-liquid interfacial area inside an aerated stirred tank bioreactor is not simple nor precise. Besides, it is not possible to separate the effect of aeration from stirring. Therefore, to investigate the deactivation of enzymes as a function of the amount of interfacial area, a bench scale bubble column was used. In this defined and controlled environment, gas bubbles rise in a stagnant liquid solution under the influence of gravitational force. The operational parameters of the system have a significant influence on the dynamic behaviour of a rising bubble. It is necessary

to achieve spherical bubbles in order to obtain an accurate estimation of the interfacial area. In the following section, the expressions to calculate the interfacial area in the bubble column are explained, and the different regimes of rising bubbles are defined along with the non-dimensional numbers that describe bubble dynamics.

Interfacial area determination

The gas-liquid interfacial area (A) per unit time generated in the bubble column was calculated using equation (5.1).

$$\frac{dA}{dt} = \frac{6 \cdot Q}{d_b} \tag{5.1}$$

where the gas flow rate (Q) was experimentally determined. The bubble diameter (d_b) was estimated using equation (5.2).

$$d_b = \left(\frac{6 \cdot \sigma \cdot d_0}{g \cdot (\rho_l - \rho_g)}\right)^{1/3} \tag{5.2}$$

which is a balance of buoyancy and surface forces (Bommarius and Karau, 2005). The bubble size was also experimentally measured to validate the estimation. The bubble diameter strongly influences the regime of the rising bubbles and is directly proportional to the diameter of the nozzle.

These equations are valid only if the bubbles do not collide with each other and remain spherical when rising in the column. The collision of the bubbles is dependent on the gas flow rate. To guarantee that the bubbles do not touch each other, the gas flow rate should be below a theoretical transition gas flow rate (Q_t) given by equation (5.3),

$$Q_t = \left(\frac{\pi}{6}\right) \cdot d_b^2 \cdot \left(\frac{L}{\theta}\right) \tag{5.3}$$

which depends on the velocity of the rising bubble (ratio of the liquid height (L) and the residence time of a bubble in the column (θ)). These two parameters were experimentally measured.

Dynamics of a Rising Bubble

A gas bubble in a quiescent solution rises due to gravitational force and its deformation and velocity depends on the balance of viscosity, buoyancy, inertia and surface tension forces. Bubbles rising

freely in infinite media can assume three different regimes, depending on the primary forces acting on the system: *spherical*, *ellipsoidal* and *spherical-cap* (Clift et al., 1978) (Figure 5.1).

The *spherical regime* is dominated by surface tension and/or viscous forces and the shape of the bubbles approximate a sphere. Bubbles are defined spherical if the ratio of minor to major axis is less than 10 %. The *ellipsoidal regime* is mainly controlled by surface tension forces and the final shape is oblate with a convex interface (perspective from the inside) around the entire surface. Ellipsoidal bubbles may suffer random wobbling motions or periodic dilatations, which can complicate the shape characterisation. Finally, the *spherical-cap* regime is dominated by inertia forces. Usually, large bubbles are in this regime and tend to assume multiple flat-type shapes (Clift et al., 1978).

The shape of a rising bubble in infinite media can then be described by three dimensionless groups that relate the forces involved in this phenomena. These are the Reynolds number, Re, Morton number, M and Bond number, Bo (also referred to as Eotvos number, Eo), which are defined by equations (5.4), (5.5) and (5.6) respectively (Clift et al., 1978; Middleman, 1998).

$$Re = \frac{\rho_L d_e U}{\mu} \tag{5.4}$$

$$M = \frac{g\mu^4 \Delta\rho}{\rho^2 \sigma^3} \tag{5.5}$$

$$Bo = \frac{g\Delta\rho d_e^2}{\sigma} \tag{5.6}$$

There are many proposed correlations for the rising velocity of a bubble (U) summarized well by Amaya-Bower & Lee (2010). In this work, it was calculated based on the measured residence time of a bubble in the column (θ) and the liquid height (L). The equivalent diameter of a bubble (d_e) is defined by equation (5.7).

$$d_e = \left(\frac{6V}{\pi}\right)^{1/3} \tag{5.7}$$

Based on these dimensionless numbers a shape regime map, presented in Figure 5.1, was proposed by Clift et al. (1978). It should be noted that the boundaries suggested between the principal regimes are somewhat arbitrary and that the graph was developed for unhindered rising bubbles in a quiescent pure water solution. Nevertheless, it can be seen that for high Re and Bo, bubbles will assume spherical-cap regime and for a high Re and intermediate Bo bubbles tend to be ellipsoidal.

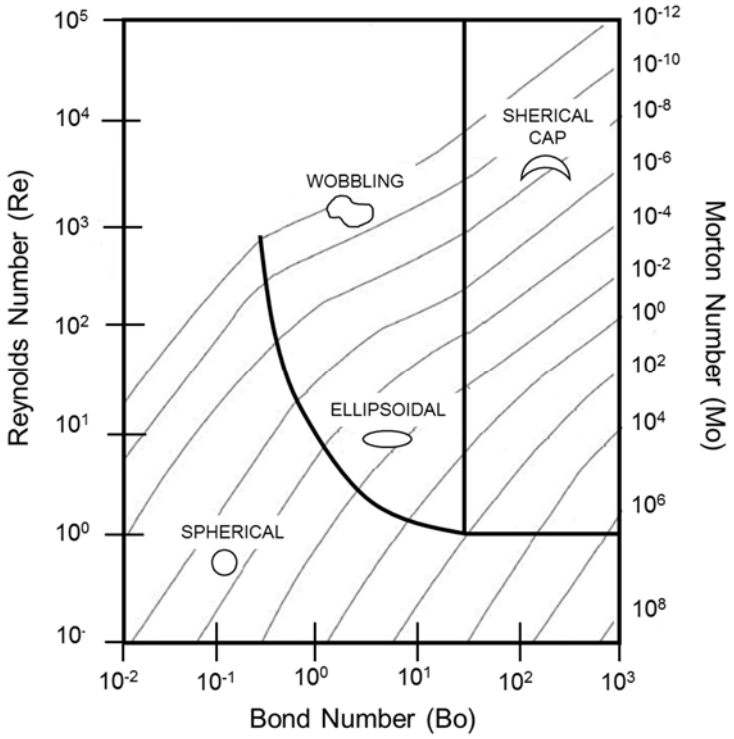

Figure 5.1. Shape regimes for bubbles ascending freely in an infinite liquid based on (Clift et al., 1978).

In the experiments carried out in the bubble column, gas bubbles rise in a confined space. When bubbles rise in bounded equipment, its shape can be affected by the walls. Also, the experiments were performed using an enzyme solution as a stagnant liquid. Proteins in solution can behave as a surfactant, since they tend to adsorb to the gas-liquid interface. It is known that the presence of surfactants also affects the shape of bubbles. Particularly, for air bubbles in aqueous media there is little viscous resistance to internal circulation so drag and rising velocity decrease with the presence of surfactants. As it can be seen in Figure 5.1, in contaminated water (with the presence of surfactants) the terminal velocity decreases with increase of the bubble diameter, for bubbles with a d_e > 0.7 mm. In addition, surfactants reduce the surface tension forces and small air bubbles tend to remain rigid in water. Consequently, all these factors have a strong influence on the bubble shape and the boundaries between regimes in Figure 5.1 and Figure 5.2 can change.

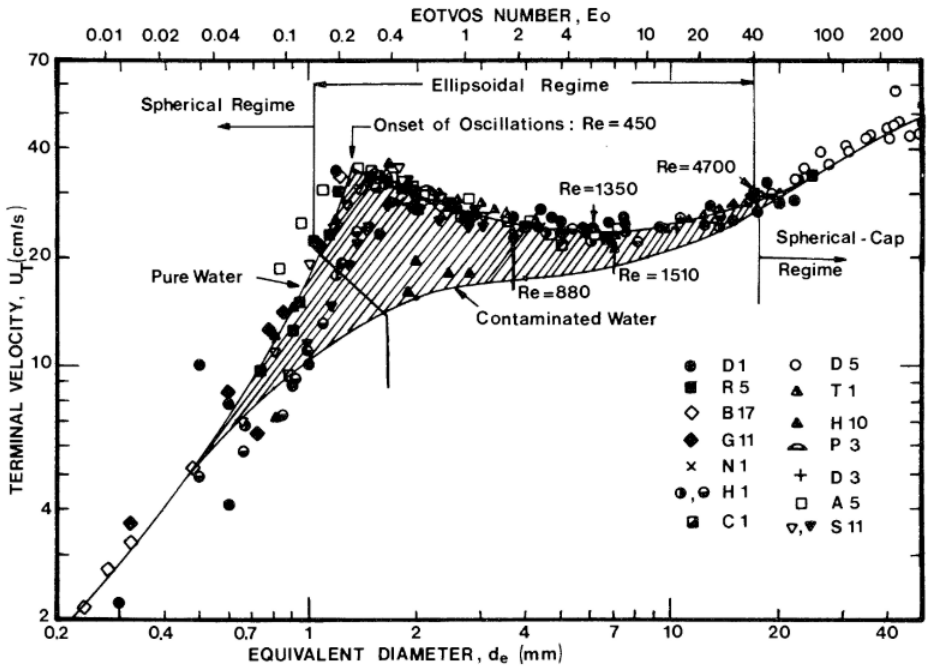

Figure 5.2. Terminal velocity of air bubbles in water at 20 °C. Contaminated water with surfactants (Clift et al., 1978).

5.4. Experimental Section

Materials

Dibasic sodium phosphate and citric acid purchased from Sigma–Aldrich (St. Louis, MO, USA) were used to prepare phosphate-citrate buffer at pH 6, 7 and 8. For pH 8 buffer sodium hydroxide solution 1 N from Sigma–Aldrich (St. Louis, MO) was used to adjust the pH. Lysates of two different NOXs from *L. sanfranciscensis* and *L. plantarum* (NoxV) were prepared according to Lountos et al. (2006) and Park et al. (2011) respectively. Dithiothreitol (DTT) was obtained from JT Baker (Phillipsburg, NJ) and NADH from Sigma–Aldrich (St. Louis, MO, USA).

Control Experiments

Control experiments were performed in glass vials (4 and 25 mL). A magnetic stirrer and a stirring plate were used when agitation was desired. Both NOXs (clarified lysate formulation) were incubated for 72 hours, at room temperature and pH 6, 7 and 8. All experiments were carried out with a clarified lysate concentration of 10 % (v/v) in phosphate-citrate buffer in a total volume of 4 mL. 1 mM of DTT was added to all solutions to prevent overoxidation of aromatic residues of the enzyme. For each pH, three different control conditions were tested: (1) incubation under a quiescent solution in 4 mL closed vials, termed "*no air*, *no mixing*", (2) incubation in the presence of gentle agitation in a closed container (4 mL vials), named "*no air*, *mixing*" and (3) incubation in the presence of air and gentle agitation, in a container with a high head space and the lid open (25

mL vials), termed "*air*, *mixing*". Samples were taken over time, stored on ice to stop further the enzyme deactivation and the residual activity was measured following the NOX activity assay procedure described below.

NOX Activity Assay

Initial activity of NOX was determined by following absorption changes of NADH consumption in a spectrophotometer at 340 nm (ε = 6.22 mM^{-1} cm^{-1}), at 25 °C with a light path of 1 cm. Absorbance was measured for 2 minutes using 0.2 mM of NADH, 1 % (v/v) of clarified lysate and phosphate citrate buffer at pH 7 (concentrations in the cuvette). The cuvettes were well mixed to ensure saturation of oxygen in the solution with air at atmospheric pressure. One unit (U) corresponds to 1 µmol of NAD^+ produced per minute. The NOX from *L. sanfranciscensis* (sfNOX) had an activity of 19 U/mL_{lysate} and NoxV from *L. plantarum* (NOX5) an activity of 50 $U/mL_{lysate.}$

Bubble Column Experiments

All stability experiments towards gas-liquid interfaces were carried out in the bubble column apparatus.

Bubble Column Setup

The bubble column was a glass tube with a length of 48 cm and an inner diameter of 6.2 mm. A needle with an inner diameter of approximately 0.6 mm was attached to the bottom of the column and operated as a nozzle. Air and nitrogen (99.9 % pure) were sparged through the nozzle at a given flow rate (Q) of 14 mL min^{-1} (2.3×10^{-7} m^3 s^{-1}). The gas bottles were connected to a mass flow controller to measure the flow rate and assure a constant value. The column had a liquid height (L) of 25 cm and the residence time of a bubble (θ) was approximately 1.7 seconds. A GoPro Hero 6 camera (frame rate of 240 fps, San Mateo, CA, USA) photographed and filmed the set-up to verify the rising bubbles regime and that the bubbles did not touch each other. The bubble diameter (d_b) was established by a photograph of the column that contained a graduated scale. A tube connected to a syringe was installed at the top of the column to fill in the column with the enzyme solution and to collect samples (sample port). Figure 5.3 presents a scheme of the bubble column apparatus and Figure 5.4 a technical drawing.

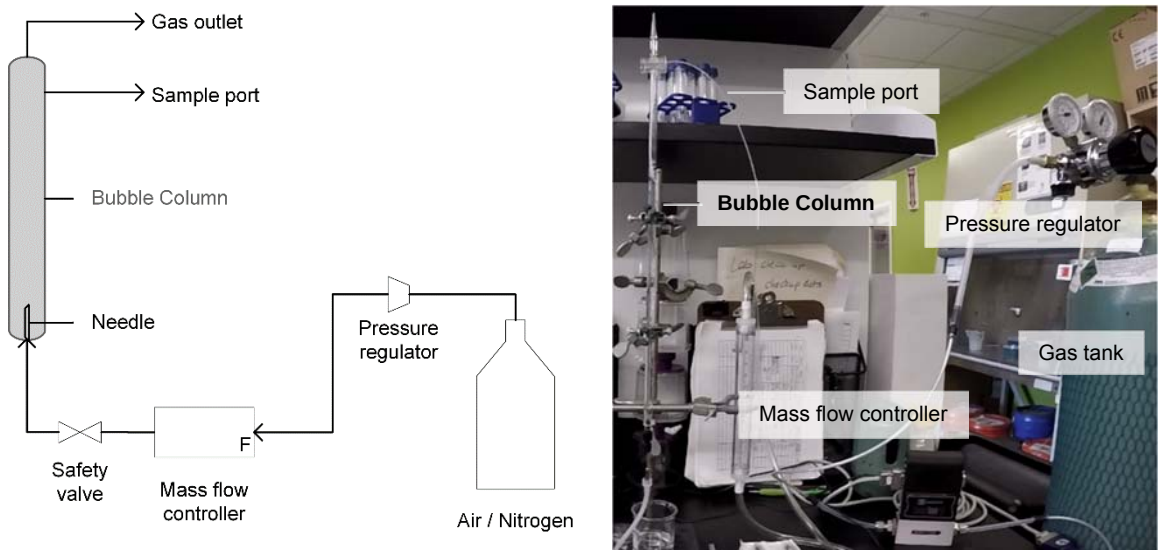

Figure 5.3. Representative diagram (left) and picture (right) of the bubble column setup.

Procedure

First, the gas flow rate was set to 14 mL min^{-1}. When it was constant, 10 mL NOX solution of 10 % (v/v) in buffer was slowly injected from the sample port. Samples were collected at regular time intervals, stored on ice to stop further enzyme deactivation and tested for residual activity following the NOX activity assay described above. Before starting an experiment, the column was cleaned with acetone so the path of the bubbles was not interrupted. The concentration of enzyme solution was kept the same to ensure constant surface tension.

sfNOX was incubated in the bubble column at pH 7 and sparged with air at room temperature. This was performed in duplicate to verify the reproducibility of the experiments. NOX5 was incubated at pH 7 and 8 (room temperature), sparging air and nitrogen for both pH conditions.

Deactivation Rate Constants

To estimate deactivation rate constants (k_d), first-order deactivation kinetics is assumed for all cases. The k_d is the slope of the natural logarithm of the residual activity over time (Sadana, 1988). The half-life was also estimated for a better comparison of the results.

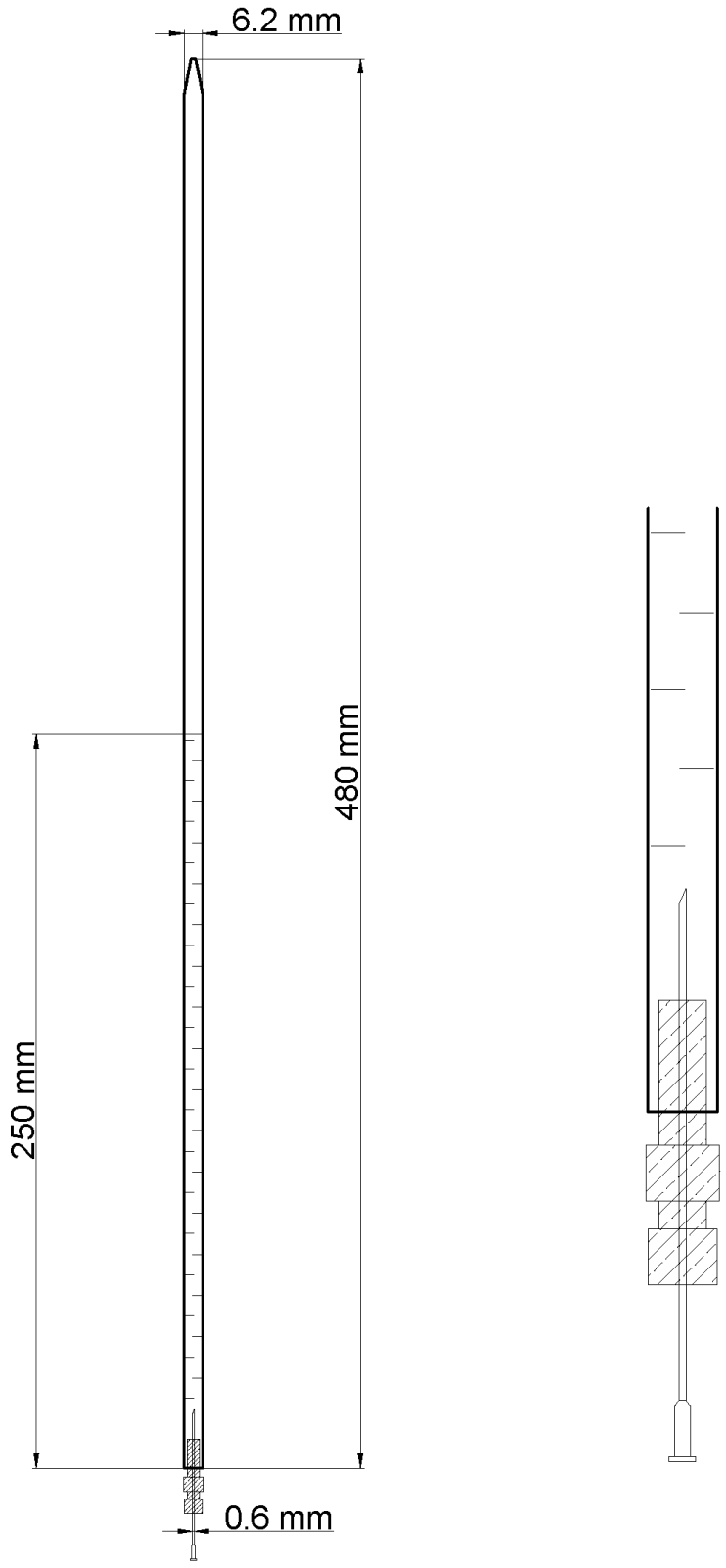

Figure 5.4. (Left) Technical drawing of the bubble column setup representing the column, the liquid height and the gas bubbles. (Right) Detail of the gas inlet.

5.5. Results and Discussion

Influence of Time and pH on the Stability of NOXs

The activity of enzymes decreases over time simply by keeping a protein in solution. Enzymes are dynamic systems and their structures change depending on the environment. To account for activity losses, dependent on time and pH, both NOXs were incubated in quiescent solutions at different pH. pH 6, 7 and 8 were selected since the reactions performed with NOXs coupled with ADHs are normally run at one of these pH conditions, dependent on the product desired. From the results presented in Figure 5.5, the two enzymes seem to be more stable at pH 7 and less stable at pH 8, as expected. Regarding stability over time, NOX 5 is a more stable enzyme than sfNOX. Therefore, NOX 5 was selected to be more extensively studied in the bubble column so a better distinction between time and the presence of gas-liquid interfacial area could be made. Furthermore, NOX 5 had higher activity than sfNOX so a better accuracy on activity assays could be obtained.

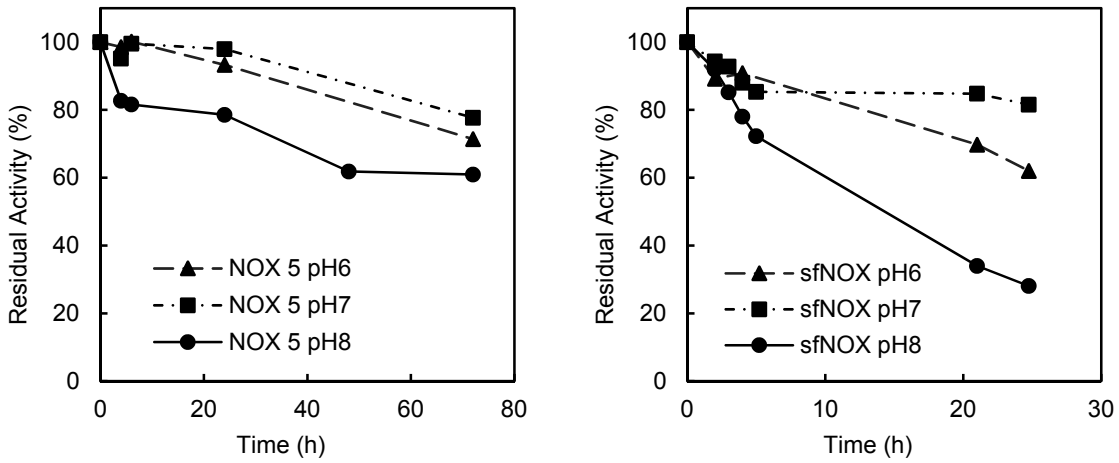

Figure 5.5. Stability of NOX 5 (left) and sfNOX (right) in quiescent conditions (*no air*, *no mixing*) room temperature, in phosphate-citrate buffer and for different pHs. All data points are an average of triplet measurements with a standard deviation below ± 5 %.

For the next step, NOX 5 stability was tested under gentle stirring and in the presence of air (diffusion of oxygen from the head space of the vial to the liquid). Results show that both mixing and the contact with the air-liquid interface have a negative effect on enzyme stability (Figure 5.6). However, it is not clear whether the presence of air increases the deactivation throughout all pHs. It should be noted that even with the lid closed, there was always some air-liquid interface and the head space increased with sampling over time. For those reasons, the separation of the effect of mixing and presence of air-surface was hard to achieve. Thus, the stability towards gas-liquid interfaces was investigated in the bubble column. Finally, it can be concluded that mixing decreased protein stability so this effect was studied separately and repeated in Chapter 4.

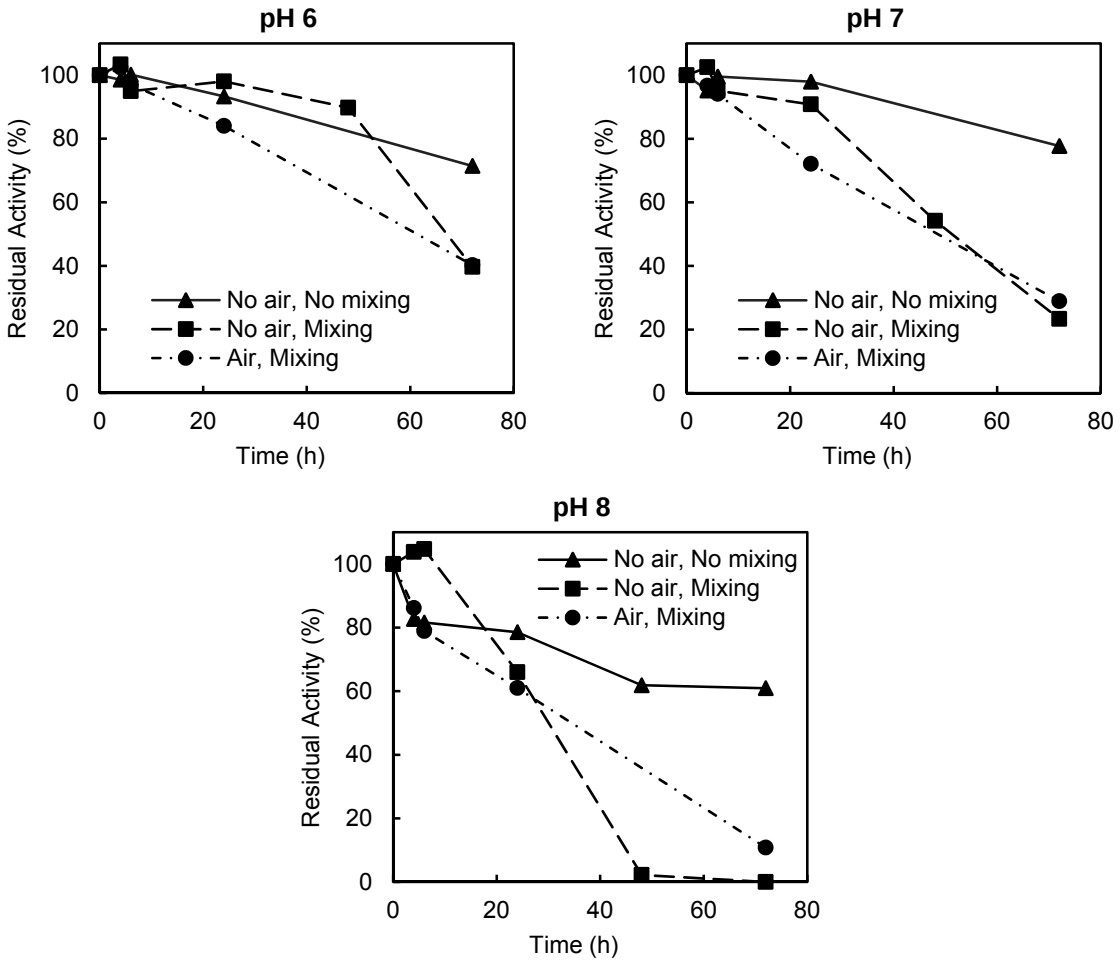

Figure 5.6. Deactivation of NOX 5 over time for pH 6, 7 and 8 at three different conditions. Experiments were carried out using phosphate-citrate buffer and the data points are an average of three measurements with a standard deviation less than ± 5 %.

Influence of Gas-Liquid Interfaces on the Stability of NOXs

To investigate the deactivation of NOXs in the presence of gas-liquid interfaces, the enzymes were incubated in a bubble column sparged with a gas phase. The enzyme was exposed to larger interfacial areas with longer incubation times. In order to quantify this area, the gas flow rate was defined so the bubbles did not collide with each other and remained in the spherical regime. Therefore, the gas flow rate selected ($Q = 2.3 \times 10^{-7}$ m^3 s^{-1}) is below the theoretical transition gas flow rate (Q_t) calculated according to equation (5.3) ($Q_t = 6.9 \times 10^{-7}$ m^3 s^{-1}).

The diameter of the bubbles was observed to be 3 mm, which was in accordance with the estimation, calculated by equation (5.2) (2.99 mm). The bubbles rose in a zig-zag and spiral pattern, hitting the column wall in the same places. Even so, from the videos, the bubbles appear to remain nearly spherical for the whole course of the experiment. Thus, the equivalent diameter (d_e) was considered equal to the bubble diameter (d_b).

Nevertheless, to theoretically verify if the bubbles were rising in a spherical regime, the dimensionless numbers *Re*, *M* and *Bo*, described in equations (5.4), (5.5) and (5.6) respectively, were estimated. For the purpose of such calculations, the surface tension was assumed equal to the air-water interface. The *Re* number of the bubbles was determined to be approximately 500, the $M = 1.7 \times 10^{-11}$ and *Bo* = 1.2 and are in accordance with Bommarius & Karau (2005). From Figure 5.1 and Figure 5.2, it can be seen that the bubbles are within the ellipsoidal or wobbling regimes. However, the bubbles were observed to be very close to spherical shape, which supports the statements that the boundaries of the graphs are arbitrary and strongly dependent on the liquid phase composition. Particularly, in this case, the enzyme solution might have a large impact on the surface tension forces that was not accounted for. Therefore, the gas bubbles were considered spherical and the calculations of the interfacial area assumed valid. Further, the liquid system was considered well mixed since results from sampling from the top and bottom of the column were identical (data not shown).

First, all results from the experiments run in the bubble column show that the deactivation of both NOXs is dependent on the increase in interfacial area (Figure 5.7 and 5.8). Also, results presented in Figure 5.7 demonstrate the replicability of the experiments performed in this apparatus, which validates the method used. It can also be seen that NOX 5 was found more stable towards gas-liquid interfaces than sfNOX but it is also more stable in quiescent conditions (without the presence of an interface). Both enzymes lost around 20 % of activity at quiescent conditions after 72 h (NOX 5) and 24 h (SfNOX). Therefore, improvements of sfNOX stability in solution may also decrease the inactivation in a gas-liquid interface environment.

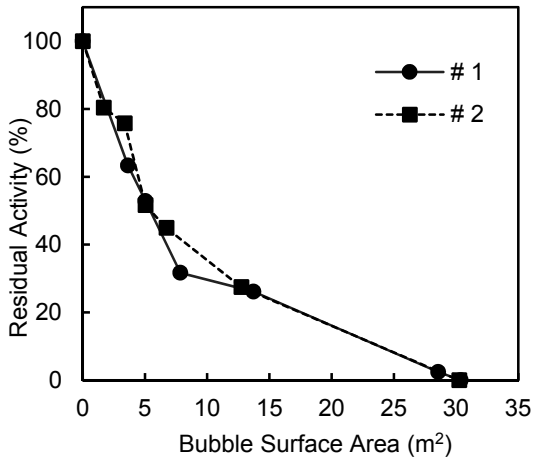

Figure 5.7. Deactivation of sfNOX in the presence of air-liquid interfaces at pH 7 with an enzyme concentration of 10 % (v/v) in phosphate-citrate buffer. The two data sets, (●) and (■), are experiments carried out at the same conditions. The data points are an average of two measurements with a standard deviation below ± 2 %.

Regarding NOX 5, experiments were carried out using air and nitrogen with the aim to establish the influence of the oxygen on the enzyme stability. Results showed that the enzyme is more stable

when nitrogen is sparged (Figure 5.8) for both pHs tested. The presence of oxygen seems to enhance the deactivation of the protein, which is most probably caused by overoxidation of the catalytically active cysteine residue, even with addition of DTT (Park et al., 2011). However, when nitrogen is sparged, the presence of the gas-liquid interface has a negative effect on the NOX stability, compared to the control experiments in quiescent conditions. Looking at Table 5.1, the influence of these parameters on the half-life of the enzyme is observed. For pH 7, the presence of the gas-liquid interface (sparging nitrogen) decreases the enzyme half-life by a factor of 5 and the presence of oxygen by a factor of 10 in comparison with the control experiment (no interface). With respect to pH, NOX 5 is more stable at pH 7 and the same behaviour in relation to the presence of gas-liquid interfacial area was observed. These observations indicate that there are multiple phenomena involved in the deactivation of the protein. Enzymes tend to adsorb to the gas-liquid interface, which is a highly hydrophobic surface with either air or nitrogen. The adsorption process induces conformational changes in the protein tertiary structure, leading to enzyme unfolding by exposure of its hydrophobic groups to the gas phase (Narsimhan and Uraizee, 1992; Wu et al., 1993). Studies performed in the presence of organic solvents (liquid-liquid interfaces) have shown that chymotrypsin is inactivated by hydrophobic organic solvents and that the inactivation is proportional to the amount of liquid-liquid interface (Ghatorae et al., 1994). It is possible that the results presented here follow the same behaviour as proteins in the presence of hydrophobic liquid-liquid interfaces.

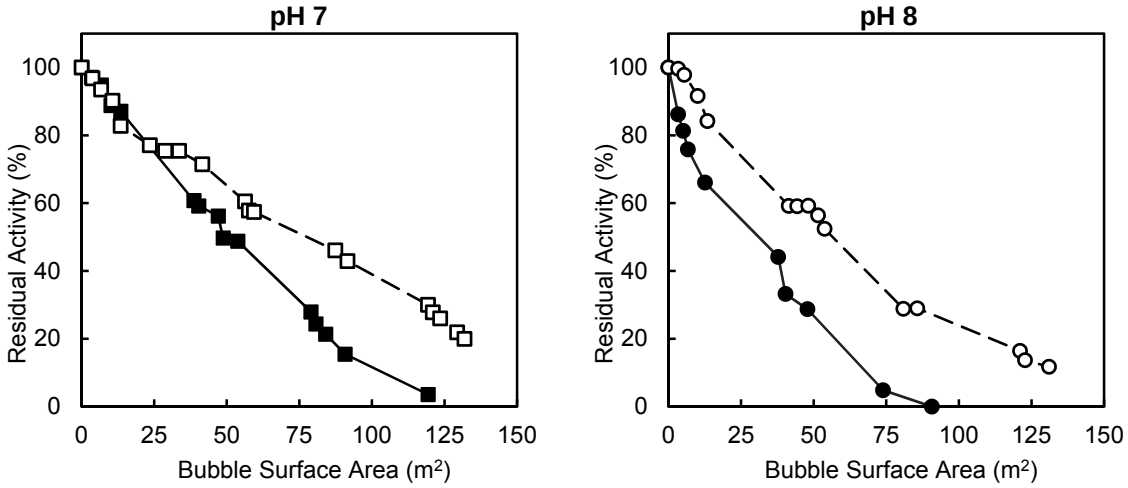

Figure 5.8. Deactivation of NOX 5 in the presence of air (full symbols) and nitrogen (empty symbols) in the bubble column, with an enzyme concentration of 10 % (v/v) in phosphate-citrate buffer, at room temperature and different pHs. All data points are an average of two measurements with a standard deviation below ± 2 %.

Finally, it can be concluded that the deactivation of the enzymes is dependent on the exposure to the gas-liquid interfacial area, and not the incubation time by comparing the results from the bubble column with the control experiments. In the control experiments, NOXs were incubated for the same time required in the bubble column to achieve such interfacial areas.

Table 5.1. Kinetic deactivation constants (k_d) and half-life of NOX 5 under different gas-liquid interface conditions and different pHs. Half-life corresponds to the time taken by the enzyme to reduce its activity by half, under the incubation conditions (calculated based on the first-order inactivation kinetics).

Conditions	**pH7**		**pH8**	
	k_d (h^{-1})	*Half-life (h)*	k_d (h^{-1})	*Half-life (h)*
No interface*	-0.0033	210	-0.0082	84
Sparging nitrogen*1	-0.017	40	-0.025	28
Sparging oxygen*1	-0.033	21	-0.056	13

* Control experiment under quiescent conditions (1)
*1 Experiments in the bubble column

5.6. Conclusions

Gas-liquid interfaces will become more routine in industrial biocatalytic oxidation reactions so the stability of biocatalysts in this specific environment needs to be better understood. The present work investigates the behaviour of NOX stability towards gas-liquid interfaces and correlates the enzyme deactivation with a quantified interfacial area. Experiments were carried out in a bubble column apparatus where the availability of the interfacial area could be controlled. Results showed that experiments run in this setup can be well replicated. Both enzymes tested were found to deactivate in the presence of gas-liquid interfaces to different extents. NOX 5 was found to be more stable towards gas-liquid interfaces than sfNOX, which emphasises that there is no clear trend on protein stability in this particular environment, even within the same enzyme type. Therefore, it can be concluded that deactivation towards gas-liquid interfaces is enzyme dependent.

The second key feature observed in this study is that both air and nitrogen deactivate NOX 5. Still, air enhances the protein deactivation. The reason for that is the presence of oxygen which may over-oxidise the cysteine catalytic residues of the enzyme. However, NOX stability decreased also when exposed to nitrogen-liquid interfaces. This observation indicates that the hydrophobicity of the interface induces changes on the protein structure. On the absorption process to the gas-liquid hydrophobic surface, the enzyme tends to expose its hydrophobic residues, which leads to unfolding and further inactivation.

Finally, results indicate that enzyme deactivation is proportional to the increase of gas-liquid interfacial area and not to the time exposed to it. This can be concluded since the NOX exposure time to bubbles was the same as the control incubation experiments where no interface was present. Therefore, availability of interfacial area is what matters.

5.7. Future Perspectives

It is essential to continue exploring the causes for enzyme deactivation towards gas-liquid interfaces in order to suggest improvement strategies to enzyme stability in such conditions. Exclusion of hydrophobicity from the gas-liquid surface could decrease the free energy that drives the enzyme to adsorb at the interface. Most of the studies done so far suggest that the addition of surface active material, which competes with the enzyme for the surface adsorption, can increase enzyme stability with gas-liquid interfaces (Bhagia et al., 2018; Donaldson et al., 1980). However, is it really feasible when running a large scale biooxidation? It will affect the interfacial area, oxygen transfer and foam formation, among other parameters. Stabilizing the biocatalyst by protein engineering may be a more efficient strategy. But, as mentioned before, the deactivation of the enzyme at the molecular level has to be understood. Therefore, future experiments using the bubble column are suggested.

Use Purified Protein

Experiments were carried out using lysate. This enzyme formulation contained multiple compounds that may affect the NOX stability. In order to understand the conformational changes in the protein structure upon deactivation, purified protein should be used in the bubble column experiments. The difference between the effects of air and nitrogen could then be better understood. Also, it would explain the differences at the molecular level between the stability of the two NOXs tested. When using purified protein, multiple parameters can be analysed such as the measurement of the flavin (NOXs cofactor) stability. Thermodynamic stability can also be measured, for instance the enzyme melting temperature (T_m) and attempt to correlate this with kinetic stability.

Run a Reaction in the Bubble Column

The stability of a protein in solution differs from its stability while catalysing a reaction. This is due to conformational changes in the enzyme structure to allow passage of the substrate and product into and out of the active site. Studying the stability of a catalytically active enzyme is the first step towards understanding the protein behaviour under these two different states. Running reactions in the bubble column, where the interfacial area can be quantified and defined, could give an indication on this concern.

Chapter 6.

General Discussion on Enzyme Stability towards Gas-Liquid Interfaces

In chapters 3, 4 and 5, the kinetic stability of NAD(P)H oxidases (NOXs) has been intensively investigated against two main stress factors: gas-liquid interface (gas supply) and mechanical stirring. These factors were selected because they are essential to develop an economically feasible process that requires supply of molecular oxygen when using an aerated stirred tank reactor. Here, the findings from these chapters are summarized and discussed in the context of process development for oxygen dependent biocatalysis.

An important factor to consider in process development is the stability of the biocatalyst, which affects the cost contribution of the enzyme towards the overall cost of a process. For instance, an unstable enzyme must be used at higher concentrations or be replaced frequently whereas, if a more stable enzyme is used, less is required to achieve the same performance. There are several methods for improving the stability of a biocatalyst and they can be divided into three major approaches: protein engineering, immobilization (Silva et al., 2007) and medium engineering (environment at which an enzyme is surrounded, enzyme formulation) (Bommarius and Broering, 2005; de Barros et al., 2018). These strategies have been extensively reviewed elsewhere (Bommarius, 2015; Bommarius and Paye, 2013; Silva et al., 2018). In order to choose the most appropriate technique, the causes for enzyme deactivation must be identified under relevant process conditions, preferably at an early stage of process development.

Enzyme stability is best characterised by a deactivation rate constant (k_d) as a function of the relevant operational conditions of the process because it allows the estimation of the biocatalyst lifetime (Bommarius and Paye, 2013). In this context, the kinetic stability of NOX was studied for the first time *in situ* on a laboratory scale aerated stirred tank reactor (250 mL). The work presented in Chapter 3 aimed to determine the k_d of NOX under a gas-liquid interfacial area within

the range of large scale bioreactors by applying mechanical stirring. Using the optical method developed, it was observed that the rate of NOX deactivation increased with an increase in gas-liquid interfacial area. However, beyond a certain point, the half-life of NOX remains constant even though the interfacial area continues to increase. This suggests that stirring alone has an impact on the enzyme deactivation. Furthermore, it was also observed that the presence of oxygen decreased enzyme stability compared to nitrogen, which indicates that protein deactivation could be caused by (over)oxidation of certain amino acid residues. Hence, it appears that enzyme deactivation results from the effects of three operating conditions: presence of mechanical stirring, presence of gas-liquid interface and presence of oxygen in the gas feed. In order to investigate the individual effects of each of these conditions, they must be isolated and studied separately.

In Chapter 4, NOX stability was studied in the presence of mechanical stirring alone, as a function of power input per volume. Despite the absence of the gas-liquid interface, the deactivation rate constant was still found to increase with an increase in power input. High power inputs result in more shear stress, since the shear rate increases with an increase in the impeller speed (Stocks, 2013). However, it has been shown that proteins are unlikely to be sensitive to shear (Thomas and Geer, 2011). But, an increase of shear rate does cause higher frequencies of protein-protein and protein-wall collisions in the bioreactor, which could explain enzyme deactivation at higher power input. With the increase of power input per volume, the frequency of enzyme collisions increases, so there is a higher probability of native protein molecules colliding and interacting with inactive proteins, which leads to enzyme deactivation (Caussette et al., 1997; Colombié et al., 2001b, 2001a). Therefore, although shear does have an indirect effect on enzyme deactivation, does not cause it.

Next, in Chapter 5, the effect of gas-liquid interfaces alone was studied on the kinetic stability of several NOXs using a laboratory scale bubble column, which is a controlled environment where the interfacial area can be quantified. Overall, the results indicated that NOXs deactivate in the presence of gas-liquid interfaces but the rates of deactivation varied for the different NOXs, under the same gas-liquid interface conditions. Moreover, it was observed that the enzymes deactivate in the presence of both nitrogen and air, yet with air the deactivation rates were higher. These results are in accordance with the observations from the experiments with air and nitrogen presented in Chapter 3, which confirms that the presence of oxygen also has an effect on enzyme deactivation.

Based on the results obtained with the NOX experiments, a regime map identifying the causes for enzyme deactivation is proposed (Figure 6.1). This map relates the effect of gas supply and mechanical stirring on the half-life of an enzyme, where gas supply represents the presence of gas-liquid interfaces and the feed gas composition. Although all of these factors affect deactivation simultaneously, each region is characterised by the dominating effect. For example, in the

molecular collisions region it is assumed that the rate of deactivation due to collisions in the reactor is higher than the rate due to the interaction with the gas-liquid interface. Furthermore, all effects depend on time, but additionally dominated by the phenomena indicated in the zones on the plot.

The proposed regime map is highly enzyme dependent since the boundaries between regions were found to vary widely for the different NOXs tested. Therefore, even in the same enzyme subclass, no clear trend can be observed. This implies that the deactivation of an enzyme must be related to its unique three dimensional structure, which is primarily determined by an enzyme amino acid sequence. The enzyme surrounding environment has a role on its stabilization. Therefore, the hydrophobic surfaces from the gas-liquid interface and protein aggregates can interact with an enzyme in solution and induce conformational changes. The hydrophobic interactions are able to expose the protein hydrophobic residues, usually buried in its interior, which induces biocatalyst deactivation. For the experiments carried out in the stirred tank reactor and in the bubble column, hydrophobic surfaces were always present, either by deactivated enzyme (protein aggregates) or by the gas-liquid interface. Therefore, enzymes sensitivity towards hydrophobic interactions can probably be the underlying phenomena for enzyme deactivation under the operational conditions tested.

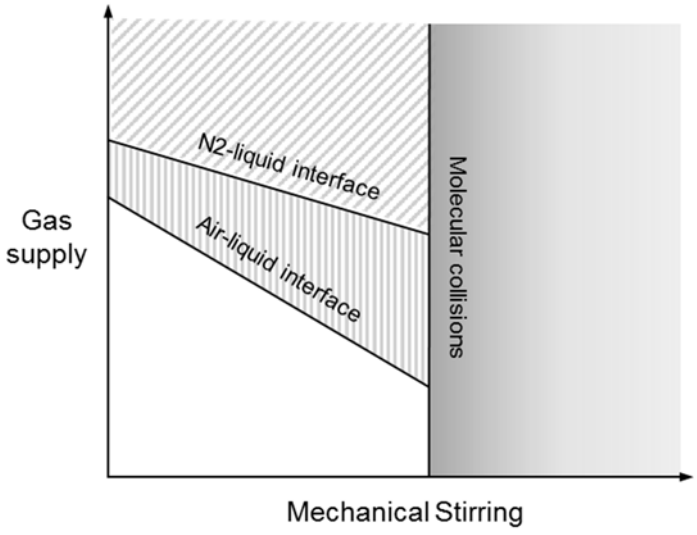

Figure 6.1. Regime map describing the dominating causes for kinetic deactivation of enzymes. Effect of gas supply and mechanical stirring on the half-life of an enzyme.

In conclusion, the experimental methodologies developed in these chapters contribute to understand enzyme deactivation and to identify the causes for stability loss. Therefore, improvements on the biocatalyst can be suggested and techniques for enzyme stabilization can be selected. Furthermore, these experiments contribute to decide the operational conditions of a process and to apply techniques to overcome the biocatalyst deactivation. The regime map allows the identification of the conditions where the enzyme stability will be most affected. Therefore, depending on the industrial targets and on the biocatalyst stability, the reactor conditions can be more carefully defined.

Chapter 7.

Towards a Scale-down Approach

7.1. Introduction

With the remarkable advances in the field of biocatalysis, there is currently a substantial interest in the development of new biocatalytic routes for oxidation reactions (Arnold, 2018; Turner and Kumar, 2018). These reactions are fundamental in the chemical industry because they convert petrochemical derived hydrocarbons into oxidised building blocks for organic synthesis. However, chemical oxidation reactions are not selective, frequently involving multiple protection and deprotection steps, and demanding stoichiometric amounts of oxidant, which leads to the generation of large amounts of chemical waste. In contrast, enzymes used as biocatalysts can selectively oxidise target substrates (Schulz et al., 2012) and require harmless oxidants, which contributes to the demands of safer and greener routes (Sheldon and Woodley, 2018). Oxidation reactions are catalysed by oxidoreductases (EC 1), which require molecular oxygen. In the case of oxidase enzymes, oxygen is used as an electron acceptor and, for oxygenases, oxygen is introduced into the substrate molecule, as illustrated in Figure 7.1 (Dong et al., 2018; Gadda, 2012; Leak et al., 2009).

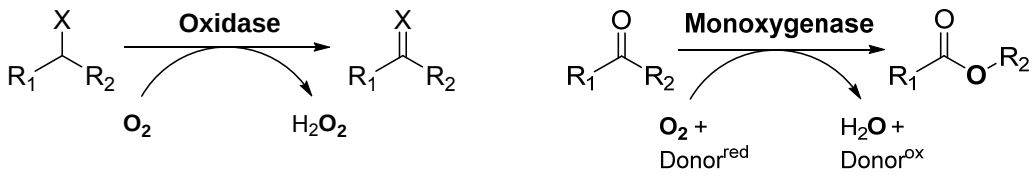

Figure 7.1. Oxidase and oxygenase catalysed oxidation reaction (X = O, NH).

From an environmental and economic perspective, the oxygen dependence of these biocatalysts appears to be an exceptional feature, since oxygen is innocuous, inexpensive and widely available. However, oxygen supply to bioreactions is one of the most challenging tasks for process engineers because of its poor solubility in aqueous solutions, which limits reaction rates. Additionally, the

presence of gas-liquid interfaces can deactivate the biocatalyst (Bhagia et al., 2018; Pedersen et al., 2015), while the process safety must also be considered as the use of oxygen presents an explosion risk, especially when an organic phase is present. Therefore, in order to evaluate the feasibility of an oxidation process, the prior requirement to implementation is that these limitations have to be identified.

7.2. Scale-down Philosophy

It is well known that biocatalytic reactions do not behave exactly the same way across all scales. In other words, a reaction performed in the laboratory has a different performance than when done in a 100 m^3 tank. Therefore, in order to understand the real limitations of reaction systems, scale-down strategies have been used to characterise them prior to scale-up. Usually, scale-down approaches consist of: (1) defining the desired large scale conditions in order to get certain characteristics of a process, (2) running experiments in small scale that mimic industrial process conditions and finally (3) analysing and comparing the results with industrial targets (Noorman, 2011). However, it is not trivial to simulate the environment of a large scale process in the laboratory because, for example, mixing and aeration are strongly dependent on the reactor and impeller size and geometry (Hudcova et al., 1989). In particular, it is extremely hard to mimic large scale operational conditions in order to obtain the same oxygen transfer rates in small scale reactors (Garcia et al., 2009; Stocks, 2013). Nevertheless, downscaling the exact environment of an enzymatic reaction is not necessary since the industrial environment is neither constant nor homogenous (Noorman, 2011). Therefore, scale-down research should focus on the aspects to which the reaction is most sensitive. Hence the question is **how to study biooxidation reactions in the laboratory**, at an early stage of the process development. In Figure 7.2, guidelines to a scale-down approach driven by industrial targets are summarized.

Guidelines for Scale-down Research

1. Keep the process under the same rate limiting mechanisms as in industrial scale.
2. The laboratory equipment should be designed in order to obtain a similar environment to industrial scale (geometric similarity may not be maintained).
3. Develop a mathematical model alongside the experiments with the utmost goal to predict the behaviour of similar systems.

Figure 7.2. Industrially driven guidelines for downscaling experiments (Noorman, 2016).

In order to establish a scale-down strategy for biocatalytic oxidations, industrial targets must be defined to design the laboratory experiments and to benchmark the current performance of a reaction system. In the following section, the targets are defined as process metrics. Furthermore,

process limitations related to oxygen supply to enzymatic oxidations are discussed and finally, a scale-down approach for oxygen dependent biocatalysis is proposed.

7.3. Industrial Requirements for Biocatalytic Processes

Considering that the ultimate purpose is to implement large-scale biocatalytic oxidation processes, laboratory experiments should be performed with industrial targets in mind. These targets depend on the process economics, which necessitate certain operational conditions, such as high substrate and product concentrations and, specifically for oxidations, the presence of gas-liquid interfaces (Woodley, 2013). These requirements, based on economic goals, can be described by process metrics (Table 7.1), which may be used to assess and lead the development of biocatalytic processes for chemical production (Lima-Ramos et al., 2014; Tufvesson et al., 2011; J.M. Woodley, 2017).

Table 7.1. Definition of process metrics for biocatalytic processes. P = product, S = substrate, τ = residence time, V = total reactor volume and B = biocatalyst. * Or space-time yield. *Reaction yield* is the yield of product on substrate and *biocatalyst yield* is the yield of product on biocatalyst.

Process Metric	**Definition**	**Units**	**Cost contribution**
Reaction yield	$\frac{m_P}{m_S}$	$g_P\ g_S^{-1}$	Raw materials
Productivity*	$\frac{m_P}{\tau \cdot V}$	$g\ L^{-1}h^{-1}$	Plant capacity (capital costs)
Product concentration	$\frac{m_P}{V}$	$g\ L^{-1}$	Downstream processing
Biocatalyst yield	$\frac{m_P}{m_B}$	$g_P\ g_B^{-1}$	Biocatalyst

It is indeed challenging to cost a process at an early stage of its development, especially new biocatalytic oxidation reactions due to limited information available concerning the full scale and process. Therefore, process metrics that consider the basic economic requirements to enable process implementation, are extremely helpful to understand the current process performance and to define development strategies. Based on previously published work (Lundemo and Woodley, 2015; Tufvesson et al., 2011) and on the experience of various industrial partners, values for the metrics have been selected and are presented in Table 7.2. As described in Table 7.1, the process metrics are defined according to the main economic cost drivers and thus have different values depending on the industrial application. Consequently, as the value of the product increases, there are less demands regarding the *process* itself. For example, for low value products the yield and

productivity are crucial metrics for process implementation whereas for high value chemicals, the metrics are not so critical due to higher economic margins for the process.

Table 7.2. Product classes and respective process metrics. The metrics were defined based on Lundemo and Woodley (2015), Tufvesson et al. (2011) and on ROBOX industrial partners experience. The biocatalyst yield is not presented due to its dependency on the biocatalyst format.

	Low value	**Medium value**	**High value**
Industry sector	Specialty chemicals	Flavours & Fragrances	Pharmaceuticals
Product Price (€ kg^{-1})	3	20	100
Reaction yield (%)	90-100	80-100	80-100
Productivity (g $L^{-1}h^{-1}$)	20	10	2
Product concentration (g L^{-1})	100	50	10

The fact that enzymatic oxidations require molecular oxygen adds an extra parameter that will impact the metrics. For instance, as demonstrated in Chapters 3 and 6, the biocatalyst stability can be affected due to gas-liquid interfaces, therefore it will influence the biocatalyst yield, product concentration and productivity. Similarly, the biocatalyst kinetics is dependent on the oxygen concentration (Chapter 2) so it has an impact on the space-time yield. The parameters that influence the metrics can also be related to the equipment and operational conditions related to mixing and aeration rate, thus the oxygen supply rate determines the maximum possible productivities. In Table 7.3, the possible limitations of an enzymatic oxidation related to the presence of oxygen and how they affect the process metrics are specified.

Table 7.3. Effect of process limitations related to oxygen supply on process metrics. Table adapted from Lundemo and Woodley (2015). STY = space-time yield, the same as productivity.

Oxygen related limitations		**React. yield**	**STY**	**Product conc.**	**Biocat. yield**
Biocatalyst	Stability towards gas-liquid interfaces		x	x	x
	Low oxygen affinity (high K_{MO})		x	x	x
	Coupling efficiency*	x			x
	Cofactor system		x		
Substrate	Oxygen solubility		x		
	Oxygen toxicity*1			x	x
Process	Oxygen transfer rate		x		
	Oxygen explosive limit		x		

* Coupling efficiency is a measure of how much of the oxygen consumed by the enzyme is used towards formation of the desired product.
*1 Oxygen toxicity is related to enzymes stability in the presence of oxygen.

7.4. Process Limitations Related to Oxygen Supply

The main process constrains caused by supplying molecular oxygen are related to reaction rate and biocatalyst stability. Therefore, different scenarios can be considered:

1. **The reaction is not fast enough**. Actually, the maximum reaction rate possible is defined by the oxygen transfer rate (OTR), which is dependent on the process operational conditions. Sometimes, the OTR is not sufficiently high to meet the industrial targets because of the slow mass transfer of oxygen from the gas to the liquid phase due to poor oxygen solubility. Moreover, the reaction rate is also determined by the biocatalyst concentration. However, once the maximum OTR is reached, increasing the enzyme concentration will not increase the reaction rate, as demonstrated in Chapter 2. Other important limitation that can affect the reaction rate is related to the low oxygen affinity of an enzyme (high K_{MO}). This parameter can be higher than the oxygen solubility in aqueous media (0.265 mM). Therefore, the enzyme cannot perform at its highest efficiency (showed in Chapter 2).

2. **The enzyme is not stable enough**. The presence of a gas-liquid interface can deactivate the biocatalyst, as presented in Chapter 3 and 5. Therefore, the enzyme may not be sufficiently stable to meet the industrial requirements. The importance of the biocatalyst stability is dependent on the product cost. For example, for a high value product, having a very stable enzyme may not be necessary to have a feasible process whereas for a low value molecule, enzyme stability pays a crucial role on the process viability. Therefore, as the cost of the product decreases, having a stable and robust enzyme becomes more important due to the low economic process margins.

These two major limitations related to oxygen supply are opposed to each other and are discussed in more detail in the sections bellow.

Rate-Related Limitations

High productivities are required to achieve economically feasible biooxidation processes and, to reach them, high oxygen transfer rates are necessary. The OTR is dependent on the reactor scale and geometry. These parameters, together with other operational conditions, define the volumetric mass transfer coefficient (k_la), which is used to characterise oxygen transfer in aerated stirred reactors. The k_la may increase with scale dependent on the coalescing conditions of the reaction medium (Table 7.4). If a biocatalytic reaction is under coalescing conditions, its oxygen transfer rate will be more dependent on the reactor scale than under non-coalescing conditions.

Table 7.4. Volumetric mass transfer coefficients (k_la) for different volumes of stirred tank reactors, under coalescing and non-coalescing conditions. Table adapted from (Noorman, 2016). For the k_la calculations, the aeration rate and power input to the rector were kept constant, 1.5 vvm and 2 W L^{-1}, respectively. *Impeller floating conditions.

Reactor volume (m^3)	**k_la (h^{-1}) Stirred tank coalescing conditions**	**k_la (h^{-1}) Stirred tank non-coalescing conditions**
0.01	169	518
0.1	191	587
1.0	266	648
10	356	662
100	421	569*

Coalescence occurs when two bubbles collide and merge to form a larger bubble, reducing the gas-liquid interfacial area. The presence of surface active compounds in solution, such as salts and proteins, influence bubble coalescence. Surfactants are compounds that reduce the surface tension between the gas and the liquid phase. When present in solution, their concentration in the film layer is enhanced and repulsion between bubbles increases, even for very small concentrations in the liquid (Keitel and Onken, 1982). Therefore, bubbles' coalescence is reduced when surface active compounds are present in solution. Proteins are surface active and therefore tend to reduce coalescence although, their action is highly dependent on the biocatalyst concentration in the reactor. Nevertheless, the effects related to the presence of enzymes in solution on coalescence are not yet well understood.

The required OTR is determined by the stoichiometric oxygen demand and the target productivities. The oxygen consumption rate is determined by the biocatalyst concentration. Theoretical oxygen demands for different oxidoreductase enzymes are summarized in Table 7.5. It should be noticed that some oxygenases may require more than the stoichiometric amount of oxygen due to low coupling efficiencies. A well-known example is the case of cytochrome P450 monooxygenases (Holtmann and Hollmann, 2016; Tavanti et al., 2018).

Table 7.5. Oxygen demand for oxidases and oxygenases assuming soluble enzyme as the catalyst format. The oxygen demand for oxygenases can be higher if uncoupling is observed.

Enzyme class	**Reaction stoichiometry**
Oxygenases	1 mol O_2 per mol product
Oxidases (coupled with catalase to scavenge H_2O_2)	0.5 mol O_2 per mol product

Ideally, the maximum oxygen transfer rate should be equal to, or higher than, the maximum oxygen demand. However, sometimes, that is not the case. For example, to produce a product with a molecular weight of 100 g mol^{-1}, with a stoichiometry of 1 mol of oxygen per mol of product and at

productivity of 10 g L^{-1} h^{-1}, the oxygen demand will be 100 mmol L^{-1} h^{-1}. This rate is close to the limit of the maximum theoretical oxygen transfer rate of a large-scale aerated stirred bioreactor with a k_la of 500 h^{-1} (Charles, 1985). Figure 7.3 shows the maximum theoretical oxygen transfer rate (OTR_{max}) at atmospheric pressure for different k_la, assuming no oxygen dissolved in the medium (OTR_{max} is equal to the saturation concentration of oxygen times the k_la). If a small scale reactor is used, the reaction will be limited by the oxygen transfer rate, since the k_la will be lower than at large-scale. Therefore, care should be taken when investigating enzymatic oxidations in the laboratory in order to not be limited by OTR. Moreover, the molecular weight of the product has a large influence on the oxygen demand. Usually, as the product market value decreases, the molecules tend to be smaller and the required productivities higher. Therefore, for the same productivity, the lower the molecular weight of the product, the higher the oxygen transfer rate required to meet the industrial targets. In this context, as biocatalysis implementation moves towards lower value products, oxygen limitations will be even more severe.

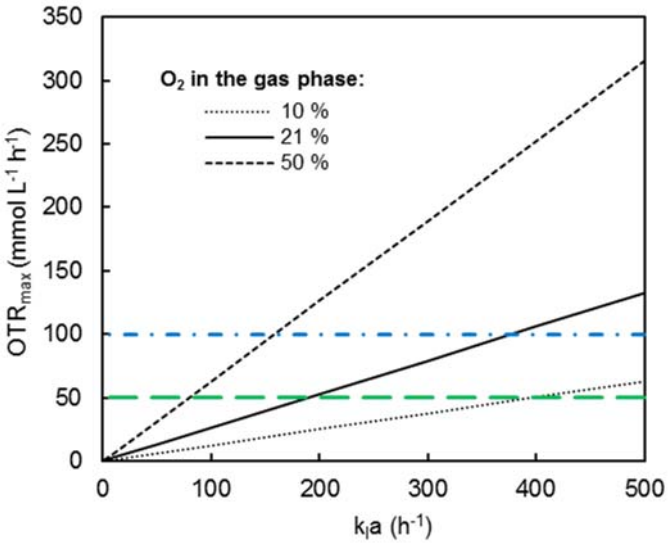

Figure 7.3. Maximum theoretical oxygen transfer rates (OTR_{max}) in a stirred reactor as function of k_la, at atmospheric pressure, assuming a constant driving force equal to the saturation concentration of oxygen, for different oxygen contents in the feed gas. Straight lines represent the oxygen demand of a biocatalytic oxidation of a 100 g mol^{-1} product at a STY of 10 g L^{-1} h^{-1}, using an oxidase (green) or an oxygenase (blue). The intersections represent the operational points where below, the reaction is limited by the oxygen transfer rate.

Since OTR increases with scale, the biocatalyst load should be reduced in bench scale experiments to study the reaction without mass transfer limitations and therefore understand other possible constrains of the reaction system. Indeed, mass transfer limitations can mask other possible limitations such as biocatalyst kinetics and stability. Therefore, identifying the region of mass transfer limitation in the reaction system should be the first stage of the experimental investigation (Nordblad et al., 2018).

It is also important to point out the safety issues related to oxygen. In order to avoid explosive mixtures, the percentage of oxygen in the inlet gas of a bioreactor may need to be reduced. This reduction results on a lower partial pressure of oxygen in the gas phase, which corresponds to a lower oxygen concentration in solution (based on Henry's law). The reduced oxygen concentration will therefore have an effect on the maximum oxygen transfer rates, which will also affect the reaction maximum productivity (Figure 7.3).

In addition to process related limitations, as mentioned before, the enzyme kinetics can also have an effect on the reaction productivities. Oxidase enzymes can have low affinity towards oxygen, meaning that oxygen concentrations using aeration at atmospheric pressure may not be sufficient to use the enzyme efficiently and consequently limit the space-time yield (Ringborg et al., 2017). The effect of enzyme kinetics on the reaction performance is described in more detail in Chapter 2. In summary, oxygen limitations for oxidases are either related to the OTR or to the enzyme efficiency, and both have in common the effect of oxygen solubility in aqueous solution.

Overall, if oxygen mass transfer is the only limitation found at bench scale, scale-up experiments should be implemented since this parameter will improve in large bioreactors. The key point is to assure that laboratory experiments are performed below oxygen mass transfer limitations so constrains related to enzyme kinetics and stability are investigated and considered.

Stability-Related Limitations

In contrast to OTR, biocatalyst stability towards gas-liquid interfaces gets worst with an increase in scale. The gas liquid interfacial area increases with the reactor volume since the k_la increases with scale (Table 7.4). Therefore the biocatalyst is more exposed to this interface. There are few studies in the literature about stability of enzymes in the presence of gas-liquid interfaces nevertheless, it has been shown that this interface can act as a denaturant and the enzyme activity is compromised (Bhagia et al., 2018; Mohanty et al., 2001). It is interesting that there are different definitions of biocatalyst stability. Here, we refer to the biocatalyst kinetic stability, in other words, the time it takes for an enzyme to irreversibly deactivate in the presence of a deactivation agent (in Chapter 4 the various types of enzyme stability are explained with more detail). Therefore, as the availability of interfacial area increases with scale, scale-down experiments should be designed aiming to mimic these conditions. Small-scale reactors should use operational conditions that allow an investigation of the effect of gas-liquid interfacial areas similar to large scale reactors. In Chapter 3, a methodology is proposed to achieve such conditions.

Considering the possible limitations of an oxygen-dependent biocatalyst, alternative methods to aerate stirred reactors for oxygen supply have been studied and are briefly described in the following section.

7.5. Alternative Oxygen Supply Methods

There are several alternative methods to aerate stirred tank reactors for oxygen supply and they can be separated based on the presence or absence of gas-liquid interfaces (Table 7.6). The main purpose of investigating different methods to aerated stirred reactors, is to achieve higher oxygen transfer rates. Therefore, the strategies used include sparging enriched air or pressurized stirred tank reactors. These options increase the oxygen solubility in aqueous solutions, since higher oxygen concentrations can be reached at higher partial pressure (Knoll et al., 2005). However, these strategies result in additional costs associated with energy consumption and the supply of pure oxygen.

Regarding bubble-free oxygen supply methods, membrane technologies are the most common. Nevertheless, membranes create an additional barrier for oxygen transfer and also contribute to additional process costs. If a membrane is submerged in the reactor, the cost is manly related to the membrane technology. On the other hand, if the membrane is located externally to the reactor, the energy required to recirculate the liquid medium is the major additional cost contributor (Pedersen et al., 2017). Although these alternatives aim to increase the oxygen transfer, OTR is not significantly improved. Therefore, membrane technologies should be used with the purpose of avoiding gas-liquid interface and not to increase the oxygen transfer rate. Additionally, if we aim to produce a low or medium value product, the additional costs are not justified and these alternatives may not be viable. However, for the production of high value molecules, alternative methods to aerated stirred reactors may be considered since the cost contribution of oxygen supply is insignificant. The decision of adopting alternative methods is dependent on the biocatalyst. For example, if the biocatalyst deactivates in the presence of gas-liquid interfaces, bubble-free oxygenation methods might be an option.

Table 7.6. Different methods of oxygen supply. Some example are fermentation processes but the principles behind oxygen transfer are the same for biocatalytic oxidations.

Oxygen Supply Methods	
Bubbling Oxygenation	***Examples***
Aerated stirred reactor	Brummund et al., 2016, 2015; Kaluzna et al., 2017
Sparging enriched air in a stirred reactor	Lara et al., 2011
Pressurized stirred reactor	Knoll et al., 2005
Use oxygen vectors in a stirred reactor	Galaction et al., 2015; Quijano et al., 2010; Rols and Goma, 1989
Use an organic cosolvent in a stirred reactor	Ramesh et al., 2016
Bubble-Free Oxygenation	
Membranes technology	Côté et al., 1988; Kaufhold et al., 2012; Moenne et al., 2013; Van Hecke et al., 2009
Enzymes (e.g. decompose H_2O_2 using catalase)	Bolivar et al., 2016; Chapman et al., 2018; Dassama et al., 2012; Morthensen et al., 2017; Schneider et al., 2012

7.6. Scale-down Approach to Investigate Biocatalytic Oxidations

Considering the aspects related to oxygen requirements of biocatalytic oxidations and the limitations related to the biocatalyst and the process, we propose a strategy to investigate these reactions based on an industrially driven scale-down philosophy. Even though industrial targets are the starting point of the suggested approach and are used to benchmark the reaction systems, the primary purpose of scale-down research should be to understand the phenomena behind the observed limitations. No doubt that scale-down experiments should be performed to characterise reaction systems and contribute to a faster scale-up of biocatalytic processes (Truppo, 2017). Though, our role as engineers and scientists is not only to identify process limitations and propose solutions, but is foremost to understand the scientific reasons for such implications. Therefore, scale-down research can contribute to the development of reasoned solutions and strategies for the improvement of biocatalytic processes and, ultimately, to accelerate its industrial implementation.

After considering the research developed in this thesis, we propose a scale-down approach to gain fundamental understanding on enzymatic oxidation reactions and to identify process limitations related to oxygen supply. This approach is illustrated in Figure 7.4 and consists of three different steps. First, the industrial environment is selected based on the process metrics and after that,

possible process limitations are defined. Second, the scale-down experiments are performed in a specific manner, depending on the rate limiting mechanism to investigate (kinetics and/or stability). In this step, the process limitations are identified and will guide further necessary experiments. Third, in order to develop an empirical model, more experiments are performed to obtain specific parameters (K_{MO}, half-life…) and the data is then used to construct a model. The process knowledge obtained will direct protein engineering research towards modifying the biocatalyst according to the industrial needs. Finally, once a model is obtained, process behaviour in large-scale bioreactors can also be predicted.

The proposed scale-down approach is integrated into a conceptual schematic overview for the development of biocatalytic processes, illustrated in Figure 7.5. The flow driver is the process economics, which defines the process metrics. After, the scale-down methodology is applied and the results follow two different paths: process behaviour predictions and protein engineering. The latter aims to modify the biocatalyst based on the process limitations found and on the industrial metrics. It should be noticed that an enzyme may be able to catalyse a target reaction however, it will only be used as a biocatalyst if its activity and stability are sufficient to meet the industrial economic targets. Therefore, the biocatalyst has to be tested to verify if the minimum activity and stability requirements are fulfilled.

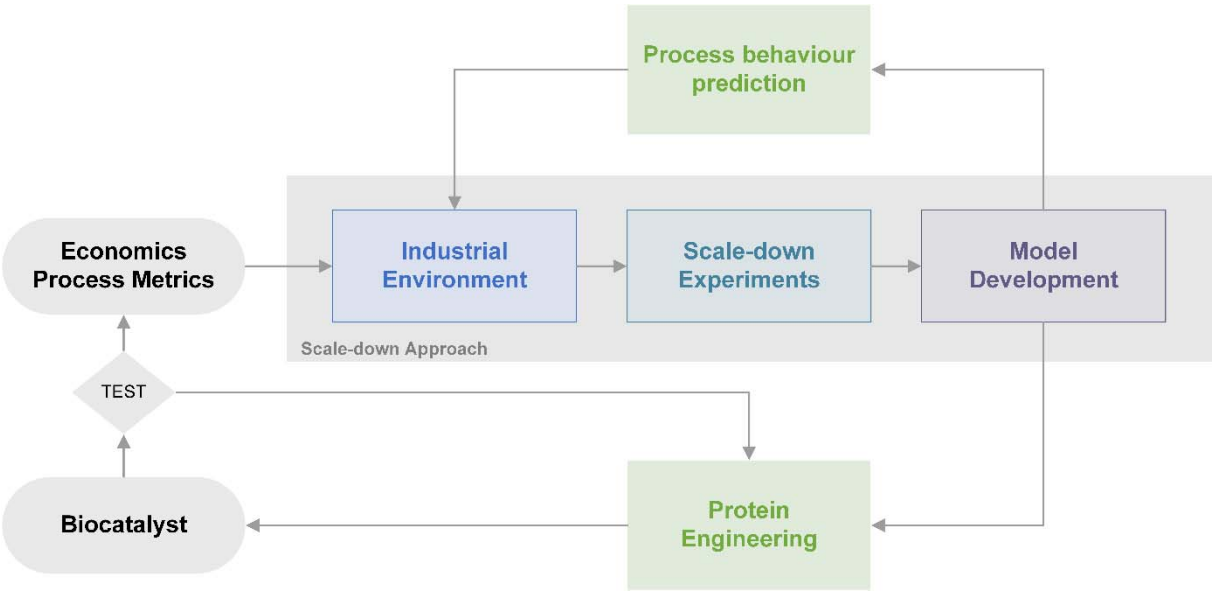

Figure 7.5. Integration of the developed scale-down approach into the biocatalytic processes development flow.

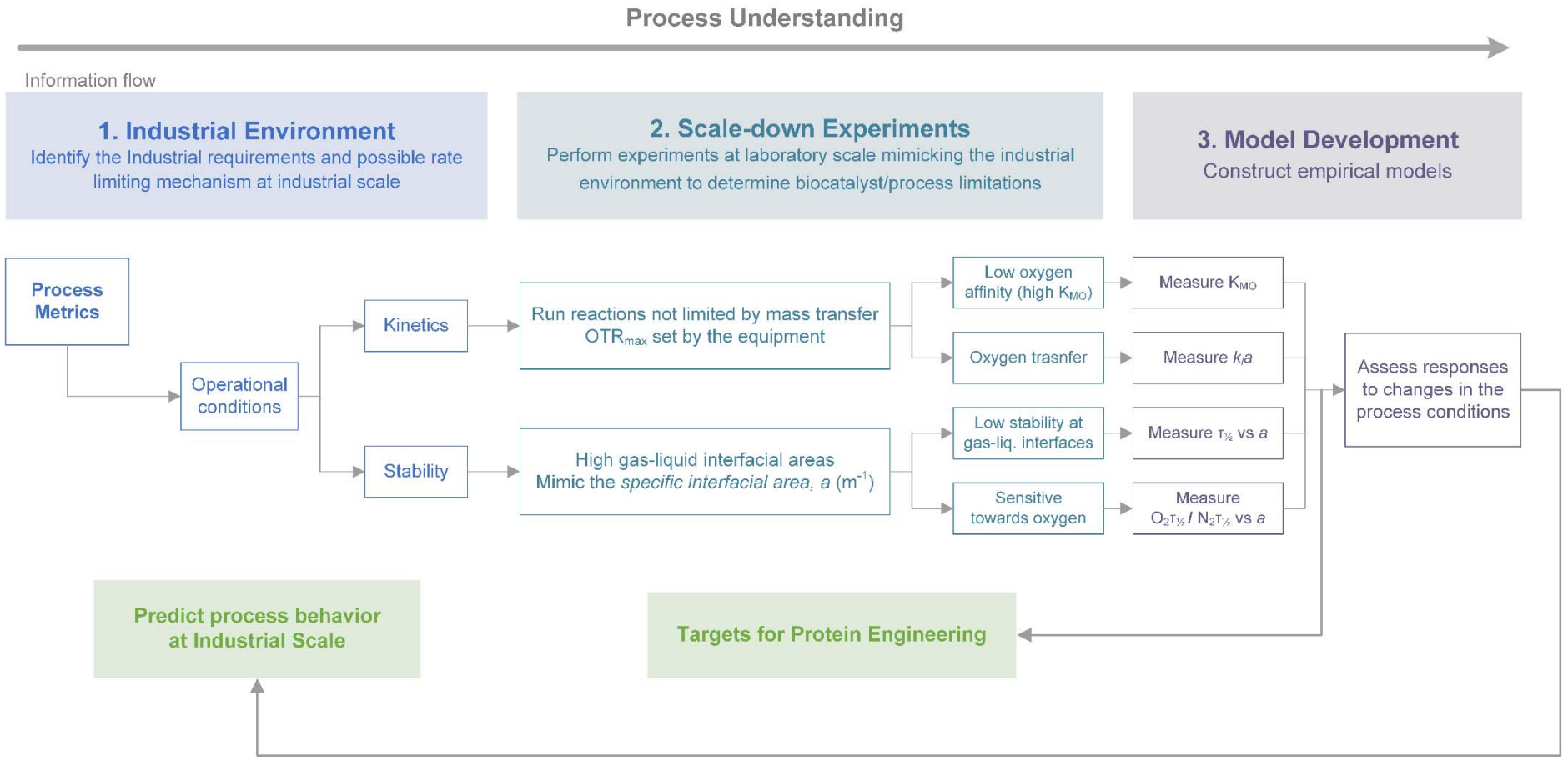

Figure 7.4. Scale-down approach to investigate oxygen dependent biocatalytic oxidation processes.

7.7. Conclusions

Biocatalytic oxidation reactions are a promising alternative to chemocatalysis even though not simple to study in the laboratory and to implement in industry. It can be concluded that the proposed scale-down approach can contribute to a better understanding of oxygen dependent biocatalytic processes and therefore to their faster implementation in industry. From the experimental strategy suggested, it can be concluded that investigating biocatalytic oxidations in the laboratory is not only about mimicking the conditions at industrial scale. A proper scale-down is about defining the rate liming step in industrial scale and simulating it in the laboratory. Contrary to what we might think, in terms of oxygen transfer rate, scale-down experiments are not about trying to mimic the oxygen transfer rates because this parameter improves with scale-up. The reaction in small scale should be run beneath oxygen transfer limitations so the other limitations of the biocatalytic system can be assessed. However, regarding stability towards gas liquid interfaces, it is advised to mimic the conditions for which the enzyme will be exposed because gas-liquid interfaces increase with scale. Therefore, in order to produce stable biocatalysts in the presence of such interfaces, harsh conditions must be tested at an early stage of the process development.

Chapter 8.

Conclusions

Biocatalytic oxidation reactions are of great interest for the synthesis of valuable chemicals. However, to date, they have rarely been implemented at industrial scale due to the complexity that results from the requirement for molecular oxygen. Multiphase systems are generally challenging to operate, but there are well known process engineering strategies to overcome possible complications. In contrast, the interaction between a multiphase system and a biocatalyst is not fully understood and it is difficult to investigate in the laboratory. In order to facilitate the implementation of enzymatic oxidations in industry, these systems have to be better understood and the process limitations should be identified at an early stage of process development. The main conclusions from the research developed in this thesis are presented below:

- A methodology based on reaction trajectory analysis facilitated the identification of the main process limitations of a glucose oxidase (GOx) catalysed reaction. It was found that the main limitations were related to biocatalyst kinetics and oxygen transfer rate. GOx kinetic parameters were investigated in more detail and the K_{MO} was determined to be higher than the solubility of oxygen in aqueous solutions. This means that the system was oxygen limited and, if this reaction is carried out under typical operational conditions (i.e. aeration at atmospheric pressure), the enzyme efficiency is compromised. Furthermore, a regime map of the main process limitations can be drawn based on industrial targets and results from the applied methodology. In conclusion, the identification of process limitations of a biocatalytic reaction system can be accelerated when a systematic experimental methodology is applied.

- For the first time, an experimental method was developed at laboratory scale in order to study enzymes' stability in the presence of gas-liquid interfacial areas, similar to large scale bioreactors. This technique enables in situ quantification of the gas-liquid interfacial area inside an aerated stirred tank reactor. The stability of NAD(P)H oxidase (NOX) was

investigated using this method and it was found that its half-life decreased with the increase in gas-liquid interfacial area, up to a certain limit, where the power input to the reactor was the major cause for enzyme deactivation. Therefore, mechanical stirring and the presence of a gas-liquid interface was investigated separately in order to understand their individual effect on enzyme deactivation. Finally, a correlation between NOX half-life and specific gas-liquid interfacial area (a) was successfully obtained.

- The effect of mechanical stirring in the absence of gas-liquid interfaces on NOX kinetic stability was investigated. It was found that NOX deactivation rate increased with an increase in the power input per volume. It is proposed that the enzyme deactivation is associated with the high frequency of molecular collisions in the reactor, caused by the stirring power input. Therefore, shear does not directly cause protein deactivation but it is indeed indirectly related to enzyme deactivation since the increase of shear rate causes higher frequency of protein-protein and protein-wall collisions.

- The kinetic stability of different NOXs variants (non-purified CFE), whose thermodynamic stability was improved, was tested under the same stirring power input conditions. The kinetic and thermodynamic stability of these enzyme was compared and no correlation was found between the enzymes half-life and melting temperature. This study demonstrates the importance of investigating enzyme kinetic stability under relevant industrial conditions, when an enzyme is used as a biocatalyst. Furthermore, these same variants were subjected to different cell lysis methods and their activity and stability are dependent on the final enzyme formulation.

- The effect of gas-liquid interfaces on NOX kinetic stability was studied in a laboratory scale bubble column, where the gas-liquid interfacial area was well defined. It was found that with the increase of interfacial area, the enzyme deactivation increased but in different ways, depending on the enzyme. These results indicate that deactivation at gas-liquid interfaces is enzyme-dependent. Furthermore, it was shown that NOX deactivation was faster when air was used instead of nitrogen. So, the presence of oxygen enhances the deactivation rates possibly by (over)oxidising certain amino acid residues of the enzyme.

- A regime map identifying the dominating causes for enzyme deactivation related to gas supply and mechanical stirring was proposed. This map is highly enzyme dependent since the boundaries between regions were found to be very different within the same enzyme subclass. This observation indicates that the hydrophobicity of the gas-liquid interface (and most likely the reactor walls) induces hydrophobic interactions with the protein, which promotes changes on its three dimensional structure causing stability loss.

- A scale-down approach for biocatalytic oxidation reactions was developed based on an industrially driven scale-down philosophy with the purpose of acquiring fundamental understanding of the biocatalyst kinetics and stability. This approach suggests that in terms of oxygen transfer rate (OTR), scale-down experiments should be run beneath the oxygen transfer limitation of the laboratory equipment and not by simulating the same OTRs achieved in a large-scale bioreactor because OTR improves with scale-up. Regarding stability towards gas-liquid interfaces, experiments should mimic the gas-liquid interfacial area of a large scale reactor, since enzymes are exposed to a larger interfacial area in industrial scale.

To conclude, a conceptual map indicating the operating window for biocatalytic oxidation reactions as a function of mechanical stirring and gas supply is presented in Figure 6.1. This window is bounded by process limitations although the limits are not well defined yet. Therefore, further research is required to better understand and quantify the limits between the different regions.

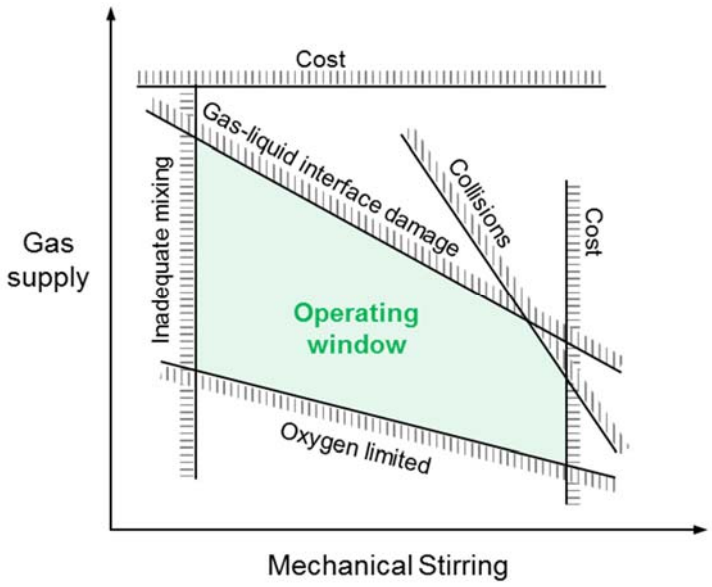

Figure 6.1. Conceptual regime map summarizing process limitations for biocatalytic oxidations.

Chapter 9.

Future Perspectives

In order to extend the work presented in this thesis, future research topics are suggested in this chapter. The lines of research here presented aim to contribute to the development and implementation of biocatalytic oxidations in industry in the foreseeable future.

- Determining the K_{MO} of oxygen dependent enzymes as a routine characterisation experiment allows the identification of oxygen limitations at an early stage of process development. The automated tube-in-tube reactor (TiTR) offers the possibility to determine the kinetics of oxygen dependent enzymes efficiently and accurately (Ringborg et al., 2017).

- To further understand the molecular explanation for enzyme deactivation at gas liquid-interfaces, hydrophobicity interactions with the enzyme should be investigated in a controlled environment, and the effect on the protein structure measured. Experiments using purified protein and a defined contact area, while changing the hydrophobicity of such an area could contribute to a better understanding of the effect. For example, the reactor surface (reactor walls) can affect enzyme deactivation depending on the hydrophobicity of the material (Colombié et al., 2001a). Therefore, changing the contact area and test materials with different hydrophobicity would indicate the effect of the reactor material on enzyme deactivation and elucidate its choice for industrial application. Experiments can also be performed using organic solvents with different hydrophobicity, although the activity of the enzyme in the presence of the organic solvent would have to be tested prior to the study. If it is shown that hydrophobicity is a major cause for enzyme deactivation in the presence of gas-liquid interfaces, screening for enzymes that are tolerant to hydrophobic interactions could generate more robust biocatalysts from the start, prior to the development of a biocatalytic oxidation process.

- The effects related to the presence of enzymes on coalescence are not well understood. The coalescence of a reaction medium affects the oxygen transfer rate of a system, which is dependent on the reactor scale (Noorman, 2016). Therefore, determining whether the presence of enzymes in solution contributes to coalescing or non-coalescing conditions would indicate the relevance of the reactor scale in the process development. Current reports pf such observations require clarification.

- Biocatalysis is moving towards the development of cascade reactions catalysed by multienzymatic systems (Sperl and Sieber, 2018). If an oxidation reaction catalysed by an oxygen dependent enzyme is present in the cascade, molecular oxygen has to be supplied. Moreover, if a common aerated stirred tank reactor is used and the cascade reaction is run in the same tank, all enzymes will be exposed to gas-liquid interfaces and their stability may be affected. Therefore, the stability of all enzymes has to be investigated towards gas-liquid interfaces and the methodology presented in this thesis offers a way to investigate this issue.

- The application of continuous flow processes in biocatalysis has been gaining great interest in recent years (Britton et al., 2018; Tamborini et al., 2018). In order to run biocatalytic processes continuously, the stability of the biocatalyst is crucial to a successful process. Therefore, investigation of the kinetic stability of enzymes should be done as part of the characterisation routine of a new biocatalyst, considering the scale-down philosophy discussed in this thesis.

- Alternative methods to an aerated stirred tank reactor that avoid gas-liquid interfaces should be further investigated, especially if the biocatalyst stability in the presence of such interfaces cannot be improved by protein engineering. For example, investigation of membrane technologies and immobilization of enzymes in a membrane system could be a possibility for continuous flow processes.

- With the great developments in the field of biocatalysis it is possible that in the near future more lower priced chemical products will be made using biocatalysis (Rudroff et al., 2018). In this context, for a more reliable and systematic implementation of industrial biocatalytic oxidations, research on enzyme stability in order to develop more robust biocatalysts is essential and the methodology presented here can be used as a guideline.

References

Abu, R., Woodley, J.M., 2015. Application of Enzyme Coupling Reactions to Shift Thermodynamically Limited Biocatalytic Reactions. *ChemCatChem* 7, 3094–3105.

Amaya-Bower, L., Lee, T., 2010. Single bubble rising dynamics for moderate Reynolds number using Lattice Boltzmann Method. *Comput Fluids* 39, 1191–1207.

Arnold, F.H., 2018. Directed Evolution: Bringing New Chemistry to Life. *Angew Chemie - Int Ed* 57, 4143–4148.

Arnold, F.H., Wintrode, P.L., Miyazaki, K., Gershenson, A., 2001. How enzymes adapt: Lessons from directed evolution. *Trends Biochem Sci* 26, 100–106.

Bach, C., Yang, J., Larsson, H., Stocks, S.M., Gernaey, K. V, Albaek, M.O., Krühne, U., 2017. Evaluation of mixing and mass transfer in a stirred pilot scale bioreactor utilizing CFD. *Chem Eng Sci* 171, 19–26.

Bhagia, S., Dhir, R., Kumar, R., Wyman, C.E., 2018. Deactivation of Cellulase at the Air-Liquid Interface Is the Main Cause of Incomplete Cellulose Conversion at Low Enzyme Loadings. *Sci Rep* 8, 1350.

Birmingham, W.R., Turner, N.J., 2018. A Single Enzyme Oxidative “cascade” via a Dual-Functional Galactose Oxidase. *ACS Catal* 8, 4025–4032.

Bolivar, J.M., Schelch, S., Pfeiffer, M., Nidetzky, B., 2016. Intensifying the O2-dependent heterogeneous biocatalysis: Superoxygenation of solid support from H2O2 by a catalase tailor-made for effective immobilization. *J Mol Catal B Enzym* 134, 302–309.

Bommarius, A.S., 2015. Biocatalysis: A Status Report. *Annu Rev Chem Biomol Eng* 6, 319–345.

Bommarius, A.S., Broering, J.M., 2005. Established and novel tools to investigate biocatalyst stability. *Biocatal Biotransformation* 23, 125–139.

Bommarius, A.S., Karau, A., 2005. Deactivation of Formate Dehydrogenase (FDH) in solution and at gas-liquid interfaces. *Biotechnol Prog* 21, 1663–1672.

Bommarius, A.S., Paye, M.F., 2013. Stabilizing biocatalysts. *Chem Soc Rev* 42, 6534.

Bornscheuer, U.T., Huisman, G.W., Kazlauskas, R.J., Lutz, S., Moore, J.C., Robins, K., 2012. Engineering the third wave of biocatalysis. *Nature* 485, 185–194.

Brummund, J., Müller, M., Schmitges, T., Kaluzna, I., Mink, D., Hilterhaus, L., Liese, A., 2016. Process development for oxidations of hydrophobic compounds applying cytochrome P450 monooxygenases in-vitro. *J Biotechnol* 233, 143–150.

Brummund, J., Sonke, T., Müller, M., 2015. Process Development for Biocatalytic Oxidations Applying Alcohol Dehydrogenases. *Org Process Res Dev* 19, 1590–1595.

Burton, S.G., 2003. Oxidizing enzymes as biocatalysts. *Trends Biotechnol* 21, 543–549.

Cahn, J.K.B., Werlang, C.A., Baumschlager, A., Brinkmann-Chen, S., Mayo, S.L., Arnold, F.H., 2017. A General Tool for Engineering the NAD/NADP Cofactor Preference of Oxidoreductases. *ACS Synth Biol* 6, 326–333.

Caussette, M., Gaunand, A., Planche, H., Colombie, S., Monsan, P., Lindet, B., 1999. Lysozyme inactivation by inert gas bubbling: kinetics in a bubble column reactor. *Enzyme Microb Technol* 24, 412–418.

Caussette, M., Planche, H., Delepine, S., Monsan, P., Gaunand, A., Lindet, B., 1997. The self catalytic enzyme inactivation induced by solvent stirring: a new example of protein conformational change induction. *Protein Eng* 10, 1235–1240.

Chaiyen, P., Fraaije, M.W., Mattevi, A., 2012. The enigmatic reaction of flavins with oxygen. *Trends Biochem Sci* 37, 373–380.

Chapman, M.R., Cosgrove, S.C., Turner, N.J., Kapur, N., Blacker, A.J., 2018. Highly Productive Oxidative Biocatalysis in Continuous Flow by Enhancing the Aqueous Equilibrium Solubility of Oxygen. *Angew Chemie - Int Ed* 57, 10535–10539.

Charles, M., 1985. Fermentation scale-up: Problems and possibilities. *Trends Biotechnol* 3, 134–139.

Charm, S.E., Wong, B.L., 1970. Enzyme inactivation with shearing. *Biotechnol Bioeng* 12, 1103–1109.

Chen, K., Arnold, F.H., 1993. Tuning the activity of an enzyme for unusual environments: sequential random mutagenesis of subtilisin E for catalysis in dimethylformamide. *Proc Natl Acad Sci* 90, 5618–5622.

Choi, J.M., Han, S.S., Kim, H.S., 2015. Industrial applications of enzyme biocatalysis: Current status and future aspects. *Biotechnol Adv* 33, 1443–1454.

Clift, R., Grace, J.R., Weber, M.E., 1978. Bubbles, Drops and Particles, Academic Press New York.

Colombié, S., Gaunand, A., Lindet, B., 2001a. Lysozyme inactivation under mechanical stirring: effect of physical and molecular interfaces. *Enzyme Microb Technol* 28, 820–826.

Colombié, S., Gaunand, A., Lindet, B., 2001b. Lysozyme inactivation and aggregation in stirred-reactor. *J Mol Catal - B Enzym* 11, 559–565.

Colombié, S., Gaunand, A., Rinaudo, M., Lindet, B., 2000. Irreversible lysozyme inactivation and aggregation induced by stirring: Kinetic study and aggregates characterisation. *Biotechnol Lett* 22, 277–283.

Cornish-Bowden, A., 2014. Reactions of More than One Substrate, in: Fundamentals of Enzyme Kinetics. pp. 189–226.

Cornish-Bowden, A., 1979. Introduction to enzyme kinetics, in: Fundamentals of Enzyme Kinetics. pp. 16–38.

Côté, P., Bersillon, J., Huyard, A., Faup, G., 1988. Bubble-Free Aeration Using Membranes : Process Analysis. *Water Pollut Control Fed* 60, 1986–1992.

Dassama, L.M.K., Yosca, T.H., Conner, D. a, Lee, M.H., Blanc, B., Streit, B.R., Green, M.T., DuBois, J.L., Krebs, C., Bollinger, J.M., 2012. O(2)-evolving chlorite dismutase as a tool for studying O(2)-utilizing enzymes. *Biochemistry* 51, 1607–16.

Davids, T., Schmidt, M., Böttcher, D., Bornscheuer, U.T., 2013. Strategies for the discovery and engineering of enzymes for biocatalysis. *Curr Opin Chem Biol* 17, 215–220.

de Barros, D.P.C., Pinto, F., Pfluck, A.C.D., Dias, A.S.A., Fernandes, P., Fonseca, L.P., 2018. Improvement of enzyme stability for alkyl esters synthesis in miniemulsion systems by using media engineering. *J Chem Technol Biotechnol* 93, 1338–1346.

Delvigne, F., Noorman, H., 2017. Scale-up/Scale-down of microbial bioprocesses: a modern light on an old issue. *Microb Biotechnol* 10, 685–687.

Demming, R.M., Fischer, M.P., Schmid, J., Hauer, B., 2018. (De)hydratases — recent developments and future perspectives. *Curr Opin Chem Biol* 43, 43–50.

Donaldson, T.L., Boonstra, E.F., Hammond, J.M., 1980. Kinetics of protein denaturation at gas-liquid interfaces. *J Colloid Interface Sci* 74, 441–450.

Dong, J.J., Fernández-Fueyo, E., Hollmann, F., Paul, C.E., Pesic, M., Schmidt, S., Wang, Y., Younes, S., Zhang, W., 2018. Biocatalytic Oxidation Reactions: A Chemist's Perspective. *Angew Chemie - Int Ed* 57, 9238–9261.

Dubey, M.K., Zehra, A., Aamir, M., Meena, M., Ahirwal, L., Singh, S., Shukla, S., Upadhyay, R.S., Bueno-Mari, R., Bajpai, V.K., 2017. Improvement strategies, cost effective production, and potential applications of fungal glucose oxidase (GOD): Current updates. *Front Microbiol* 8, 1–22.

Dumeignil, F., Guehl, M., Gimbernat, A., Capron, M., Lopes Ferreira, N., Froidevaux, R., Girardon, J.-S., Wojcieszak, R., Dhulster, P., Delcroix, D., 2018. From sequential chemoenzymatic synthesis to integrated hybrid catalysis: Taking the best of both worlds to open up the scope of possibilities for a sustainable future. *Catal Sci Technol* DOI: 10.1039/C8CY01190G.

Ferrandi, E.E., Monti, D., Riva, S., 2014. New Trends in the In Situ Enzymatic Recycling of NAD(P)(H) Cofactors, in: Cascade Biocatalysis: Integrating Stereoselective and Environmentally Friendly Reactions. pp. 23–42.

Findrik, Z., Valentović, I., Vasić-Rački, D., 2014. A mathematical model of oxidative deamination of amino acid catalyzed by two D-amino acid oxidases and influence of aeration on enzyme stability. *Appl Biochem Biotechnol* 172, 3092–3105.

Gabelle, J.C., Augier, F., Carvalho, A., Rousset, R., Morchain, J., 2011. Effect of tank size on kLa and mixing time in aerated stirred reactors with non-newtonian fluids. *Can J Chem Eng* 89, 1139–1153.

Gadda, G., 2012. Oxygen activation in flavoprotein oxidases: The importance of being positive. *Biochemistry* 51, 2662–2669.

Galaction, A., Blaga, A.C., Ciobanu, C.P., Turnea, M., Ca, D., 2015. Distribution of Oxygen Transfer Rates in Stirred Bioreactor for Different Fermentation Broths - Oxygen-Vector Dispersions. *Environ Eng Manag J* 14, 433–447.

Garcia-Ochoa, F., Gomez, E., 2009. Bioreactor scale-up and oxygen transfer rate in microbial processes: An overview. *Biotechnol Adv* 27, 153–176.

Garcia-Ochoa, F., Gomez, E., 2004. Theoretical prediction of gas-liquid mass transfer coefficient, specific area and hold-up in sparged stirred tanks. *Chem Eng Sci* 59, 2489–2501.

Garcia, J.R., Cha, H.J., Rao, G., Marten, M.R., Bentley, W.E., 2009. Microbial nar-GFP cell sensors reveal oxygen limitations in highly agitated and aerated laboratory-scale fermentors. *Microb Cell Fact* 8, 6–12.

Ghadge, R.S., Patwardhan, A.W., Sawant, S.B., Joshi, J.B., 2005. Effect of flow pattern on cellulase deactivation in stirred tank bioreactors. *Chem Eng Sci* 60, 1067–1083.

Ghatorae, A.S., Guerra, M.J., Bell, G., Halling, P.J., 1994. Immiscible organic solvent inactivation of urease, chymotrypsin, lipase, and ribonuclease: Separation of dissolved solvent and interfacial effects. *Biotechnol Bioeng* 44, 1355–1361.

Gibson, Q.H., Swoboda, B.E., Massey, V., 1964. Kinetics and Mechanism of Action of Glucose Oxidase. *J Biol Chem* 239, 3927–3934.

Gkotsi, D.S., Dhaliwal, J., McLachlan, M.M., Mulholand, K.R., Goss, R.J., 2018. Halogenases: powerful tools for biocatalysis (mechanisms applications and scope). *Curr Opin Chem Biol* 43, 119–126.

Goswami, P., Chinnadayyala, S.S.R., Chakraborty, M., Kumar, A.K., Kakoti, A., 2013. An overview on alcohol oxidases and their potential applications. *Appl Microbiol Biotechnol* 97, 4259–4275.

Grogan, G., 2018. Synthesis of chiral amines using redox biocatalysis. *Curr Opin Chem Biol* 43, 15–22.

Grompone von Gioi, R., Jakubowicz, J., Morel, J.-M., Randall, G., 2012. LSD: a Line Segment Detector. *Image Process Line*.

Hammer, S.C., Knight, A.M., Arnold, F.H., 2017. Design and evolution of enzymes for non-natural chemistry. *Curr Opin Green Sustain Chem* 7, 23–30.

Hardy, N., Augier, F., Nienow, A.W., Béal, C., Ben Chaabane, F., 2017. Scale-up agitation criteria for Trichoderma reesei fermentation. *Chem Eng Sci* 172, 158–168.

Hewitt, C.J., Nienow, A.W., 2007. The Scale-Up of Microbial Batch and Fed-Batch Fermentation Processes. *Adv Appl Microbiol* 62, 105–135.

Hollmann, F., Arends, I.W.C.E., Buehler, K., Schallmey, A., Bühler, B., 2011. Enzyme-mediated oxidations for the chemist. *Green Chem.* 13, 226–265.

Holtmann, D., Hollmann, F., 2016. The Oxygen Dilemma: A Severe Challenge for the Application of Monooxygenases? *ChemBioChem* 1391–1398.

Hoschek, A., Bühler, B., Schmid, A., 2017. Overcoming the Gas–Liquid Mass Transfer of Oxygen by Coupling Photosynthetic Water Oxidation with Biocatalytic Oxyfunctionalization. *Angew Chemie - Int Ed* 56, 15146–15149.

Hudcova, V., Machon, V., Nienow, A.W., 1989. Gas–liquid dispersion with dual Rushton impellers. *Biotechnol Bioeng* 34, 617–628.

Hummel, W., Gröger, H., 2014. Strategies for regeneration of nicotinamide coenzymes emphasizing self-sufficient closed-loop recycling systems. *J Biotechnol* 191, 22–31.

Junker, B., Maciejak, W., Darnell, B., Lester, M., Pollack, M., 2007. Feasibility of an in situ measurement device for bubble size and distribution. *Bioprocess Biosyst Eng* 30, 313–326.

Kaluzna, I., Brummund, J., Schuermann, M., 2017. Production of diclofenac metabolites by applying cytochrome P450 technology. *Chim Oggi/Chemistry Today* 35, 55–58.

Kaufhold, D., Kopf, F., Wolff, C., Beutel, S., Hilterhaus, L., Hoffmann, M., Scheper, T., Schlüter, M., Liese, A., 2012. Generation of Dean vortices and enhancement of oxygen transfer rates in membrane contactors for different hollow fiber geometries. *J Memb Sci* 423–424, 342–347.

Keitel, G., and Onken, U. (1982). The effect of solutes on bubble size in air-water dispersions. *Chem Eng Commun* 17, 85–98.

Knoll, A., Maier, B., Tscherrig, H., Büchs, J., 2005. The oxygen mass transfer, carbon dioxide inhibition, heat removal, and the energy and cost efficiencies of high pressure fermentation. *Adv Biochem Eng Biotechnol* 92, 77–99.

Kolmogorov, A.N., 1991. The local structure of turbulence in incompressible viscous fluid for very large Reynolds numbers. *Proc R Soc Lond A* 434, 9–13.

Kroutil, W., Mang, H., Edegger, K., Faber, K., 2004. Biocatalytic oxidation of primary and secondary alcohols. *Adv Synth Catal* 346, 125–142.

Laakkonen, M., Moilanen, P., Miettinen, T., Saari, K., Honkanen, M., Saarenrinne, P., Aittamaa, J., 2005. Local bubble size distributions in agitated vessel comparison of three experimental techniques. *Chem Eng Res Des* 83, 50–58.

Lalonde, J., 2016. Highly engineered biocatalysts for efficient small molecule pharmaceutical synthesis. *Curr Opin Biotechnol* 42, 152–158.

Lara, A.R., Knabben, I., Regestein, L., Sassi, J., Caspeta, L., Ramírez, O.T., Büchs, J., 2011. Comparison of oxygen enriched air vs. pressure cultivations to increase oxygen transfer and to scale-up plasmid DNA production fermentations. *Eng Life Sci* 11, 382–386.

Law, H.E.M., Baldwin, C.V.F., Chen, B.H., Woodley, J.M., 2006. Process limitations in a whole-cell catalysed oxidation: Sensitivity analysis. *Chem Eng Sci* 61, 6646–6652.

Leak, D.J., Sheldon, R.A., Woodley, J.M., Adlercreutz, P., 2009. Biocatalysts for selective introduction of oxygen. *Biocatal Biotransformation* 27, 1–26.

Leskovac, V., Trivi´ctrivi´c, S., Wohlfahrt, G., Kandrač, J., Peričin, D., 2005. Glucose oxidase from Aspergillus niger: the mechanism of action with molecular oxygen, quinones, and one-electron acceptors. *Int J Biochem Cell Biol* 37, 731–750.

Lima-Ramos, J., Tufvesson, P., Woodley, J.M., 2014. Application of environmental and economic metrics to guide the development of biocatalytic processes. *Green Process Synth* 3, 195–213.

Liu, J., Wu, S., Li, Z., 2018. Recent advances in enzymatic oxidation of alcohols. *Curr Opin Chem Biol* 43, 77–86.

Lountos, G.T., Jiang, R., Wellborn, W.B., Thaler, T.L., Bommarius, A.S., Orville, A.M., April, R. V, Re, V., Recei, M., June, V., 2006. The Crystal Structure of NAD(P)H Oxidase from Lactobacillus sanfranciscensis : Insights into the Conversion of O2 into Two Water Molecules by the Flavoenzyme. *Biochemistry* 45, 9648–9659.

Lowe, D.G., 1985. Perceptual organization and visual recognition. *Comput Vision, Graph Image Process* 31, 394.

Lundemo, M.T., Woodley, J.M., 2015. Guidelines for development and implementation of biocatalytic P450 processes. *Appl Microbiol Biotechnol* 99, 2465–2483.

Ma, S.K., Gruber, J., Davis, C., Newman, L., Gray, D., Wang, A., Grate, J., Huisman, G.W., Sheldon, R.A., 2010. A green-by-design biocatalytic process for atorvastatin intermediate. *Green Chem* 12, 81–86.

Martínez, A.T., Ruiz-Dueñas, F.J., Camarero, S., Serrano, A., Linde, D., Lund, H., Vind, J., Tovborg, M., Herold-Majumdar, O.M., Hofrichter, M., Liers, C., Ullrich, R., Scheibner, K., Sannia, G., Piscitelli, A., Pezzella, C., Sener, M.E., Kılıç, S., Van Berkel, W.J.H., Guallar, V., Lucas, M.F., Zuhse, R., Ludwig, R., Hollmann, F., Fernández-Fueyo, E., Record, E., Faulds, C.B., Tortajada, M., Winckelmann, I., Rasmussen, J.-A., Gelo-Pujic, M., Gutiérrez, A., Del Río, J.C., Rencoret, J., Alcalde, M., 2017. Oxidoreductases on their way to industrial biotransformations. *Biotechnol Adv* 35, 815–831.

Mattevi, A., 2006. To be or not to be an oxidase: challenging the oxygen reactivity of flavoenzymes. *Trends Biochem Sci* 31, 276–283.

Middleman, S., 1998. An Introduction to Mass and Heat Transfer: Principles of Analysis and Design. John Wiley & Sons, New York.

Moenne, M.I., Mouret, J.R., Sablayrolles, J.M., Agosin, E., Farines, V., 2013. Control of bubble-free oxygenation with silicone tubing during alcoholic fermentation. *Process Biochem* 48, 1453–1461.

Mohanty, M., Ghadge, R.S., Patil, N.S., Sawant, S.B., Joshi, J.B., Deshpande, A. V., 2001. Deactivation of lipase at gas-liquid interface in stirred vessel. *Chem Eng Sci* 56, 3401–3408.

Morthensen, S.T., Meyer, A.S., Jørgensen, H., Pinelo, M., 2017. Significance of membrane bioreactor design on the biocatalytic performance of glucose oxidase and catalase: Free vs. immobilized enzyme systems. *Biochem Eng J* 117, 41–47.

Narsimhan, G., Uraizee, F., 1992. Kinetics of Adsorption of Globular Proteins at an Air-Water Interface. *Biotechnol Prog* 8, 187–196.

Neubauer, P., Junne, S., 2010. Scale-down simulators for metabolic analysis of large-scale bioprocesses. *Curr Opin Biotechnol* 21, 114–121.

Nienow, A.W., Nordkvist, M., Boulton, C.A., 2011. Scale-down/scale-up studies leading to improved commercial beer fermentation. *Biotechnol J* 6, 911–925.

Nienow, A.W., Scott, W.H., Hewitt, C.J., Thomas, C.R., Lewis, G., Amanullah, A., Kiss, R., Meier, S.J., 2013. Scale-down studies for assessing the impact of different stress parameters on growth and product quality during animal cell culture. *Chem Eng Res Des* 91, 2265–2274.

Noorman, H., 2016. Scale-Up and Scale-Down, in: Villadsen, J. (Ed.), Fundamental Bioengineering. Wiley-VCH Verlag GmbH & Co. KGaA, Weinheim, pp. 463–498.

Noorman, H., 2011. An industrial perspective on bioreactor scale-down: What we can learn from combined large-scale bioprocess and model fluid studies. *Biotechnol J* 6, 934–943.

Nordblad, M., Dias Gomes, M., Meissner, M.P., Ramesh, H., Woodley, J.M., 2018. Scoping Biocatalyst Performance using Reaction Trajectory Analysis. *Org Process Res Dev* 22, 1101–1114.

Nordkvist, M., Nielsen, P.M., Villadsen, J., 2007. Oxidation of Lactose to Lactobionic Acid by a Microdochium nivale Carbohydrate Oxidase: Kinetics and Operational Stability. *Biotechnol Bioeng* 97, 694–707.

Onken, U., Liefke, E., 1989. Effect of Total and Partial Pressure (Oxygen and Carbon Dioxide) on Aerobic Microbial Processes, in: Advances in Biochemical Engineering/Biotechnology. pp. 137–169.

Park, J.T., Hirano, J.I., Thangavel, V., Riebel, B.R., Bommarius, A.S., 2011. NAD(P)H oxidase v from Lactobacillus plantarum (NoxV) displays enhanced operational stability even in absence of reducing agents. *J Mol Catal B Enzym* 71, 159–165.

Patil, N.S., Ghadge, R.S., Sawant, S.B., Joshi, J.B., 2000. Lipase deactivation at gas–liquid interface and its subsequent reactivation. *AIChE J* 46, 1280–1283.

Pătrăucean, V., Gurdjos, P., Von Gioi, R.G., 2012. A parameterless line segment and elliptical arc detector with enhanced ellipse fitting, in: Lecture Notes in Computer Science (Including Subseries Lecture Notes in Artificial Intelligence and Lecture Notes in Bioinformatics). pp. 572–585.

Paul, E.L., Atiemo-obeng, V.A., Kresta, S.M., 2004. Handbook of Industrial Mixing.

Pedersen, A.T., Birmingham, W.R., Rehn, G., Charnock, S.J., Turner, N.J., Woodley, J.M., 2015. Process requirements of galactose oxidase catalyzed oxidation of alcohols. *Org Process Res Dev* 19, 1580–1589.

Pedersen, A.T., Woodley, J.M., Krühne, U., 2017. Oxygen Dependent Biocatalytic Processes Pedersen,. Kgs. Lyngby: Technical University of Denmark (DTU).

Perriman, A.W., Henderson, M.J., Holt, S.A., White, J.W., 2007. Effect of the air-water interface on the stability of beta-lactoglobulin. *J Phys Chem B* 111, 13527–13537.

Petschacher, B., Staunig, N., Müller, M., Schürmann, M., Mink, D., De Wildeman, S., Gruber, K., Glieder, A., 2014. Cofactor Specificity Engineering of Streptococcus mutans NADH Oxidase 2 for NAD(P)(+) Regeneration in Biocatalytic Oxidations. *Comput Struct Biotechnol J* 9, e201402005.

Pickl, M., Fuchs, M., Glueck, S.M., Faber, K., 2015. The substrate tolerance of alcohol oxidases. *Appl Microbiol Biotechnol* 99, 6617–6642.

Polizzi, K.M., Bommarius, A.S., Broering, J.M., Chaparro-Riggers, J.F., 2007. Stability of biocatalysts. *Curr Opin Chem Biol* 11, 220–225.

Pollard, D.J., Woodley, J.M., 2007. Biocatalysis for pharmaceutical intermediates: the future is now. *Trends Biotechnol* 25, 66–73.

Porter, J.L., Rusli, R.A., Ollis, D.L., 2016. Directed Evolution of Enzymes for Industrial Biocatalysis. *ChemBioChem* 17, 197–203.

Price, J., Nordblad, M., Martel, H.H., Chrabas, B., Wang, H., Nielsen, P.M., Woodley, J.M., 2016. Scale-up of industrial biodiesel production to 40 m3 using a liquid lipase formulation. *Biotechnol Bioeng* 113, 1719–1728.

Quijano, G., Hernandez, M., Villaverde, S., Thalasso, F., Mu??oz, R., 2010. A step-forward in the characterization and potential applications of solid and liquid oxygen transfer vectors. *Appl Microbiol Biotechnol* 85, 543–551.

Raimundo, P.M., Cartellier, A., Beneventi, D., Forret, A., Augier, F., 2016. A new technique for in-situ measurements of bubble characteristics in bubble columns operated in the heterogeneous regime. *Chem Eng Sci* 155, 504–523.

Ramesh, H., Mayr, T., Hobisch, M., Borisov, S., Klimant, I., Krühne, U., Woodley, J.M., 2016. Measurement of oxygen transfer from air into organic solvents. *J Chem Technol Biotechnol* 91, 832–836.

Rehn, G., Pedersen, A.T., Woodley, J.M., 2016. Application of NAD(P)H oxidase for cofactor regeneration in dehydrogenase catalyzed oxidations. *J Mol Catal B Enzym* 134, 331–339.

Ringborg, R.H., Toftgaard Pedersen, A., Woodley, J.M., 2017. Automated Determination of Oxygen-Dependent Enzyme Kinetics in a Tube-in-Tube Flow Reactor. *ChemCatChem* 9, 3273.

Ringborg, R.H., Woodley, J.M., 2016. The application of reaction engineering to biocatalysis. *React Chem Eng* 1, 10–22.

Rols, J.L., Goma, G., 1989. Enhancement of oxygen transfer rates in fermentation using oxygen-vectors. *Biotechnol Adv* 7, 1–14.

Romero, E., Gómez Castellanos, J.R., Gadda, G., Fraaije, M.W., Mattevi, A., 2018. Same Substrate, Many Reactions: Oxygen Activation in Flavoenzymes. *Chem Rev* 118,1742-1769.

Sadana, A., 1988. Enzyme Deactivation. *Biotechnol Adv* 6, 349–446.

Sanchez-Ruiz, J.M., 2010. Protein kinetic stability. *Biophys Chem* 148, 1–15.

Savile, C.K., Janey, J.M., Mundorff, E.C., Moore, J.C., Tam, S., Jarvis, W.R., Colbeck, J.C., Krebber, A., Fleitz, F.J., Brands, J., Devine, P.N., Huisman, G.W., Hughes, G.J., 2010. Biocatalytic Asymmetric Synthesis of Chiral Amines from Ketones Applied to Sitagliptin Manufacture. *Science* 329, 305–308.

Schneider, K., Dorscheid, S., Witte, K., Giffhorn, F., Heinzle, E., 2012. Controlled feeding of hydrogen peroxide as oxygen source improves production of 5-ketofructose From L-sorbose using engineered pyranose 2-oxidase from Peniophora gigantea. *Biotechnol Bioeng* 109, 2941–2945.

Schulz, S., Girhard, M., Urlacher, V.B., 2012. Biocatalysis: Key to Selective Oxidations. *ChemCatChem* 4, 1889–1895.

Sheldon, R.A., Woodley, J.M., 2018. Role of Biocatalysis in Sustainable Chemistry. *Chem Rev* 118, 801–838.

Silva, C., Martins, M., Jing, S., Fu, J., Cavaco-Paulo, A., 2018. Practical insights on enzyme stabilization. *Crit Rev Biotechnol* 38, 335–350.

Silva, C., Silva, C.J., Zille, A., Guebitz, G.M., Cavaco-Paulo, A., 2007. Laccase immobilization on enzymatically functionalized polyamide 6,6 fibres. *Enzyme Microb Technol* 41, 867–875.

Slavica, A., Dib, I., Nidetzky, B., 2005. Single-site oxidation, cysteine 108 to cysteine sulfinic acid, in D-amino acid oxidase from Trigonopsis variabilis and its structural and functional consequences. *Appl Environ Microbiol* 71, 8061–8068.

Stocks, S.M., 2013. Industrial enzyme production for the food and beverage industries: Process scale up and scale down, Microbial Production of Food Ingredients, Enzymes and Nutraceuticals. Woodhead Publishing Limited.

Strohmeier, G.A., Pichler, H., May, O., Gruber-Khadjawi, M., 2011. Application of designed enzymes in organic synthesis. *Chem Rev* 111, 4141–4164.

Tavanti, M., Porter, J.L., Sabatini, S., Turner, N.J., Flitsch, S.L., 2018. Panel of New Thermostable CYP116B Self-Sufficient Cytochrome P450 Monooxygenases that Catalyze C–H Activation with a Diverse Substrate Scope. *ChemCatChem* 10, 1042–1051.

Thomas, C.R., Dunnill, P., 1979. Action of shear on enzymes: Studies with catalase and urease. *Biotechnol Bioeng* 21, 2279–2302.

Thomas, C.R., Geer, D., 2011. Effects of shear on proteins in solution. *Biotechnol Lett* 33, 443–456.

Thomas, C.R., Nienow, A.W., Dunnill, P., 1979. Action of shear on enzymes: Studies with Alcohol Dehydrogenase. *Biotechnol Bioeng* 21, 2263–2278.

Tirrell, M., Middleman, S., 1975. Shear modification of enzyme kinetics. *Biotechnol Bioeng* 17, 299–303.

Toftgaard Pedersen, A., de Carvalho, T.M., Sutherland, E., Rehn, G., Ashe, R., Woodley, J.M., 2017. Characterization of a continuous agitated cell reactor for oxygen dependent biocatalysis. *Biotechnol Bioeng* 114, 1222–1230.

Truppo, M.D., 2017. Biocatalysis in the Pharmaceutical Industry: The Need for Speed. *ACS Med Chem Lett* 8, 476–480.

Truppo, M.D., 2012. Cofactor Recycling for Enzyme Catalyzed Processes, in: Comprehensive Chirality. pp. 46–70.

Tufvesson, P., Lima-Ramos, J., Nordblad, M., Woodley, J.M., 2011. Guidelines and cost analysis for catalyst production in biocatalytic processes. *Org Process Res Dev* 15, 266–274.

Turner, N.J., 2012. Oxidation of C-N Bonds. *Enzym Catal Org Synth Third Ed* 3, 1535–1552.

Turner, N.J., 2011. Enantioselective Oxidation of C-O and C-N bonds using oxidases. *Chem Rev* 111, 4073–4087.

Turner, N.J., 2009. Directed evolution drives the next generation of biocatalysts. *Nat Chem Biol* 5, 567–573.

Turner, N.J., Kumar, R., 2018. Editorial overview: Biocatalysis and biotransformation: The golden age of biocatalysis. *Curr Opin Chem Biol* 43, A1–A3.

Van't Riet, K., 1979. Review of Measuring Methods and Results in Nonviscous Gas-Liquid Mass Transfer in Stirred Vessels. *Ind Eng Chem Process Des Dev* 18, 357–364.

Van Hecke, W., Haltrich, D., Frahm, B., Brod, H., Dewulf, J., Van Langenhove, H., Ludwig, R., 2011. A biocatalytic cascade reaction sensitive to the gas-liquid interface: Modeling and upscaling in a dynamic membrane aeration reactor. *J Mol Catal B Enzym* 68, 154–161.

Van Hecke, W., Ludwig, R., Dewulf, J., Auly, M., Messiaen, T., Haltrich, D., Van Langenhove, H., 2009. Bubble-free oxygenation of a bi-enzymatic system: Effect on biocatalyst stability. *Biotechnol Bioeng* 102, 122–131.

Vennestrøm, P.N.R., Christensen, C.H., Pedersen, S., Grunwaldt, J.-D., Woodley, J.M., 2010. Next-Generation Catalysis for Renewables: Combining Enzymatic with Inorganic Heterogeneous Catalysis for Bulk Chemical Production. *ChemCatChem* 2, 249–258.

Wang, Y., Lan, D., Durrani, R., Hollmann, F., 2017. Peroxygenases en route to becoming dream catalysts. What are the opportunities and challenges? *Curr Opin Chem Biol* 37, 1–9.

Whitman, W.G., 1962. The two-film theory of gas absortion. *J Heat Mass Transf* 5, 429–433.

Whitman, W.G., 1923. The Two-Film Theory of Gas Absorption. *Chem Metall Eng* 29, 146–148.

Wong, C.M., Wong, K.H., Chen, X.D., 2008. Glucose oxidase: Natural occurrence, function, properties and industrial applications. *Appl Microbiol Biotechnol* 78, 927–938.

Woodley, J.M., 2017. Bioprocess intensification for the effective production of chemical products. *Comput Chem Eng* 105, 297–307.

Woodley, J.M., 2017. Integrating protein engineering with process design for biocatalysis. *Philos Trans R Soc A Math Phys Eng Sci* 376, 20170062.

Woodley, J.M., 2013. Protein engineering of enzymes for process applications. *Curr Opin Chem Biol* 17, 310–316.

Woodley, J.M., 2008. New opportunities for biocatalysis: making pharmaceutical processes greener. *Trends Biotechnol* 26, 321–327.

Woodley, J.M., Breuer, M., Mink, D., 2013. A future perspective on the role of industrial biotechnology for chemicals production. *Chem Eng Res Des* 91, 2029–2036.

Wu, H., Fan, Y., Sheng, J., Sui, S.F., 1993. Induction of Changes in the Secondary Structure of Globular-Proteins by a Hydrophobic Surface. *Eur Biophys J with Biophys Lett* 22, 201–205.

Xu, F., 2005. Applications of oxidoreductases: recent progress. *Ind Biotechnol Spring* 1, 38.

Xue, R., Woodley, J.M., 2012. Process technology for multi-enzymatic reaction systems. *Bioresour Technol* 115, 183–195.

Process and Systems Engineering Centre (PROSYS)
Department of Chemical and Biochemical Engineering
Technical University of Denmark
Søltofts Plads, Building 229
DK - 2800 Kgs. Lyngby
Denmark

Phone: +45 45 25 28 00
Web: www.kt.dtu.dk/forskning/prosys